School of Pharmacy

An Investigation of p53's Differential Activation of Cell Cycle Arrest and Apoptosis

Yuan Zhang

This thesis is presented for the Degree of
Master of Pharmacy
of
Curtin University of Technology

August 2008

DECLARATION

This thesis contains no material which has been accepted for the award of any other degree or diploma in any university.

To the best of my knowledge and belief this thesis contains no material previously published by any other person except where due acknowledgment has been made.

Signature: _____

Date: _____

ACKNOWLEDGEMENTS

I wish to express my sincere gratitude to Dr Brett Dix, my supervisor, who provides me with very useful guidance in this project and valuable suggestions about my writing. Without his help, this project would be impossible.

I would like to thank Dr. Simon Fox, Erin Bolitho and Inez Czerwionka who assisted me with laboratory works in the past 2 years. It is their kind help enables me achieve more than I expect.

I should also be grateful to my family for supporting me studying overseas and continuous encouragement to maintain my study spirit.

ABSTRACT

The p53 tumour suppressor protein lies at the hub of a very complex network of cellular pathways including apoptosis, cell cycle arrest, DNA repair and cellular senescence. However, the mechanism of why and how p53 switches between apoptosis and cell cycle arrest, thereby determining a cell's fate, remains a mystery to us.

To enable us to investigate this ability of p53 to switch between cell cycle arrest and apoptosis, we developed a model which demonstrates similar p53 expression patterns but different functional outcomes.

Treating cells with Cisplatin (a common chemotherapeutic drug) and Nutlin-3 (an MDM-2 inhibitor) results in similar high levels of p53 accumulation but different cellular responses. Cisplatin-treated cells undergo apoptosis while Nutlin-treated cells enter cell cycle arrest.

Using this model, we explored the localization of p53 and in particular a C-terminal Ser 392 moiety in an attempt to identify how p53 is able to preferentially activate cell cycle arrest or apoptotic pathway.

TABLE OF CONTENTS

LIST OF FIGURES

LIST OF TABLES

ABBREVIATIONS

AP: alkaline phosphatase

BCL-2: B-cell CLL/lymphoma 2

BCIP: bromo-4-chloro-3-indolyl phosphate

BER: base-excision-repair

BH3: BCL-2 homology domain 3

cDNA: complementary DNA

DAPI: 4', 6-diamidino-2-phenylindole, dihydrochloride

DBD: DNA-binding domain

DMEM: Dulbecco's modified eagle's medium

DNA: deoxyribonucleic acid

dNTP: deoxyribonucleotide triphosphates

FACS: fluorescence-activated cell sorting

FADD: Fas (TNFRSF6)-associated via death domain

FCS: fetal calf serum

g: G-force

g: gram

GGR: global genome repair

hr: hour

IgG: immunoglobulin G

LFS: Li-Fraumeni Syndrome

L: litre

MDM-2: murine double minute 2

min: minute

ml: millilitre

mM: millimolar

MMR: mismatch-repair

MOMP: mitochondrial outer membrane permeabilization

NBT: nitro blue tetrazolium

NER: nucleotide-excision-repair

NES: nuclear export signal

NIBA: narrow interference blue A

NLS: nuclear localization signal

PBS: phosphate-buffered saline

PI: propidium iodide

PI-A: propidium iodide absorbance

RB: retinoblastoma

REG: regulatory region

RIPA buffer: RadioImmunoPrecipitation buffer

RNA: ribonuclease acid

ROS: reactive oxygen species

RT-PCR: reverse transcription polymerase chain reaction

s: second

SDS-PAGE: sodium dodecyl sulfate polyacrylamide gel electrophoresis

SEM: standard error of the mean

TA: transcriptional activation

TAE: tris-acetate, EDTA buffer

TBS: tris buffered saline

TCR: transcription-coupled repair

TET: tetramerization

U: unit

UV: ultraviolet

WG: wide green

5-FU: 5-fluorouracil

µg: micrograms

µl: microlitre

CHAPTER I

Literature Review

1.1 An introduction to p53

p53, was incorrectly described as an oncogene when it was first discovered by Linzer and Levine in SV40-transformed cells (1). However, abundant data subsequently proved p53 to be a tumour suppressor. p53 is defined as the true "guardian of the genome" due to its essential role in preventing cells from undergoing tumorigenesis by initializing various cellular responses. Studies have shown that more than 50% of human tumours contain a mutation or deletion of the *TP53* gene (2), and nearly 90% of p53 gene mutations are missense mutations leading to the synthesis of a stable but inactivated protein. This is different from most tumour suppressor genes which are usually unable to or aberrantly synthesize their product because of a frameshift or nonsense mutation (3). Studies of p53-null mice have shown that 75% of these mice developed tumours by six months of age and all were dead by 10 months (4). In humans, Li-Fraumeni syndrome (LFS) patients, carrying germline p53 mutations, are more prone to cancer and over 50% of these patients will develop tumours by age 30 (3). Additionally, p53 has demonstrated an ability to help maintain chromosome stability and in studies on fibroblasts from LFS patients, loss of p53 function leads to an abnormal karyotype with altered chromosome structure and number (5).

p53 plays a key role in mediating several important cellular responses including apoptosis, cell cycle arrest, DNA repair and cellular senescence. Because of its importance in tumour control, it has been widely studied in the search for more effective cancer therapies. During the last 10 years, numerous papers about p53 have been published, and significant progress in understanding the mechanism of p53 action has been achieved. However, gaps still exist in our knowledge regarding the global regulation of p53. Restoration of wild-type p53 function in p53-deficient or

p53-null tumour cells exhibit a promising future for cancer therapy and we hope one day will lead to a significant improvement in the treatment of human cancer.

1.2 The structure of the p53 protein

p53 is a nuclear protein which acts as a transcription factor. The gene encoding p53 is located on the short arm of chromosome 17 at 17p13.105-p12 (6). The open reading frame of p53 encodes for a protein of 393 amino acids (53kDa).

The structure of p53 (***Fig 1.1***) can generally be divided into three functional domains: a transcriptional activation domain (codons 1~101), a sequence-specific DNA-binding domain (codons 102~292), and a tetramerization domain (293~393). The transactivation domain is located at the N-terminus of the protein. This region interacts with components of the transcriptional machinery including p300/CBP, a regulator of chromatin remodeling (7). The regulatory protein MDM-2 can inhibit the transcriptional activity of p53 when binding to this region. Adjacent to the MDM-2 binding region, a proline-rich domain is found. This domain has been shown to be important for p53's tumour suppressor activity (8). The central domain is involved in sequence specific binding to DNA and is the region most commonly mutated. The C-terminus contains the tetramerization domain (TET) where a negative regulatory region (REG, codons 363-393) has been identified and three nuclear localization signals (NLS, codons 305–322, 369–375, 379–384) are clustered. The nuclear export signal (NES, codons 11–27, 339–352) and post-translational modification sites including phosphorylation, acetylation and sumoylation sites are located in the amino terminus and the carboxy terminus (9). Notably, p53 is active as a transcription factor only in tetrameric form because tetramerization of p53 is believed to mask the NES at its C-terminus thus keeping p53 in the nucleus (9). It is also suggested that DNA damage-induced phosphorylation may inhibit NES activity thus preventing p53 from exporting to the cytoplasm where it could be degraded through ubiquitin-mediated proteolysis (7). The stability and activity of p53 are tightly regulated by these

modifications. The role of modification has been of interest to many investigators. Understanding how these modifications contribute to the stability, location, binding, activation, and target site selectivity of p53 remains an active area of research.

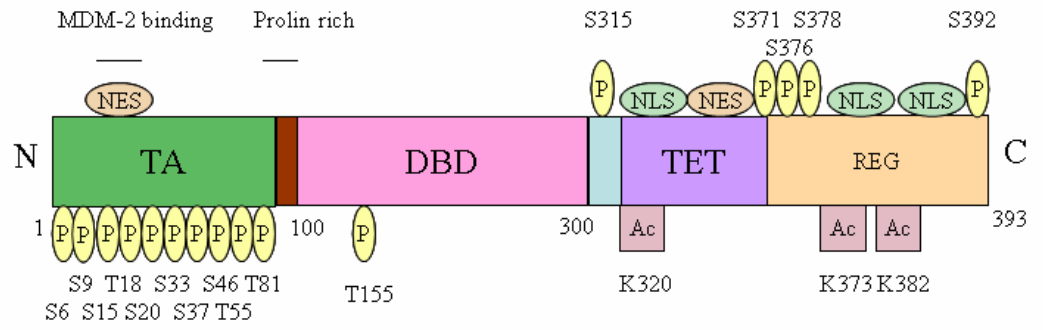

Fig 1.1: The structure of p53

The p53 protein comprises three domains including an N-terminal region containing the transactivation domain (TA), a core containing the sequence-specific DNA-binding domain (DBD) and a tetramerization domain with multiple functions (TET). The P indicates phosphorylation sites and Ac acetylation sites, NES stands for nuclear export signal and NLS for nuclear localization signal. Modified from Resnick-Silverman, L (7).

1.3 The p53 pathway in tumour control

1.3.1 p53 and its negative regulator MDM-2

p53 plays an important part in mediating a cell's response to DNA damage, hypoxia and genomic damage. p53 is maintained at relative low levels by its key negative regulator, MDM-2, in unstressed cells. After exposure to genotoxic stress, p53 protein is transiently stabilized due to its detachment from MDM-2 and accumulated in the nucleus.

MDM-2 was discovered in a mouse double minute chromosome. The protein contains an N-terminal p53 interaction domain, a central acidic domain, a Zinc finger domain and a C-terminal RING domain. The phosphorylation of residues in the central acidic domain appears to be important for regulation of MDM-2 function (10). Furthermore, this region contains several nuclear export and import signals that are associated with nuclear-cytoplasmic localization of MDM-2. The RING domain

of MDM-2 shows E3 ubiquitin ligase activity (11). MDM-2 has been shown to be amplified in 20% ~ 40% human sarcomas as a consequence of down-regulation of p53 (6).

The stability and activity of p53 primarily depends on its interaction with the MDM-2 protein. MDM-2 can block p53's transcriptional activity by binding to its N-terminal region and functions as an E3 ubiquitin ligase leading to degradation of p53 by the proteosome. *MDM-2* in turn is a transcriptional target of p53 creating an autoregulatory feedback loop (12). However, a recent study of the interaction between p53 and MDM-2 is seen to be much more complex than previously assumed. The binding of MDM-2 and p53 is largely affected by post-translational modifications, conformation changes, and other cofactors involved in their transcription (9, 13). For example, part of the N-terminal region of p53, from residues 15 to 26, is known for binding to a structured domain of MDM-2. Phosphorylation in this region, such as serine-15 and serine-20, can inhibit the binding of p53 to MDM-2 thus preventing p53's degradation (6). Moreover, proline isomerase Pin1 has recently been found to induce conformation change in p53 thus inhibiting the binding and/or stimulating the detachment of MDM-2 (13). Other cofactors involved in p53-MDM-2-binding include HAUSP, YY1, ΔN-p53 (13). These cofactors are either known to promote or to suppress the binding of p53 to MDM-2 in different ways. MDM-2 functions as an E3 ubiquitin ligase, targeting p53 and itself for degradation by the proteasome. Interestingly, recent studies have found that MDM-2 is able to induce both mono-ubiquitination and poly-ubiquitination on p53 depending on the p53: MDM-2 ratio (14). When sufficient MDM-2 is present, p53 will be poly-ubiquitinated otherwise it will be mono-ubiquitinated (14). However, the role of mono-ubiquitination and poly-ubiquitination in p53 regulation remains unclear. A widely accepted theory suggests that mono-ubiquitination is associated with p53 nuclear export while poly-ubiquitination leads to rapid p53 degradation (15). why p53 is exported to the cytoplasm is still under investigation. One possibility is that mono-ubiquitination of p53 can promote its translocation to

the mitochondria where p53 is able to interact with the BCL-2 family proteins leading to apoptosis independent of transcriptional activation (reviewed in 1.3.3.2 The transcription-independent pathway) (16).

Notably, abrogation of MDM-2 binding is not the only mechanism responsible for stabilization of p53. Other proteins such as calpain 1, beta-catenin and JNK also contribute to the stabilization of p53 (17).

1.3.2 MDM-2 and its antagonists

Nutlin-3 is a synthetic compound. It binds to the p53 interaction domain on MDM-2 disrupting MDM-2 and p53 binding (18). This leads to indirect accumulation of p53 in the nucleus, providing potential as an anti-cancer drug. p14ARF is also an MDM-2 inhibitor, binding to MDM-2 and inhibiting the degradation of p53 (19).

1.3.3 p53 regulation

p53's role in regulating cellular responses to stress can be mainly divided into transcription-dependent pathways and transcription-independent pathways (***Fig 1.2***). Following genotoxic stress, p53 becomes stabilized and accumulates in the nucleus primarily due to post-translational modifications. The primary consequences of p53 accumulation are cell cycle arrest or apoptotic cell death (8).

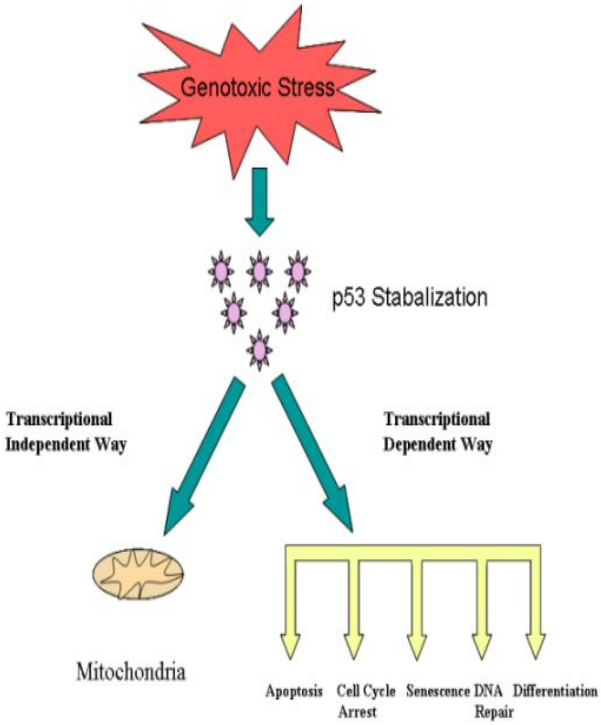

Fig 1.2: The p53 pathway

The initiating stimuli in the p53 pathway are diverse and may include UV radiation, ionizing radiation, hypoxia, hyperoxia, telomeric deterioration, cytokines, growth factors deprivation, activated oncogenes, metabolic changes, cell-cell contact, virus infection, and treatment with chemotherapeutic drugs. p53 becomes stabilized and activated by post-translational modifications and is capable of transactivating downstream targets involved in different cellular responses. Moreover, it can initialize apoptosis by localizing to the mitochondria (7).

1.3.3.1 The transcription-dependent pathway

p53 exerts its function largely as a transcription factor. Hundreds of genes have been reported to be activated or repressed by p53, however, only a few of them have been studied in detail (20).

Post-translational modifications such as acetylation and phosphorylation have shown to contribute to p53's DNA-binding activity. Acetylation of p53 by some important transcriptional co-activators such as p300/CBP and PCAF is reported to disturb the interaction between the C-terminal domain and core DNA-binding domain, thereby allowing the core DNA-binding domain to assume an active conformation (9, 21). When p53 is activated, it can up-regulate or suppress its target genes in order to drive cells into apoptosis, cell cycle arrest or DNA repair (22). Table 1.1 summarizes some important target genes activated by p53 which are involved in apoptosis, cell cycle arrest and DNA repair.

Apoptosis	Intrinsic pathway	*BAX* *PUMA* *NOXA* *APAF1* *P53AIP1* *PTEN*
	Extrinsic pathway	*TRAIL* *CD95* *DR4, DR5* *FAS/APO-1*
Cell Cycle Arrest	G_1/S Checkpoint	*CDKN1A* ($P21^{WAF1/CIP1}$) *BTG2* *MCG10* *GADD45*
	G_2/M Checkpoint	*CDKN1A* *GADD45* *SFN* (14-3-3σ) *BTG2* *REPRIMO* *GTSE-1* *HZF* *MCG10*
DNA Repair	mismatch repair (MMR)	*MLH1* *MSH2* *PCNA* *PMS2*
	base-excision repair (BER)	*OGG1* *APE*
	nucleotide-excision repair (NER)	*XPC* *DDB2(XPE)*

Table 1.1: Genes up-regulated by p53 in response to cellular stress *(9, 21).*

1.3.3.1a p53's role in apoptosis

p53 combats tumour growth by its ability to mediate apoptosis (programmed cell death). Apoptosis can be activated by either the extrinsic pathway or the intrinsic pathway (***Fig 1.3***). Both pathways have an independent group of "initiator" caspases and a group of "effector" caspases that execute the final cell death program (23). In the extrinsic pathway, death receptors on the cell surface become active when binding to their specific ligand, and recruit FADD, initiator procaspase-8 and procaspase-10, resulting in receptor trimerization. The high local concentration of the procaspase molecules activates initiator caspases by autocatalysis and initiates downstream proteolytic processing of the effector caspases-3, -6, and-7 which will carry out the cell death program (7, 24). The intrinsic pathway doesn't require death receptor signalling but can lead to the activation of effector caspases as well. This process begins with the mitochondrial outer membrane permeabilisation (MOMP) caused by activated pro-apoptotic BCL-2 family members leading to leakage of cytochrome c into the cytoplasm. Subsequently, cytochrome c complexes with the cytoplasmic protein Apaf-1 which then oligomerizes and binds to procaspase-9 resulting in the formation of an apoptosome. This allows procaspase-9 to enzymatically self-activate and in turn activate down stream effector caspases-3, -6, and-7. The intrinsic pathway converges with the extrinsic pathway at the level of effector caspase activation and these effector caspases carry out the apoptotic cell death program (7).

p53 initializes the extrinsic apoptotic pathway by up-regulating target genes such as death receptor-4 (*DR4*), death receptor-5(*DR5*) (24), *TRAIL*, *FAS* receptor (*CD95*) and the FAS/APO-1 ligand (25). p53 can also promote the intrinsic pathway by up-regulating target genes involved in disrupting mitochondrial membrane, such as pro-apoptotic BCL-2 family members *BAX*, *PUMA*, and *NOXA*. *APAF1* and *p53AIP1* are also reported to be up-regulated by p53 in the intrinsic pathway (21). In addition, it has recently been found that p53 may play a direct role in mediating the intrinsic pathway (reviewed in 1.3.3.2 The transcription-independent pathway).

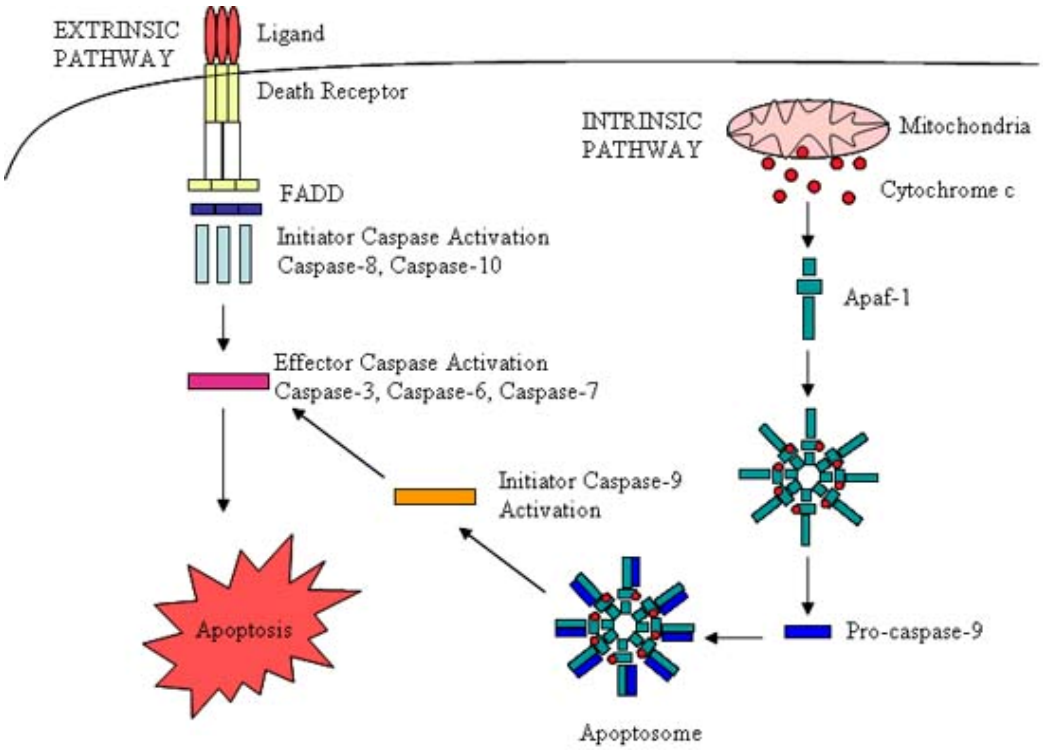

Fig 1.3: Apoptosis pathway

The extrinsic pathway comprises death receptor activation, FADD recruitment, initiator caspase activation and effector caspase activation. The intrinsic pathway begins with mitochondrial damage leading to cytochrome C leakage. The subsequent formation of apoptosome by cytochrome C, Apaf-1, pro-caspase-9 leads to caspase-9 activation. Activated caspase-9 eventually causes apoptosis through caspase-3 activation (23).

1.3.3.1b p53's role in cell cycle arrest

Cell cycle is comprised of four distinct phases: G_1, S (DNA replication), G_2, and M (the cell division). Activation of each phase depends on the regulation of genes involved in this progression. Two kinds of molecules, cyclins and cyclin-dependent-kinases (CDK), are identified as the key regulators in the progression of cell cycle (26). CDKs are inactive and cannot phosphorylate target proteins involved in regulating the entry to the next cell cycle phase in the absence of the cyclins. Different Cyclin-CDK complexes target different downstream proteins. Cyclin D-CDK4 is the first complex produced in response to growth signals. Cyclin D-CDK4 phosphorylates RB (Retinoblastoma) which dissociates from the E2F/DP1/RB complex and activates E2F (27). E2F is an important transcription factor for many genes including Cyclin E, Cyclin A, DNA polymerase and thymidine polymerase

which are all required in cell cycle progression (28). As the cell cycle proceeds, Cyclin E is synthesised and binds to CDK2. This complex is capable of driving cells from G_1 to S. Similarly, Cyclin A-CDK2 and Cyclin B-CDC2 (also called Cyclin B-CDK1) complexes are responsible for G2 to M transitions (29).

Regulation of cell-cycle arrest genes by active p53 may initialize growth arrest at one of two cell cycle checkpoints (G_1/S checkpoint and G_2/M checkpoint). Cyclin-dependent kinase inhibitor 1A (*CDKN1A, P21*$^{WAF1/CIP1}$) for instance, is one of the most important cell-cycle arrest genes controlled by p53. The encoded protein p21 binds to the complex cyclin-CDK2 or cyclin–CDK4 and inhibits their activity which is required for G_1 to S phase progression (30). While p21 is the major initiator of p53-mediated G_1 arrest, other genes are also involved, such as *GADD45* and *BTG2* (21). *BTG2* mediates G_1/S checkpoint entry by inhibiting Cyclin D1 and Cyclin E1 (31). *GADD45* is found to bind to PCNA, a component of CDK complexes and a protein involved in DNA replication, thus inhibiting entry into S phase (32).

p53 mediates G_2/M arrest by regulating many target genes involved in G_2/M progression. For instance, p53 regulates p21 which inhibits G_2/M progression by inactivating the Cyclin B-CDC2 complex (33). Moreover, p53 can up-regulate 14-3-3σ which suppresses the activity of phophatase CDC25C. CDC25C activates CDC2 protein kinase by dephosphorylation and this is associated with entry into mitosis (34). It is also reported that 14-3-3σ sequesters Cyclin E-CDK2 and Cyclin B-CDC2 in the cytoplasm thereby regulating G_1 and G_2 arrest (34). Furthermore, *GADD45*, *BTG2* and *REPRIMO* have been reported to regulate the G_2/M checkpoint by inhibiting Cyclin B-CDC2 kinase activity (33, 35-39).

1.3.3.1c p53's role in senescence

Permanent cell cycle arrest is also known as senescence. p53 regulates replicative senescence and pre-mature senescence. Both of the senescence pathways involve the p53-p21-Rb system (40). Replicative senescence often occurs after telomere shortening (21). At G_1/S phase, p53 stimulates p21 expression, which binds to cyclin-CDK4 and holds the complex inactive. An inactive cyclin-CDK4 complex cannot phosphorylate RB and unphosphorylated RB binds to E2F rendering it

inactive. Thus, cell cycle progression is suspended. The fact that $p53^{-/-}$ and $p21^{-/-}$ HCT116 cells are less able to undergo senescence following DNA damage supports the important role of p53 and p21 in the regulation of cell senescence (41).

1.3.3.1d p53's role in DNA repair

In human cells, normal metabolic activities and various environmental stresses such as ultraviolet-irradiation (UV), reactive oxygen species (ROS), chemotherapeutic drugs, and chemical carcinogens can cause DNA damage. Depending on the type of DNA lesion, p53 can initialize multiple DNA repair pathways to restore the integrity and normal function of cellular genome.

p53 mediates base-excision-repair (BER) for a single mutated DNA base caused by oxidation, alkylation, hydrolysis, or deamination through promoting several key proteins associated with BER (21). The activity of 8-oxoguanine glycosylase (OGG1) and apurinic endonuclease (APE) is reported to be promoted by p53 (42). OGG1 is known for breaking the β-N glycosidic bond and creating an apurinic site. APE recognizes this site and facilitates DNA polymerase to complete the repair (43).

Mismatches may occur during the process of DNA replication. p53 can regulate several key proteins in mismatch-repair (MMR) including MSH2, MLH1, PCNA and PMS2 via a transcription-dependent mechanism (21). MSH2 can recognize mismatches (44) while MLH1 is responsible for recruiting additional repair enzymes (45). PCNA can facilitate the repair of mismatched bases by MSH2 (46), and PMS2 is a sensor of DNA damage (47).

Nucleotide-excision-repair (NER) occurs when pyrimidine dimers are formed due to UV irradiation and chemical carcinogens. NER can be further categorized into two classes: transcription-coupled repair (TCR) and global genome repair (GGR). The difference between these two pathways is TCR can only repair template strand DNA while GGR can repair both DNA strands (21). p53 is reported to transactivate genes involved in GGR including xeroderma pigmentosum C (*XPC*) (48) and DNA damage-binding 2 (*DDB2/XPE*) (49). Supporting the effectiveness of p53 in GGR,

100% of $XPC^{-/-}$ mice develop lung cancer (50) and LFS fibroblasts demonstrate defects in GGR (51).

1.3.3.2 The transcription-independent pathway

BCL-2 family members play an important role in p53 regulated apoptosis, although how exactly the BCL-2 family proteins regulate cell death is still an unresolved question. However, their role in triggering mitochondrial outer membrane permeabilisation (MOMP) which causes subsequent cytochrome c release has been widely recognised (52).

BCL-2 family members can be divided into three groups. (i) The anti-apoptotic, also known as the pro-survival, BCL-2 family members including BCL-2 itself, BCL-XL, BCL-W, A1 and MCL-1, which are essential for cell survival. (ii) The pro-apoptotic BCL-2 family members comprising BAX, BAK, BOK, BCL-G and BFK which play a direct role in MOMP. Studies indicate that most BCL-2 proteins seem to be localised to the mitochondria while BCL-XL and BCL-W are distributed between the cytosol and mitochondrial membrane. BAX normally localises in the cytosol, with only a small portion in the mitochondria membrane. Evidence suggests that BAX will transport from the cytosol to the mitochondrial membrane following an apoptotic signal (53). Although the binding of pro-apoptotic and anti-apoptotic group members is unclear, the finding that BAX is constitutively complexed with the BCL-XL and MCL-1 provide a basis for a model suggesting that BAX and BAK can only be activated once they are no longer kept in check by anti-apoptotic members (54). (iii) The BH3-only proteins can be further divided into two groups. The activators include BIM and BID that can activate pro-apoptotic members directly. The other group known as enabler includes BAD, BMF, NOXA, BIK, HRK and PUMA. These proteins can inhibit the activity of the anti-apoptotic group thus releasing the pro-apoptotic group. Of note, PUMA and NOXA are reported to be transcriptionally induced by p53 whereas other BH3-only proteins are thought to be regulated at the post-translational level (55).

The relationship between p53 and BCL-2 family members is largely involved in p53-regulated apoptosis. In addition to p53's role in regulating the transcription of BCL-2 family members, it is also reported that a portion of p53, translocated to the mitochondria, can function similar to BH3-only proteins thus leading to a transcription-independent pathway of apoptosis. In other words, p53 can either act as an 'activator' to directly activate pro-apoptotic group or as an 'enabler' to block anti-apoptotic group (56) (***Fig 1.4***).

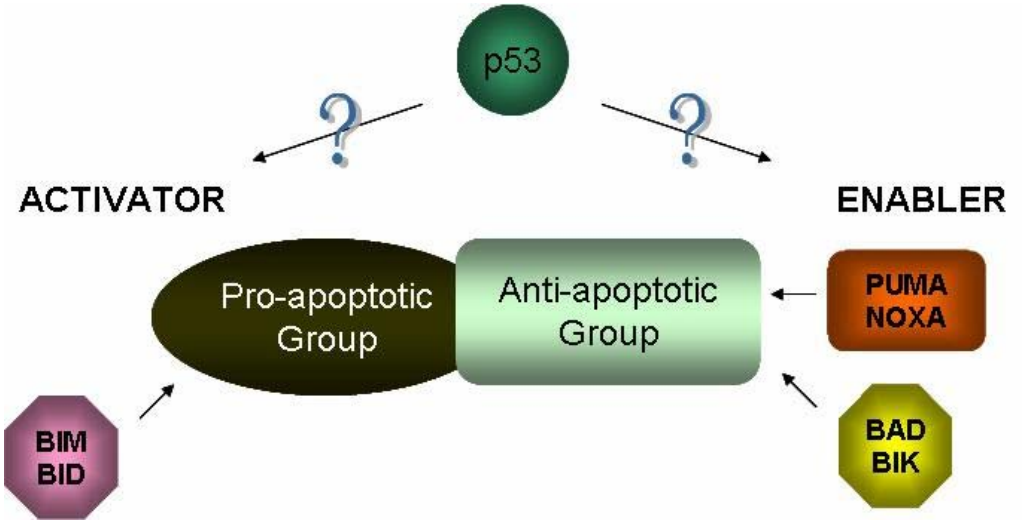

Fig 1.4: p53 and BCL-2 family members

The mechanism of how p53 translocates to the mitochondria remains unclear. Based upon data showing nuclear p53 contributes little translocated p53 to the mitochondria (14, 57), a hypothesis proposed by Natasha D Marchenko *et al* suggests a separate p53 pool in the cytoplasm which might be the major source of translocated p53. The cytoplasmic p53 can be mono-ubiquitinated by MDM-2. This process is thought to promote p53 translocation to the mitochondria. Their evidence also shows that p53 is deubiquitinated by HAUSP before its interaction with BCL-2 family members (14). Furthermore, the studies conducted by Susan Erster *et al* indicate that mitochondrial p53 translocation triggers a rapid first wave of caspase 3 activation and apoptosis (detectable by 30min following stress in thymus and spleen), and the transcription-

dependent pathway triggering the second wave of death occurs a few hours later (58).

1.4 A focus on phosphorylation of p53

Under normal conditions, p53 is maintained at low levels via MDM-2 regulated degradation. p53 can be activated following a number of cellular stresses, including DNA damage, hypoxia and genomic damage. It has been well established that stress signals, especially the signals caused by DNA damaging agents, such as chemotherapeutic drugs, can induce p53 up-regulation mainly at the protein level (59, 60).

There are a number of chemotherapeutic drugs reported to lead to p53 responses by inducing DNA damage. For instance, Cisplatin acts by crosslinking DNA, making it impossible for cells to duplicate their DNA for mitosis. It is suggested that Cisplatin treatment can induce G_2/M arrest and apoptosis in cancer cells (61). Doxorubicin is one of the DNA intercalators which inhibit DNA replication in cancer cells. 5-fluorouracil (5-FU) acts as a thymidylate synthase inhibitor which inhibits the synthesis of thymidine monophosphate in DNA synthesis.

Following DNA damage, activation of p53 occurs in association with a rapid increase in the level. This then results in activation of a number of downstream genes responsible for apoptosis, cell-cycle arrest or DNA repair. It is suggested that this regulation is mainly brought about by post-translational modification of the p53 polypeptide such as phosphorylation, dephosphorylation, acetylation, deacetylation and glycosylation.

Various studies have underscored the importance of phosphorylation at several key serine sites including 15, 20, 33, 37, 46, 47, 315, 376, 378 and 392 in the activation of p53 (62). p53 can be phosphorylated by numerous kinases including ATM (Ataxia

telangiectasia mutated kinase), ATR (Ataxia telangiectasia RAD3-related kinase), p38, HIPK2 (homeodomain-interacting protein kinase2), CHK1 (Checkpoint kinase-1) and CHK2 (Checkpoint kinase-2). In brief, phosphorylation at N-terminal sites may inhibit the interaction between p53 and its negative regulator MDM-2, thus promoting p53 levels and transcriptional activity, whereas phosphorylation at C-terminal sites may enhance the sequence-specific DNA binding potential of the protein (63).

In addition to the post-translational modification, recent studies have been shown that several RNA-binding proteins such as HuR (Hu antigen R), ribosomal protein L26 (RPL26), and nucleolin can increase p53 levels after DNA damage by promoting p53's translation (64). Phosphorylation of MDM-2 at several key residues is also known to contribute to stabilization of p53 (***Fig 1.5***).

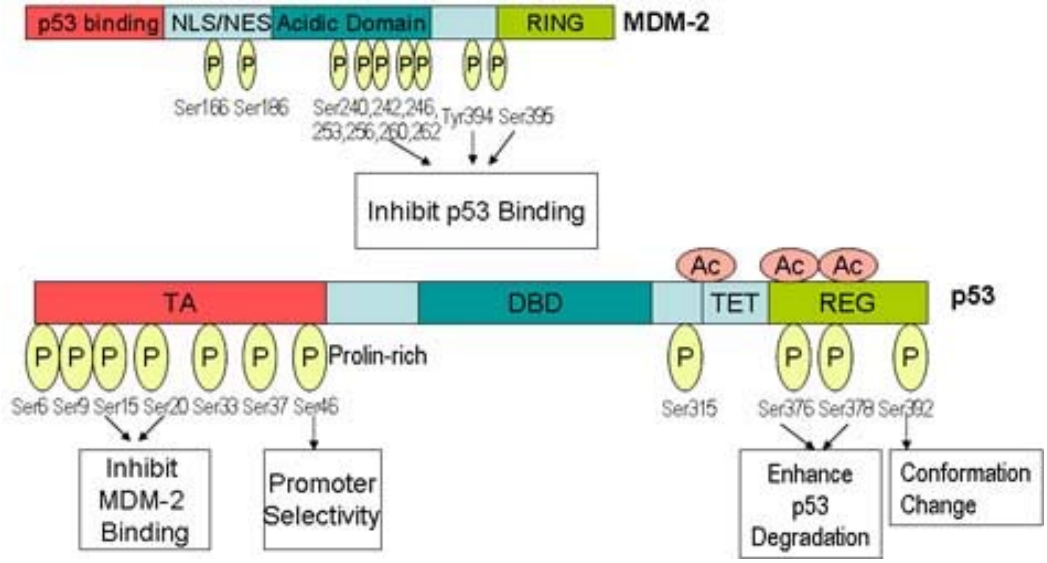

Fig 1.5: DNA damage-induced post-translational modification of p53 and MDM2

The different domains of p53 and MDM-2 are highlighted in different color. The Phosphorylation and acetylation sites are indicated by yellow and red ellipses respectively. Boxes containing text summarize the biological consequences of relevant modification sites. Modified from Meek, D.W. (22).

p53 can be phosphorylated on serine-15 by a series of kinases. Phosphorylation at this site is thought to instigate a series of subsequent p53 post-translational modifications including acetylation on C-terminal sites which may contribute to the stabilization of p53 by impairing ubiquitination (22). Furthermore, together with phosphorylation at serine-20, p53 could no longer interact with MDM-2 (17). This leads to a prolonged half-life of p53 and enables interaction with transcriptional coactivators, TBP, TAFs and/or other components of the transcriptional apparatus (65). As a NES is located at codon 11~27, phosphorylation at serine-15 and 20 are also thought to inhibit the NES signal thus preventing p53 from being exported outside the nucleus (66). Studies indicate that phosphorylation at serine-6 appears as strong as serine-15 in response to DNA damage while phosphorylation at serine-9 is less strong than the other two (67).

Phosphorylation of serine-33/37 is known to increase the affinity of p53 for coactivators PCAF and p300 and promote the acetylation of p53 C-terminal residues

lysine-382 and lysine-320 (68). Acetylation at either of these sites is known to enhance p53 sequence-specific DNA binding. Another critical N-terminal residue is serine-46. Previous observations have shown that serine-46-phosphorylated p53 targets the promoter of the tumour suppressor PTEN in preference to MDM-2 (69). Moreover, phosphorylation of serine-46 can regulate p53AIP1 (p53-regulated Apoptosis-Inducing Protein 1) transcriptional activation. This protein is reported to induce apoptosis by dissipation of mitochondrial inner membrane potential (70). However, there are studies indicating that phosphorylation at serine-46 is not always sufficient to induce p53AIP1 depending on the type of cell line and treatment delivered (71). The adjacent serine-47 is also known to enhance the ability of p53 to induce apoptosis (9).

Several critical phosphorylation sites in the C-terminal region of p53 including serine-315, serine-371, serine-376, serine-378 and serine-392 are well known. A previous study has demonstrated that phosphorylation of serine-392, in response to UV radiation, could induce conformational changes in the tetramerization domain, which may enhance the activity of the core DNA binding domain (72). In addition, phosphorylation of serine 392 is suggested to be related to nuclear export (73). Although most of the phosphorylation sites on p53 can lead to an increase in stability and activity, some phosphorylation sites are reported to be associated with enhanced p53 degradation such as serine-376 and -378 (74).

Table1.2 summarises several key phosphorylation sites of p53 and their general functions:

C-terminal	Serine-6, -9	1. Amplify the biomedical affect of the initial phosphorylation like serine-15
	Serine-15, -20	1. Promote acetylation at C-terminal site 2. Disturb MDM-2 binding 3. Stimulate transcription factors such as p300, CBP, PCAF 4. Blocking NES signal
	Serine-33, -37	1. Promote acetylation at C-terminal site 2. Stimulate transcription factors such as p300 and PCAF
	Serine-46, -47	1. Bind to PTEN 2. Induce p53AIP1
N-terminal	Serine-315	1. Retain nuclear p53 during E2F1/p53-mediated cell cycle arrest
	Serine-215, -376, -378	1. Enhance p53 degradation
	Serine-392	1. Conformational change 2. Related to NES

Table 1.2: Key phosphorylation sites of p53 (22, 59, 65, 67-72, 74-76)

Post-translational modifications have been proved critical for the stabilization and activation of p53 in the nucleus. It is also speculated that post-translational modifications may play an important part in p53's translocation to the mitochondria. Although there are several phosphorylation sites reported to be related to p53 nuclear export such as phosphorylation at Serine 392 and Serine 315, whether it is associated with p53 translocation to the mitochondria remains unclear.

1.5 The ability of p53 to differentiate between life and death

As described before, p53 can initiate both cell survival and cell death pathways. It has been suggested that p53 can differentiate between these two pathways according to the intensity of the DNA damage signal. When DNA damage is mild, p53 is more likely to promote cell survival by regulating cell cycle arrest or DNA repair. When excessive DNA damage is accumulated, p53 chooses to regulate cell senescence or apoptosis in order to prevent tumorigenesis (21). Nevertheless, the mechanisms by which p53 decides between the alternatives of apoptosis or cell-cycle arrest remain to be elucidated. There are several hypotheses proposed to explain the differential ability of p53. Studies have shown that the affinity of p53 to the promoters of its target genes, the overall levels of p53, the post-translational modifications of p53 , the differential transcriptional cofactors involved in a specific response and its translocation to the mitochondria may contribute to determine the fate of cells (77, 78).

1.5.1 The levels of p53

Accumulating evidence has shown that the differential ability of p53 to regulate cell-cycle arrest and apoptosis is associated with the levels of p53 (79). Paul B. S. Lai and colleagues have shown that apoptosis was induced in HCC cells with high levels of p53 expression while lower p53 expression could only trigger cell-cycle arrest (80). Based on this observation, some people have proposed the idea that cell-cycle arrest genes have higher affinity p53-binding sequences while apoptotic genes have lower affinity p53-binding sequences. When p53 achieves a certain threshold level, the apoptosis pathway is turned on (22). Although the level of p53 proteins may contribute to the selection of apoptosis or growth arrest, other factors may also influence the choice between apoptosis and cell-cycle arrest.

1.5.2 Other proteins that bind to p53

In addition to the BCL-2 family proteins which are demonstrated to bind to p53 thereby leading to apoptosis, there are some other proteins that bind to p53 and help mediate different cellular responses.

The E2F family (E2F1-8) play an important role in p53-induced cell-cycle arrest. E2F family members are key transcription factors in the control of cell cycle progression. The tumour suppressor RB can bind E2F family members thereby inhibiting its ability to activate cyclins and CDKs which will drive the cells to proliferation (81). Similar to RB, p53 can bind E2F1-3 and inactivate them. As E2F also has a Cyclin A binding site, p53 and Cyclin A can compete for binding to E2F1-3 to determine whether the cell undergoes cell-cycle arrest or not (82). In addition, E2F's binding to p53 can mask the NES thus preventing p53 nuclear export and promoting its transcriptional ability (83).

ASPP family members are identified as critical regulators of the apoptotic, but not cell cycle arrest function of p53. There are three members in this family: ASPP1, ASPP2 and inhibitory iASPP (83). Studies have shown that the binding of ASPP1 and ASPP2 to p53 can selectively activate the binding of p53 to the promoters of pro-apoptotic genes, such as *BAX* and *PIG3*, but not to the promoters of cell cycle arrest genes like *CDKN1A* (84). Furthermore, the binding of ASPP1 and ASPP2 to p53 family members, p63 and p73, can indirectly enhance the apoptotic function of p53 (85). iASPP inhibits p53-mediated apoptosis by promoting the transforming activity of oncogenes *RAS* and *E1A* (86).

YB1 has been shown to bind to p53. This interaction is seen to suppress p53-regulated $p21^{WAF1/CIP1}$ transactivation (87). In addition, the fact that YB-1 reduce apoptosis in a p53-dependent manner suggests its role as an oncoprotein (88).

Different from other kinds of p53-binding proteins, Pin1 is an enzyme that catalyses phosphorylation-directed prolyl-isomerization. Pin1 catalyses cis/trans isomerisation at phosphorylated Ser-Pro or Thr-Pro motifs present in many proteins including p53. It is suggested that conformational changes can retain some of the Pin1's substrates in a phosphorylated cis-conformation which can no longer be dephosphorylated or degraded by phosphatases and ubiquitin ligases (89). Evidence showing that Pin1 is present at p53 target promoters suggests Pin may contribute to promoter selection by stabilizing p53 (83). In addition to the suggestion that Pin1 may contribute to the stabilization of p53, it is also reported that Pin1 can induce conformational change on serine-46 which is important in p53-mediated apoptosis but not in cell cycle arrest (90).

1.5.3 p53 and its transcriptional cofactors

It is suggested that promoter selection plays an essential part in determining the response to p53. Some transcriptional cofactors are reported to influence promoter selection. For instance, p53 and Miz are required for activating the expression of the $P21^{WAF1/CIP1}$ gene rather than apoptotic genes (91). On the other hand, SLUG represses the expression of PUMA by binding to its promoter (92). Changes in the conformation of p53 itself may also allow the differential recognition of target-gene promoters (77). This is supported by the observation that p53 demonstrates a high degree of flexibility in binding to DNA (93).

p53-regulated transactivation of target genes is widely recognized as the main reason for its capability to differentiate between cell survival and death. As more and more new genes are reported to be involved in p53 regulation, it seems very difficult to elucidate the global regulation of p53 in transcriptional activation. However, working on how these proteins coordinate and contribute to p53-regulated cellular responses will help to clarify the mechanism of p53 regulation.

1.5.4 Post-translational modification of p53

Post-translational modification plays an important part in the selective response of p53. Studies have found that phosphorylation at serine-15 and 20 are necessary for apoptosis but not cell cycle arrest (94). Phosphorylation at serine-46 has been shown to contribute to apoptotic gene activation (69). In addition to its direct influence on p53 target genes, post-translational modification can also regulate the interaction of p53 and its binding proteins which will have an effect on the final cellular responses initiated by p53 (77).

1.5.5 The transcription-independent pathway

The importance of the transcription-independent pathway in p53-regulated apoptosis remains controversial. The studies showing 5-fluorouracil (5-FU) and Doxorubicin (Adriamycin) elicit totally different cellular responses in HCT116 cells despite similar p53 mediated transcription profiles raises a remarkable possibility that at least in certain contexts, the p53 transcription-independent pathway may play a major role in p53-regulated apoptosis (78, 95).

1.6 p53's role in anti-cancer drug development

Because of its central role in activating apoptosis and cell cycle arrest, p53 has become an appealing target for anti-cancer drug designs. Restoration of wt-p53 function in p53-deficient or p53-null tumour cell lines is a major strategy for re-activating p53-regulated apoptosis in tumour cells. The approaches to achieve this goal include retrovirus-mediated *TP53*-gene therapy, adenovirus-mediated *TP53*-gene therapy (Ad5CMV-p53), and synthetic drugs to inhibit p53-MDM-2 binding (96).

Retroviruses are common vectors for gene therapy. They can integrate into the genome of infected cells and require cell division for transduction (97). It has been

reported that the injection of the retroviral vector containing wt-*TP53* gene into tumour cells leads to nearly 50% tumour regression in 7 patients after 5 months (96). However, retroviral vectors still have some disadvantages. For instance, they may cause damage to the genome and the transduction efficiency is relatively low especially in non-dividing cells (98). Ad5CMV-p53 is a recombinant E1-deleted serotype 5 adenoviral vector encoding-*TP53*. It has demonstrated its efficiency in wt-p53 expression, tumour cell growth inhibition and selectivity of tumour cell killing in vivo (99-101).

Disrupting the binding between p53 and its negative regulator MDM-2 seems the most direct way to accumulate p53. Synthetic compounds, like Nutlin-3, are designed to displace p53 from the p53-binding pocket on MDM-2 (102). It has been reported that this molecule effectively induces p53 up-regulation, cell-cycle arrest and apoptosis in tumour cells (96).

Other chemical compounds like polyamines have been shown to activate p53 in many cultured cell lines (103). p53 inhibitors like Pifithrin have been used to protect wt-p53 cells from apoptosis induced by irradiation and various cytotoxic drugs including Doxorubicin and Etoposide thus reducing side-effects of radiation therapy and chemotherapy (104). CP31398, Ellipticine and PRIMA-1 are drugs designed to re-activate the wt-p53 activity in mutant p53 (105). Interestingly, PRIMA-1 and another small molecule kinase inhibitor LY2119301 have been shown to induce apoptosis in a way that is independent of p53 mediated transcriptional activation (106).

1.7 Significance of p53

p53 plays a key role in regulating cellular stress induced by hypoxia, DNA damage, and UV radiation. It acts as a tumour suppressor by inducing apoptosis, cell cycle arrest, and DNA repair. These responses can inhibit uncontrolled cell proliferation

and prevent neoplastic transformation. Thus, p53 has been targeted as an innovative tool for anti-cancer treatment. However, numerous questions about the global regulation of p53 need to be elucidated especially its differential ability to induce cell death and survival. How to activate the apoptotic ability of p53 in tumour cells while protecting normal cells becomes the ultimate goal for medical scientists. Transactivation of p53 target genes in tumour cells appears promising for the treatment of cancer, but targeting the transcriptionally independent mechanism for activating apoptosis could be an alternative approach. In this thesis, we will focus on post-translational modifications, especially phosphorylation and subcelluar localization of p53 which may be related to its differential ability in regulating cellular responses.

1.8 Hypotheses and Aims

Hypotheses:

1. Phosphorylation of p53 at Serine 392 leads to cytoplasmic accumulation and activation of apoptosis.
2. In the absence of phosphorylation at Serine 392, p53 accumulates in the nucleus and activates cell cycle arrest genes.

Aims:

1. To construct a model that demonstrates high-level p53 expression and independently induces apoptotic and cell cycle arrest responses.
2. Using this model investigate localization of p53 following apoptotic and cell cycle arrest induction.
3. Using this model analyse expression of p53 inducible genes following apoptotic and cell cycle arrest induction.
4. Using this model study the accumulation and localisation of p53 phosphorylated at Serine 392 following apoptotic and cell cycle arrest induction.

CHAPTER Π

Material and Methods

2.1 Cell lines and culture

Human cancer cell lines A549 (lung carcinoma) and RKO (colon carcinoma) were obtained from the American Type Culture Collection (107), and both of them express wild-type p53 (108). Dulbecco's modified Eagle's medium (DMEM) supplemented with foetal calf serum (FCS 10%v/v), L-glutamine (300mM), benzylpenicillin (100U/ml) and streptomycin (100μg/ml) was used for cell culture. Cultures were incubated at 37^{o}C/10% CO_2 in a humidified environment and harvested when they reached 80%~ 90% confluence.

2.2 Reagents

Nutlin-3 (Sigma-Aldrich, Australia) was prepared by dissolving in absolute ethanol. Cisplatin aqueous solution (1mg/ml) was obtained from Mayne, Australia. Other chemicals or reagents not detailed below were purchased from Sigma-Aldrich (Australia).

2.3 Immunofluorescence

Immunofluorescence was used to detect p53 protein and phosphorylated p53 protein. Samples were viewed using an Olympus BX51 fluorescence microscope.

(i) Sample preparation

Cells were harvested when they reached 80%~ 90% confluence and cell concentration was adjusted to 2×10^5/ml. 1×10^4 cells were then seeded onto the centre of sterile 180μm glass coverslips contained in a 6-well plate (BD Biosciences,

Australia). Seeded plates were then incubated at 37°C/10% CO_2 for one and a half hours to allow cells to attach to the coverslips. A further 2ml of medium was then added and cells were incubated overnight.

(ii) Treatment

The chemotherapeutic drugs Cisplatin (1mg/ml), Doxorubicin (0.1g/L), 5-FU (10mM) and MDM-2 antagonist Nutlin-3 (1mM) were used to treat cells.

(iii) Mitochondrial staining

Mito-Tracker® probes were used to stain mitochondria in live cells. 500nM Mito-Tracker Red CMXRos (Invitrogen, Australia) was prepared in DMEM, and 1ml of the solution was applied to each coverslip. Coverslips were then incubated at 37°C/10% CO_2 for 30 minutes and washed briefly with 1× Phosphate-buffered saline (PBS) [(1)]. If mitochondrial staining is required, all the steps below should be protected from light.

(iv) Cell fixation and permeabilisation

DMEM or DMEM containing Mito-tracker was aspirated off, and coverslips were rinsed with 1×PBS. PBS was aspirated off, and cells were fixed using freshly prepared 4% paraformaldehyde solution [(2)] for 20 minutes at room temperature. Coverslips were rinsed with 1×PBS, and washed 3×10 minutes with 0.2% Triton X-100 in Tris Buffered Saline (TBS) [(3)] on an orbital mixer to allow permeabilisation.

(v) Nuclear staining

Aqueous DAPI (4',6-diamidino-2-phenylindole, dihydrochloride) solution was applied to each well at a final concentration of 300nM. Samples were protected from light, and incubated for 10 minutes at room temperature, and then washed for 3×5 minutes with 1×PBS on an orbital mixer.

(vi) Detection of p53 and p53 phosphorylated at Ser 392 (phospho-Ser392-p53)

Samples requiring p53 or phospho-Ser392-p53 detection were incubated at 37^{o}C/10% CO_2 in blocking buffer (2% FCS, 0.2% Triton X-100 in Tris Buffered Saline, freshly prepared) for 1 hour. Coverslips were removed from the 6-well plates, and excess fluid was dried from the edges of the coverslips. Cell patches were incubated with the primary mouse anti-p53 monoclonal antibody DO-1 (Oncogene Research, USA), or rabbit anti-p53 (Phospho-Ser 392) polyclonal antibody (Cayman Chemical, USA) at a 1:1000 dilution in blocking buffer for one hour at room temperature. 25µl diluted antibody solution was applied directly onto each cell patch. If double staining was required, an equal volume of each primary antibody solution was mixed and 50µl mixture applied to each cell patch.

Coverslips were returned to 6-well plates, and washed 3×10 minutes in 1×PBS to remove excess primary antibody. Coverslips were again removed from the 6-well plates, and dried. Cell patches were incubated with the secondary antibody at room temperature for 1 hour protected from light. The secondary antibody chosen for detecting p53 was Alexa Fluor® 488 goat anti-mouse IgG (Invitrogen, Australia). For phospho-Ser392-p53, Alexa Fluor® 568 goat anti-rabbit IgG (Invitrogen, Australia) was used when staining in conjunction with Alexa Fluor® 488. When double staining with Mito-Tracker Red CMXRox is required, Alexa Fluor® 488 goat anti-rabbit IgG (Invitrogen, Australia) was used instead of Alexa Fluor® 568 goat anti-rabbit IgG. The secondary antibody dilution (1:400) was prepared freshly in

1×TBS, and 25µl of the dilution was applied to each cell patch. For double staining, an equal volume of each secondary antibody solution was mixed and 50µl applied to each cell patch.

The coverslips were again returned to the 6-well plates, and washed 3×10 minutes in 1×PBS to remove excess secondary antibody.

(vii) Slides preparation and visualisation

All coverslips were mounted in the centre of glass microscope slides, using anti-fade mounting media [(4)]. Slides were sealed with nail varnish, labelled and stored protected from light at room temperature until visualised using an Olympus BX51 fluorescence microscope at the Pharmacy Research Laboratory, Curtin University of Technology. Photographic images were captured using an Olympus DP70 digital camera.

Alexa Fluor® 488 probes (excitation max: 495nm, emission max: 519nm) were visualised using a NIBA (Narrow Interference Blue A) mirror unit. Alexa Fluor® 568 probes (excitation max: 578nm, emission max: 603nm) and Mito-Tracker Red CMXRos (excitation max: 579nm, emission max: 599nm) were visualised using a WG (Wide-Green) mirror unit. DAPI-stained nuclei (excitation max: 372nm, emission max: 456nm) were visualised using a UV (wide-ultraviolet) mirror unit.

(viii) Controls for immunofluorescence

Fixed cells were stained with antibodies specific to p53 and phospho-Ser392-p53. p53 expressing slides with p53 primary antibodies and Alexa Fluor 488 secondary antibodies were used to adjust the fluorescence microscope so that no fluorescence was identified in the wide green wavelength. The left-hand image was viewed in a narrow blue wavelength and the right-hand image was viewed in a wide green

wavelength. This setting was used to view phospho-Ser392-p53 in double staining slides (***Fig 2.1***).

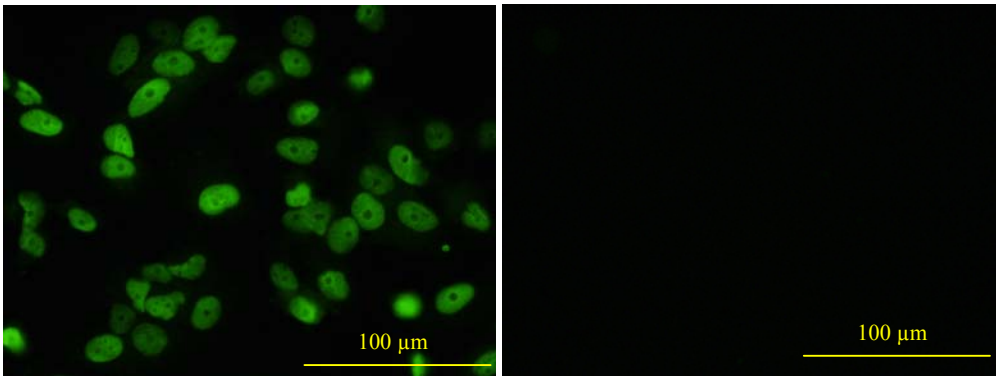

Fig 2.1: Controls for phospho-Ser392-p53 detection in wide green wavelength

A549 cells were treated with 10µg/ml Cisplatin for 24hours. Fixed cells were stained with p53 primary antibodies and corresponding Alexa Fluor 488 secondary antibodies. The left-hand image was taken using NIBA mirror unit and the right-hand image was taken using WG mirror unit.

Similarly, phospho-Ser392-p53 expressing slides containing primary antibodies and Alexa Fluor 568 secondary antibodies were used to adjust the fluorescence microscope so that no fluorescence was identified in the narrow blue wavelength. The left-hand image was viewed in a wide green wavelength and the right-hand image was viewed in a narrow blue wavelength. This setting was used to view p53 in double staining slides (***Fig 2.2***).

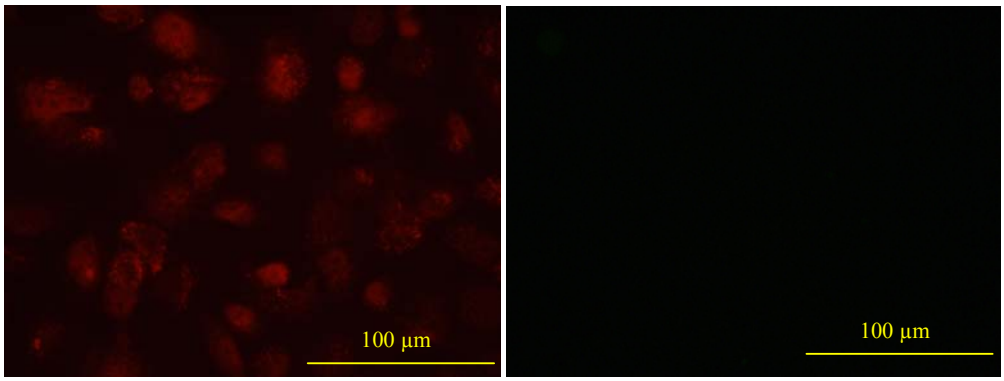

Fig 2.2: Controls for p53 detection in narrow blue wavelength

A549 cells were treated with 10µg/ml Cisplatin for 24hours. Fixed cells were stained with phospho-Ser392-p53 primary antibodies and corresponding Alexa Fluor 568 secondary antibodies. The left-hand image was taken using WG mirror unit and the right-hand image was taken using NIBA mirror unit.

In phospho-Ser392-p53 and mitochondria double staining slides, fixed cells were stained with a mitochondrial specific dye and phospho-Ser392-p53 specific antibodies. Controls with Mito-Tracker Red CMXRos staining alone were used to determine the settings of the fluorescence microscope so that no fluorescence from mito-tracker was observed in the narrow blue wavelength. The left-hand image was viewed in the wide green wavelength and the right-hand image was viewed in the narrow blue wavelength. This setting was used to view phospho-Ser392-p53 (***Fig 2.3***).

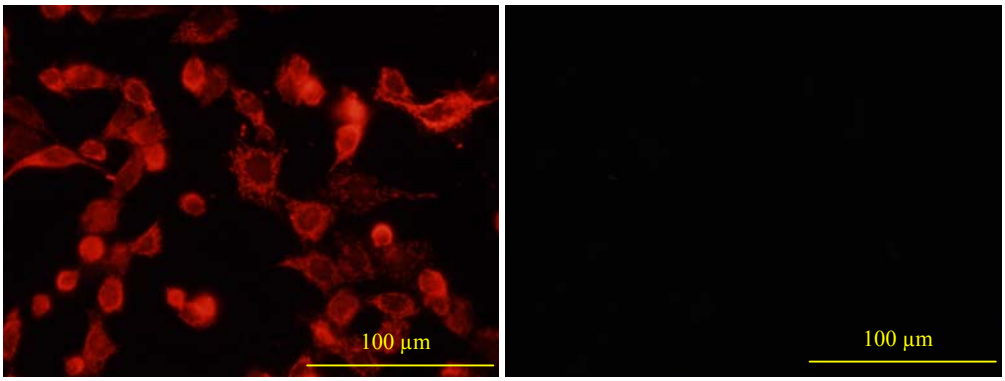

Fig 2.3：Controls for phospho-Ser392-p53 detection in narrow blue wavelength

A549 cells were treated with 10μg/ml Cisplatin for 24hours. Fixed cells were stained with Mito-Tracker Red CMXRos. The left-hand image was taken using WG mirror unit and the right-hand image was taken using NIBA mirror unit.

Controls with phoshpo-Ser392-p53 staining alone were used to determine the setting of fluorescence microscope so that no fluorescence from phospho-Ser392-p53 was observed in the wide green wavelength. The left-hand image was viewed in the narrow blue wavelength and the right-hand image was viewed in the wide green wavelength. This setting was used to view mitochondrial staining (***Fig 2.4***).

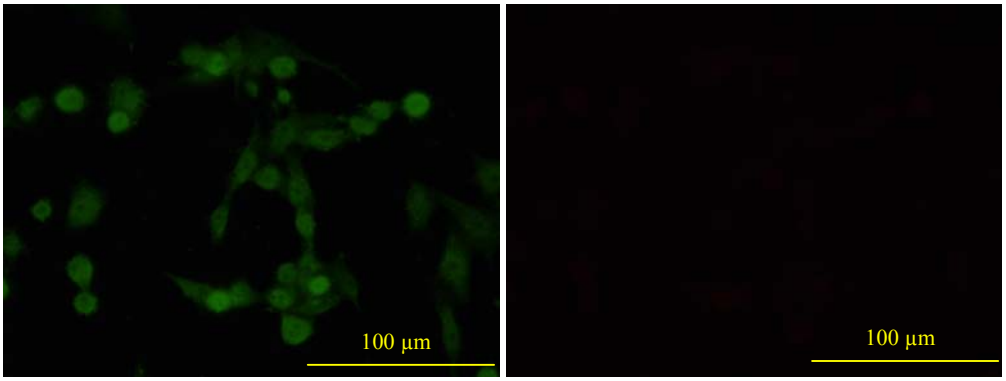

Fig 2.4: Controls for mitochondria detection in wide green wavelength

A549 cells were treated with 10μg/ml Cisplatin for 24hours. Fixed cells were stained with phospho-Ser392-p53 primary antibodies and corresponding Alexa Fluor 488 secondary antibodies. The left-hand image was taken using NIBA mirror unit and the right-hand image was taken using WG mirror unit.

2.4 Trypan blue cell-death assay

Trypan Blue is a dye that is used to determine the viability of a cell. Living cells exclude the dye, whereas dead cells will take up the blue dye. The blue stain is easily visible, and cells can be counted using a light microscope.

Cells were seeded into 6-well tissue culture plates at a density of $1\sim2\times10^5$/well, and were incubated overnight at 37^oC/10% CO_2. Treatments were added to each well at the desired concentration. Plates were again incubated for 24 hours, 48 hours and 72 hours.

The medium containing dead and floating cells was transferred into a 15ml tube. The well was rinsed with 1×PBS and the PBS was also transferred to the same tube. Cells were harvested using trypsin-EDTA (JRH Biosciences, Australia), resuspended in 1ml medium, and transferred into the same tube. Harvested cells were centrifuged at 400g for 10 minutes, supernatant was removed, and the cell pellet was resuspended in 0.5ml medium. 20μl of sample suspension was added to 20μl 0.5% trypan blue dye, and mixed thoroughly. The stained cell suspension was transferred to a

haemocytometer for counting. Data was collected in terms of viable and dead (stained) cells counted per sample.

2.5 Fluorescence-activated cell sorting analysis

(i) Sample preparation

Cell-cycle arrest and apoptosis were investigated using flow cytometry (BD FACSCanto^{TM} II, excitation max: 488nm, emission max: 585nm). Cells were grown in 6-well plates until they reached 90%~ 100% confluences. Samples were then treated with Nutlin-3 or Cisplatin and incubated for the required time at 37^{o}C/10% CO_2.

Cells were harvested and centrifuged at 400g for 10 minutes. The supernatant was then discarded, and the cell pellet was resuspended in 2ml of sample buffer (0.1% w/v glucose in 1×PBS, Ca^{2+} and Mg^{2+} free, filtered at 0.22μm and stored at 4^{o}C). The supernatant was discarded and this step was repeated. The cell suspension was adjusted to produce a cell density of 1×10^{6} cells/ml in sample buffer. 1ml of this solution was centrifuged at 400g for 10 minutes. The supernatant was then carefully removed, leaving about 100μl of residual solution. The samples were then agitated through a vortex to produce a slurry, and 1ml of ice-cold ethanol (70%) was gradually added into each tube. Tubes were capped, and stored at 4^{o}C to fix overnight.

(ii) Nucleic acid staining

Propidium iodide (PI-Sigma, Australia, excitation max: 536nm, emission max: 617nm) stock solution was prepared as a 0.1%w/v solution in sterile Milli-Q water (filtered at 0.22μm and store at 4^{o}C, protected from light). A propidium iodide

staining solution was then freshly prepared by adding 0.5ml PI stock solution, 21mg of RNase A (Promega) and made up to 10ml with sample buffer.

Samples were briefly re-agitated with a vortex, and centrifuged at 4000g for 10 minutes. The supernatant was removed, and cells were resuspended in residual solution to produce a slurry using a vortex. 1ml of PI staining solution was added to each sample and mixed thoroughly with a vortex. Samples were then incubated for at least 30 minutes before analysing by flow cytometry.

2.6 Reverse transcription polymerase chain reaction (RT-PCR)

RT-PCR was used to determine target gene expression. Cells were seeded in a 6-well plate, and were exposed to 10μg/ml Cisplatin and 10μM Nutlin-3 when they reached 70%~ 80% confluence. The plates were incubated for 4 hours, 6 hours and 8 hours.

(i) RNA extraction

Total RNA was extracted from cells using Ultraspec^{TM} RNA reagent (Biotecx, USA). Medium was removed from 6-well plate, and 300μl of Ultraspec^{TM} RNA reagent was added to each well. After passing the lysate several times through a pipette, it was transferred to a 1.5ml microcentrifuge tube and rested on ice for 10 minutes for dissociation of nucleoprotein complexes. RNA extraction was performed by adding 0.2ml of chloroform to the lysate, and the mixture was shaken vigorously and placed on ice for 5 minutes. The mixture was centrifuged at 11000g for 15 minutes and the aqueous layer containing RNA was removed to a new 1.5ml microcentrifuge tube. An equal volume of isopropyl alcohol was added to the aqueous layer to precipitate RNA, and the sample was agitated using a vortex and returned to ice for 10 minutes. The sample was then centrifuged for 10 minutes at 11000g, the supernatant was removed, and the residual pellet was washed twice with 75% ethanol. After centrifugation for 5 minutes at 4000g, ethanol was removed and

the residual ethanol was evaporated in air. The RNA pellet was resuspended in 20µl of 1mM sodium citrate buffer and samples were stored at -80 ^{o}C until required.

Solutions were analysed by spectrophotometry to quantify the amount of RNA in each sample. The concentration of RNA was calculated by preparing 1:60 dilution with RNase-free water, and measuring the sample at 260nm using a Shimadzu UV-Vis 1240 spectrophotometer.

(ii) DNase treatment

RNA samples were treated with DNase enzymes to exclude genomic DNA contamination. 5µl of RQ1 RNase-free DNase (Promega) was added to tubes containing 5~10µg of sample RNA and 2µl of 10× reaction buffer. RNase-free water was added to adjust the volume to 20µl. Samples were incubated at 37^{o}C for 30 minutes, followed by the addition of 2µl of RQ1 DNase Stop solution (Promega). Samples were incubated at 65 ^{o}C for 10 minutes and then incubated on ice for 1 minute. Samples were centrifuged briefly and kept on ice for the reverse transcription reaction.

(iii) Reverse transcription

To transcribe RNA into cDNA, the following reagents were used to prepare a 20µl reaction:

4µl	$MgCl_2$ (25mM)
2µl	Reverse Transcription 10×Buffer
2µl	dNTP Mixture (5mM)
0.5µl	RNAse inhibitor
1µl	AMV Reverse Transcriptase (10units/µl)
1µl	Random Primers (0.5µg/ µl)
2~4µl (1µg)	Sample RNA
7.5~5.5µl	Nuclease-Free Water

The mixture was incubated at room temperature for 10 minutes to allow primer extension, and then incubated at 42°C for 30 minutes to allow cDNA synthesis. The samples were heated at 99°C for 5 minutes, and then incubated at 4°C for 5 minutes to inactivate the reverse transcriptase. This reaction was performed using the PTC-100 thermal cycler (MJ Research, USA)

The human *CDKN1A* (*P21*$^{WAF1/CIP1}$), *GADD45A, BAX*, *G3PDH, BIK, BIM, NOXA* gene sequence was obtained from the Genbank online genetic-sequence database (http://www.ncbi.nlm.nih.gov/) and Primer 3 software was used to design forward and reverse gene-specific primers that bind to corresponding cDNA sequences, as follows:

Gene Name	Genbank Accession Number	Primer Sequence (5'-3')
CDKN1A	NM_000389	F: GAGCGATGGAACTTCGACTT
		R: CAGGTCCACATGGTCTTCCT
GADD45A	EF614238	F: ACGAGGACGACGACAGAGAGAT
		R: GCAGGATCCTTCCATTGAGA
BAX	NM_004324	F: TTTGCTTCAGGGTTTCATCC
		R: CAGTTGAAGTTGCCGTCAGA
G3PDH	NM_002046	F: ACCACAGTCCATGCCATCAC
		R: TCCACCACCCTGTTGCTGTA
BIK	NM_001197	F: ACCTGGACCCTATGGAGGAC
		R: GGTGAAACCGTCCATGAAAC
BIM	AY351528	F: AGATCCCCGCTTTTCATCTT
		R: TCTTGGGCGATCCATATCTC
NOXA	NM_021127	F: AAGAAGGCGCGCAAGAAC
		R: TCCTGAGCAGAAGAGTTTGGA

(iv) Polymerase chain reaction

PCR was used to investigate target gene expression. The following reagents were used to create a standard 25µl reaction:

17.32µl	H_2O
2.5µl	10×Buffer
2µl	$MgCl_2$ (25mM)
1µl	dNTP (5mM)
1µl	Primer mix (5 µM each)
0.18µl	Taq (units/µl)
1µl	cDNA

To increase the accuracy, a 'master-mix' solution of the above ingredients without cDNA was prepared. 1µl of cDNA was then added to each tube containing 24µl of the mixture.

Basic cycling program for RT-PCR was performed as below:

Denaturation:	95 ^{o}C for 3 minutes
Cycling:	95 ^{o}C for 20s
	55 ^{o}C for 20s
	72 ^{o}C for 60s
	×40 Cycles
Extension:	72 ^{o}C for 5 minutes
Hold:	10 ^{o}C

The amplified products were analysed on a 2% agarose gel by electrophoresis. 10µl of amplified product was mixed with 2µl of 6×loading buffer and loaded onto an agarose gel in 1×TAE buffer (40mM Tris-acetate, 1mM EDTA). A 100bp molecular

weight marker was included on the gel. The gel was electrophoresed at 80V for 45 minutes and stained with SYBR® Safe (Invitrogen) diluted 1:10000 in 1×TAE buffer. The gel was placed under UV light and photographed using Kodak EDAS 120 digital camera.

2.7 Real-time polymerase chain reaction (Real-Time PCR)

Real-Time PCR was used to investigate target gene expression in a quantitative way. A RotorGene 2000 real-time amplification instrument (Corbett Research, Australia) and an EvaGreen detection protocol were used to perform this experiment. The final 10µl reaction was composed of 1µl cDNA, the final concentration of 0.2µM dNTP, 5U/µl Taq thermostable DNA polymerase, 1×DNA polymerase buffer, 1:20,000 EvaGreen dye (Biotium, USA) and optimal concentration of $MgCl_2$ and primer. The final volume was adjusted to 10µl using DNase-free water. To increase the accuracy of preparing the 10µl reaction, a large "master-mix" stock solution of the above ingredients (excluding the cDNA samples) was prepared. 2.5µl of cDNA was added to 22.5µl of the "master-mix" in a 0.6ml PCR tube (Axygen, USA) to create 25µl of complete real-time PCR reaction mixture. From this, duplicate 10µl samples were dispensed into 0.1ml tubes compatible with the RotorGene 2000 amplification instrument (Corbett Research, Australia).

Typical cycling conditions for real-time PCR experiments are as follows:

Denaturation:	95 ^{o}C for 5 minutes
Denaturation:	95 ^{o}C for 20s
Annealing of primers:	55 ^{o}C for 20s
Extension and fluorescence acquisition:	72 ^{o}C for 45s
Extension and fluorescence acquisition:	Optimised temperature for 20s
	×45 Cycles
Final extension:	72 ^{o}C for 60s

Standard curves for each gene analysed were performed to indicate the efficiency of the amplification process. Ten-fold serial dilutions of cDNA standards were prepared and processed using the real-time PCR protocol. The concentration of each standard was assigned as 1,000, 100, 10, 1 and 0. For genes that have relatively low expression, a standard assigned as 1,000, 200, 40, 8, 1.6 and 0 was created. The concentration of each sample was calculated based upon the standard curves.

Melt curve analyses were used to measure the melting point of the product, and melting point discrepancies between samples indicated contamination, inappropriate optimisation or the presence of primer-dimer artefacts.

(i) Optimisation of Mg^{2+} and primer concentrations

The concentration of Mg^{2+} and primer were essential for the efficiency of the amplification. Optimisation of Mg^{2+} and primer concentration was performed for each gene. A series of reactions containing 2~7 mM Mg^{2+} or 0.1~1.0μM were processed in duplicate according to the real-time PCR protocol. The quantitation and melt curves were analysed to determine which concentration of Mg^{2+} and primers could yield the best efficiency of amplification and a specific melt curve. Optimised primer concentration, $MgCl_2$ concentration and data acquisition temperature determined are as follows:

Gene	$MgCl_2$ Concentration	Primer Concentration	Acquisition Temperature
P21	4mM	0.5μM	92 ^oC
NOXA	4mM	0.5μM	88 ^oC

(ii) Housekeeping genes

Housekeeping genes should be expressed at similar level in all cells, but this can vary due to different treatments. To choose the most stable housekeeping genes, several

common genes including *G3PDH*, *18S*, *HPRT1*, *UBC* were analysed and the most stable ones were found to be *18S*, *HPRT1*, *UBC*:

Gene	Genebank Accession Number	Primer Sequences (5'~3')
18S	K03432	F:GTAACCCGTTGAACCCCATT
		R:CCATCCAATCGGTAGTAGCG
HPRT1	NM_000194	F:TGACACTGGCAAAACAATGCA
		R:GGTCCTTTTCACCAGCAAGCT
UBC	NM_021009	F:ATTTGGGTCGCGGTTCTTG
		R:TGCCTTGACATTCTCGATGGT

2.8 Western blotting

Western Blotting was used to investigate the level of proteins. Cells were seeded in 6-well plates and incubated at 37^{o}C/10% CO_2. Cells were treated when they reached 90% confluence.

(i) Protein extraction

Total protein was extracted using RadioImmunoPrecipitation Assay Buffer (RIPA buffer) [(5)]. 0.3ml of ice-cold RIPA buffer with protease inhibitor was applied to each well. The plates were placed on a rocker at 4^{o}C for 1 hour. The lysate was then transferred into Eppendorf tubes, and disrupted by pipetting vigorously. Tubes were centrifuged at 11000g at 4^{o}C for 30 minutes. The supernatant was then transferred into a new tube and stored at -80^{o}C.

(ii) Protein quantitation

Protein Quntitation was performed using a BCA protein Assay kit (Pierce, USA). Complying with manufacturer's instructions, the following steps were performed:
Diluted Albumin standards were prepared at the following concentrations:

2000µg/ml, 1500µg/ml, 1000µg/ml, 750µg/ml, 500µg/ml, 250µg/ml, 125µg/ml 25µg/ml and 0µg/ml.

A Working Reagent (WR) was freshly prepared by mixing 50 parts of BCA Reagent A with 1 part of BCA Reagent B.

25µl of each standard or unknown sample was added into its own microplate well and 200µl of the WR was added to each well and mixed thoroughly. The plate was incubated at 37^{o}C/10% CO_2 for 30 minutes and the absorbance was measured at 595nm using a Bio-Rad Model 3550 microplate reader.

(iii) Sodium dodecyl sulfate polyacrylamide gel electrophoresis (SDS-PAGE)

Protein loading was normalised for each sample, usually 10~20µg/well. Each sample was mixed with an equal volume of sample buffer [(6)], and heated at 100^{o}C for 5 minutes. Samples were loaded into each well of a pre-cast polyacrylamide electrophoresisGels (NuSep, Australia) in a tank filled with 1×Running buffer [(7)]. A MW marker was loaded at the same time. The SDS-PAGE gel was run at 150V for 90 minutes.

(iv) Protein blot

Gels, Immobilon P membrane (Millipore, USA), filter papers, and pads were laid down on a graphite plate in the following order:

Pad, filter paper, membrane, gel, filter paper and pad. The bubbles between filter papers and membrane and gels were removed. The graphite plate was locked and the 'Sandwich' was then put in a tank filled with ice-cold 1×Transfer buffer [(8)]. The setting for transfer was 90V for 75 minutes. To confirm transfer, the membrane was stained with 0.1% Ponceau S in 5% acetic acid and destained with Milli-Q water. The membrane was blocked in blocking buffer (5%w/v Albumin from bovine serum in TBST [(9)]) for 1 hour in room temperature.

(v) Protein detection

Mouse anti-p53 monoclonal antibody DO-1 for detecting p53 was diluted 1:1000 in blocking buffer. 10ml of diluted primary antibody was applied to each membrane. Mouse anti-β-actin monoclonal antibody was diluted 1:5000 and 10ml of the diluted solution was applied to each membrane. Membranes were incubated with the primary antibodies at $4^{o}C$ overnight and washed for 3×10min in TBST at room temperature before adding secondary antibody. Alkaline Phosphatase Conjugated anti-mouse (Chemicon, Australia) antibody was diluted 1:2000 in TBST. 10ml of diluted secondary antibodies was applied to each membrane. Membranes were incubated with secondary antibody at room temperature for 30 minutes. Membranes were then washed for 3×10min in TBST in room temperature before adding BCIP/NBT Alkaline Phosphatase Substrate Solution for colour development. 30µl 50mg/ml 5-Bromo-4-chloro-3-indolyl phosphate (BCIP) and 60µl 50mg/ml Nitro blue tetrazolium (NBT) were mixed in 10ml alkaline phosphatase (AP) buffer. The 10ml solution was then applied to each membrane.

After colour developed to the desired level, membranes were rinsed with Milli-Q water and dried between two sheets of filter paper.

2.9 Commonly used buffers

(1) 10×Phosphate-buffered saline (PBS):

80g NaCl

2g KCl

14.4g Na_2HPO_4

2.4g KH_2PO_4

Add 800ml Milli-Q water

Adjust pH value to 7.2~7.4

Add Milli-Q water to 1000ml

(2) 4% paraformaldehyde (10ml):

0.4g paraformaldehyde was added in 8ml Milli-Q water. 5µl 1mM NaOH was added to help paraformaldehyde dissolve. The solution was then kept in 60 ^{o}C oven for 1 hour to let the paraformaldehyde dissolve completely. The total volume was adjusted to 10ml using filtered 1×PBS. The pH should be 7.8~8.0.

Note: The solution can only last for 4 days in 4 ^{o}C fridge.

(3) 1×Tris Buffered Saline (TBS):

8g NaCl

0.2g KCl

3g Tris Base

Adjust pH value to 7.2~7.4

Add Milli-Q water to 1000ml

(4) Anti-fade mounting media:

1M Trizma Base was titrated with 1M $NaH_2PO_4.H_2O$ dropwise to make up the Tris-PO_4 Buffer. 5ml Tris-PO_4 Buffer was mixed up with 75 ml Milli-Q water in Ehrlinmeyer flask. 20g polyvinyl alcohol was added to the solution. The flask was incubated in 60 ^{o}C Oven with a lid on for about 4 to 5 hours to let the polyvinyl alcohol dissolve. 30ml of glycerol and 100mg chlorobutanol was then added to the solution. The anti-fade mounting media was stored at -20^{o}C and the working aliquot was at 4^{o}C.

(5) RadioImmunoPrecipitation Assay Buffer (RIPA Buffer):

5ml of 1M Tris pH 8: 6.057g in 50ml Milli-Q water

3ml of 5M NaCl: 14.610g in 50ml Milli-Q water

Triton X-100: 1ml

5ml of 10% Na Deoxycholate: 5g in 50ml Milli-Q water

1ml of 10%SDS: 5g in 50ml Milli-Q water

Milli-Q H_2O: 85ml

Take 10ml when using, and add 1 tablet of protease inhibitor. Keep the solution on ice.

(6) Sample Buffer:

10ml of 0.5M Tris pH 6.8: 3.0285g in 50ml Milli-Q water

16ml of 10% SDS

2ml of 0.1% bromophenol blue: 0.05g in 50 ml Milli-Q water

8ml of glycerol

2ml of Milli-Q H_2O

beta-mercaptoethanol is added at a ratio of 1:19 to the total volume of sample buffer.

(7)10×Running Buffer:

Tris Base 29g

Glycine 144g

SDS 10g

Milli-Q H_2O to 1000ml

Using 1×running buffer

(8)10×Transfer Buffer:

Tris Base 15.15g

Glycine 72g

Milli-Q H_2O to 500ml

1×Transfer Buffer: 100ml 10×Transfer Buffer + 200ml methanol +700ml Milli-Q water

(9) TBST:

50µl Tween-20 in 100ml TBS

CHAPTER III

Identifying a model of p53 accumulation

3.1 Accumulation of p53 in response to various anti-cancer drugs

Cisplatin, Doxorubicin and 5-FU are reported to induce p53 responses by causing DNA damage (reviewed in Chapter I, 1.4) and Nutlin-3 is an experimental compound binding to MDM-2 and inhibiting its interaction with p53. To identify whether p53 expression was increased following treatment with these common anti-cancer drugs and Nutlin-3, we treated the cells with 10μg/ml Cisplatin (109), 1μM Doxorubicin (62), 10μM Nutlin-3 (109), and 50μM 5-fluorouracil (109) respectively for 24 hours. A549 and RKO cells were chosen because they are commonly used human cell lines which both express wt-p53. Western blotting was used to investigate the level of p53 proteins. Ethanol was used as a control to indicate the level of p53 in untreated cells.

As we can see from the results (***Fig 3.1***), although the sensitivity to the drugs varied between cell lines, all drugs resulted in increased p53 expression. While Cisplatin appeared to induce maximal p53 expression in A549 cells, Doxorubicin induced maximal p53 expression in RKO cells. Unfortunately, Doxorubicin is a fluorescent compound thus making it unsuitable for immunofluorescence which we intended to use in the future experiment. Therefore, we chose Cisplatin as a suitable inducer for p53 accumulation. Because Nutlin-3 had an entirely different mechanism of action to the other chemotherapeutical drugs, we also chose to investigate how p53 accumulates in response to this agent.

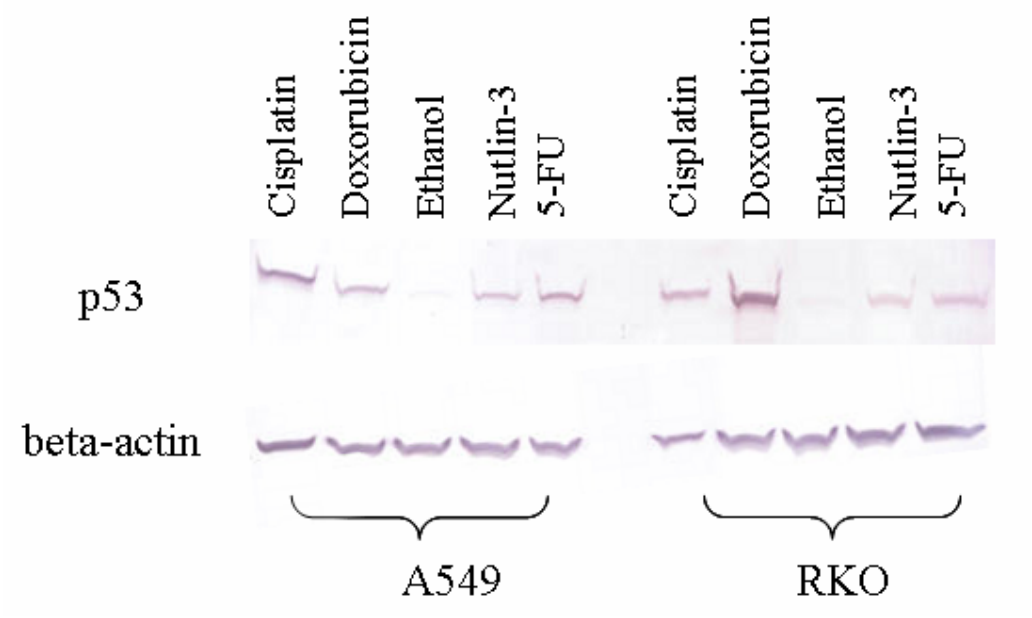

Fig 3.1: Accumulation of p53 is induced by various anti-cancer drugs
A549 and RKO cell lines were treated with Nutlin-3, Cisplatin, Doxorubicin and 5-fluorouracil. Ethanol (the solvent of Nutlin-3) was used as a control. β-actin was used as a loading control.

3.2 Optimal dosage required for maximal p53 accumulation

To identify the optimal dosage for maximal p53 accumulation, we treated A549 and RKO cells with a range of doses of Cisplatin and Nutlin-3 for 24 hours.

To identify p53 accumulation, we used immunofluorescent microscopy and a primary antibody directed against p53 proteins (DO-1). This primary antibody was detected by a fluorescently tagged secondary antibody (Alexa Fluor® 488).

A549 and RKO cells were treated with a range of doses of Cisplatin (0μg/ml, 1μg/ml, 2μg/ml, 5μg/ml, 10μg/ml, 20μg/ml) and Nutlin-3 (0μM, 1μM, 2μM, 5μM, 10μM, 20μM) and levels of p53 protein were identified by immunofluorescence 24 hours later (***Fig 3.2-Fig 3.5***).

From the images below, maximal p53 staining was shown in A549 and RKO cells treated with 10µg/ml Cisplatin. In A549 cells, the fluorescent intensity in the sample treated with 20µg/ml Cisplatin fell down slightly while there was no further increase in intensity in RKO cells treated with 20µg/ml Cisplatin. In Nutlin-treated samples, maximal p53 staining was reached at 10µM and no further increase in intensity was evident at 20µM. In both cell lines, a decrease in cell numbers was observed following 20µg/ml Cisplatin due to the cell death associated with this treatment.

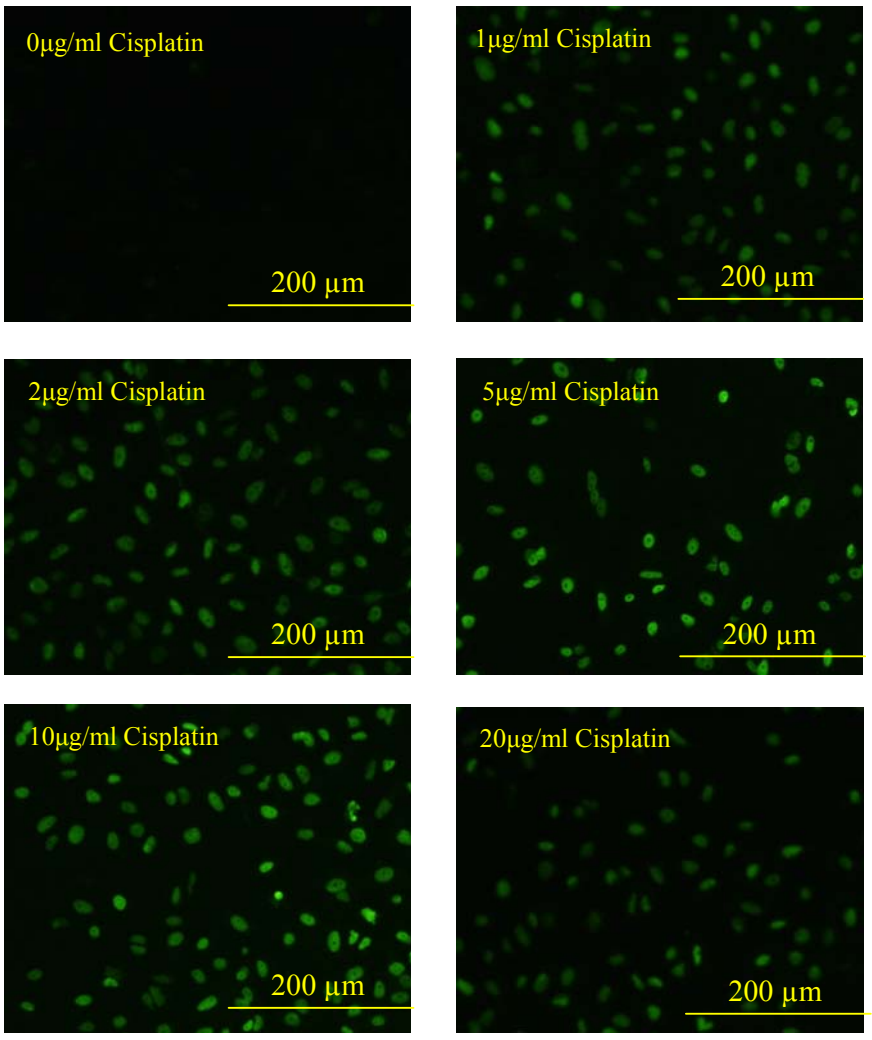

Fig 3.2: Optimising Cisplatin dosage for maximal p53 accumulation in A549 cells

A549 cells were treated with various dosages of Cisplatin. Immunofluorescence was performed after 24 hours treatment. Images were viewed under NIBA mirror unit at 100×magnification.

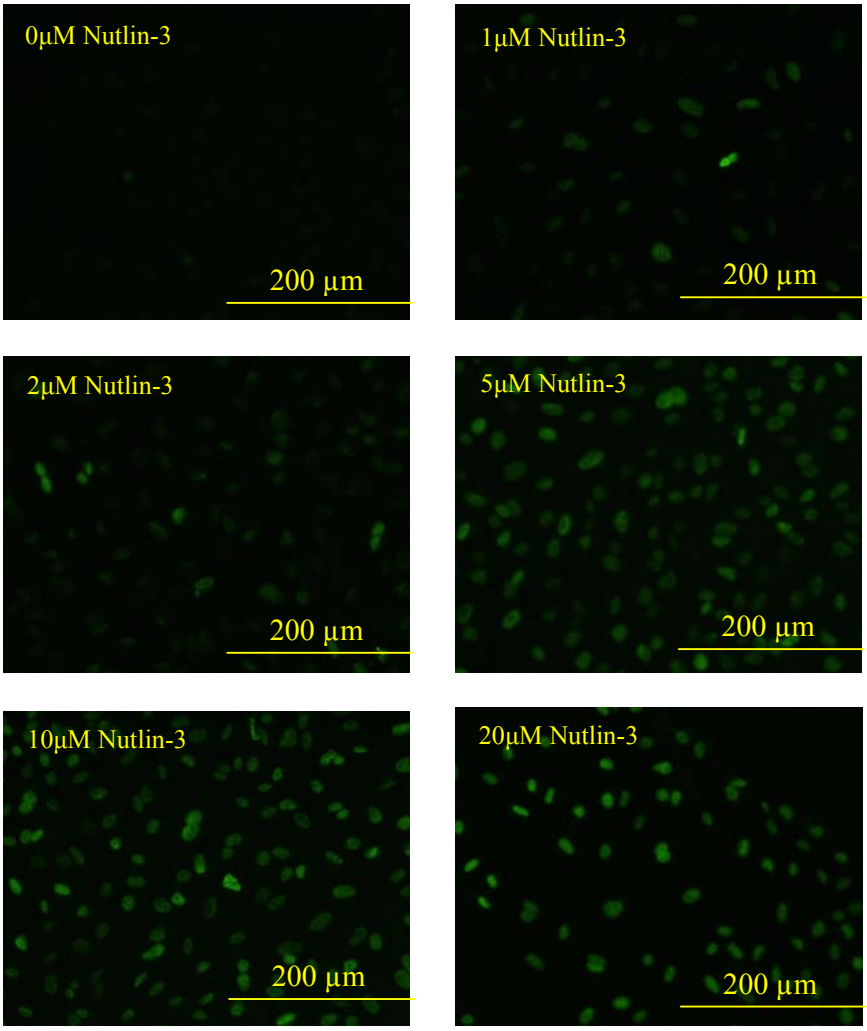

Fig 3.3: Optimising Nutlin-3 dosage for maximal p53 accumulation in A549 cells

A549 cells were treated with various dosages of Nutlin-3. Immunofluorescence was performed after 24 hours treatment. Images were viewed under NIBA mirror unit at 100×magnification.

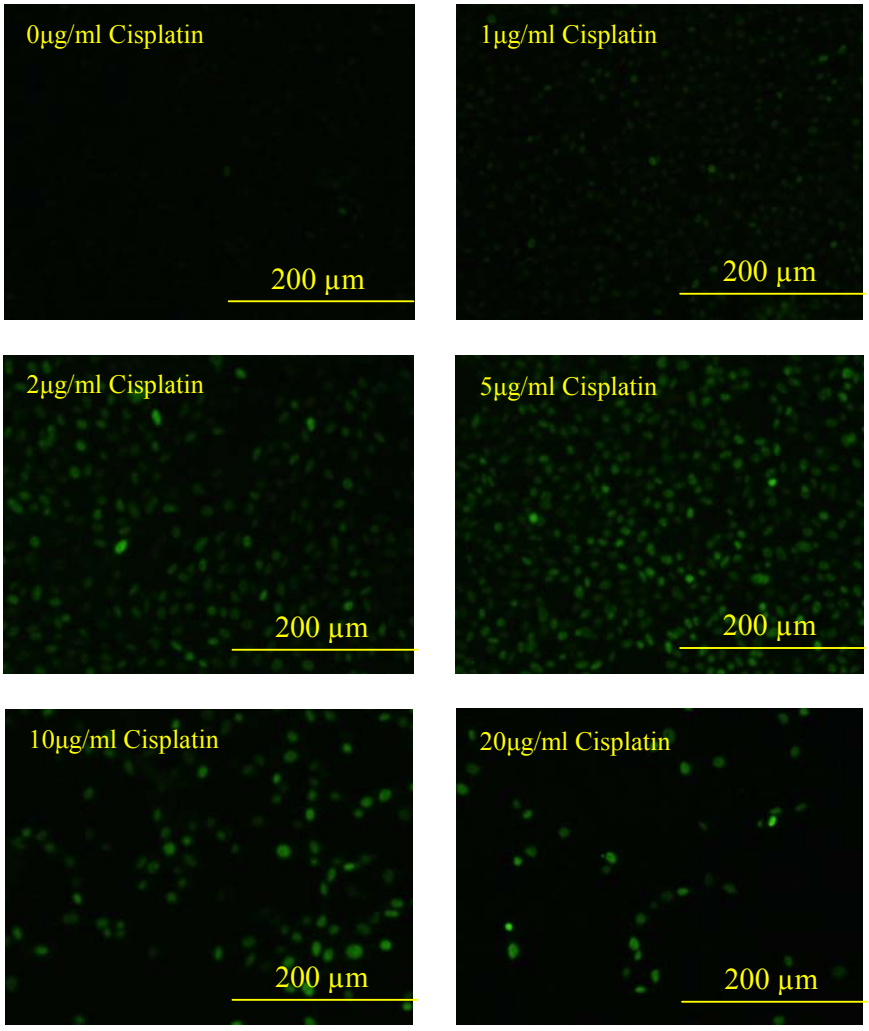

Fig 3.4: Optimising Cisplatin dosage for maximal p53 accumulation in RKO cells

RKO cells were treated with various dosages of Cisplatin. Immunofluorescence was performed after 24 hours treatment. Images were viewed under NIBA mirror unit at 100×magnification.

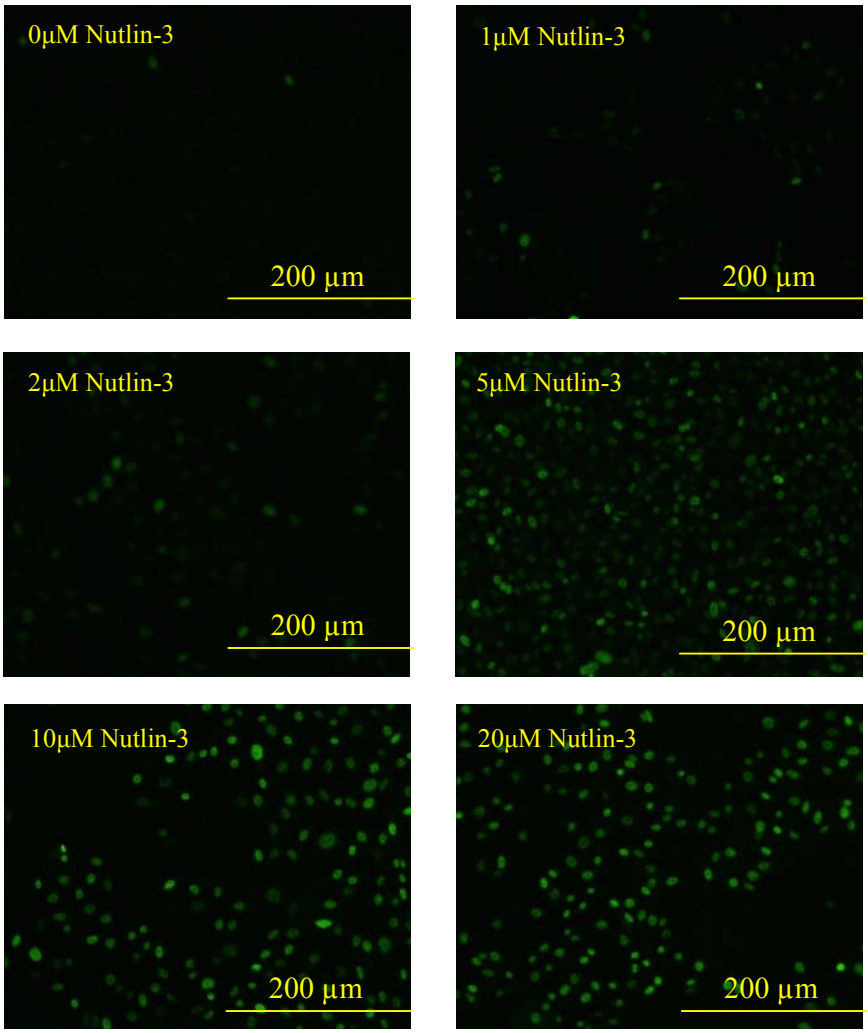

Fig 3.5: Optimising Nutlin-3 dosage for maximal p53 accumulation in RKO cells

RKO cells were treated with various dosages of Nutlin-3. Immunofluorescence was performed after 24 hours treatment. Images were viewed under NIBA mirror unit at 100×magnification.

3.3 Optimal time required for maximal p53 accumulation

To identify the optimal time for maximal p53 accumulation, A549 and RKO cells were treated with 10ug/ml Cisplatin and 10uM Nutlin-3 and levels of p53 protein were identified by immunofluorescence at 0, 2, 4 , 8 , 12 , 16, 20 , and 24 hours after treatment. From the images shown below (***Fig 3.6-Fig 3.9***), maximal p53 staining was reached between 12 hours and 24 hours in both cell lines following either Cisplatin or Nutlin-3 treatment. A general observation was that at the latter time point, cell number was decreased due to cell death associated with Cisplatin

treatment. However, this was not the case in Nutlin-treated samples. For the purposes of this experiment we chose 24 hours as demonstrating maximal p53 accumulation.

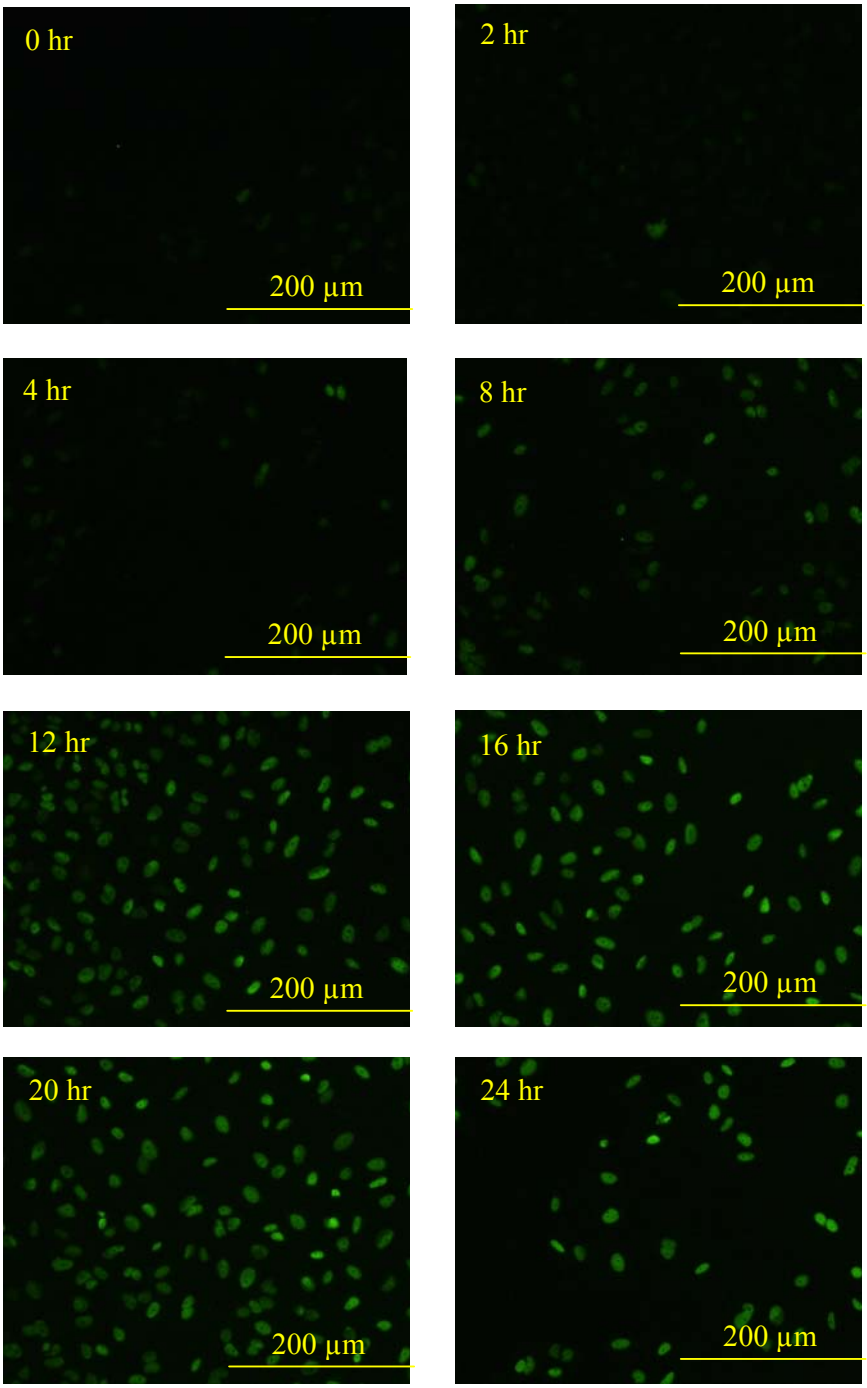

Fig 3.6: Identifying optimal time for maximal p53 accumulation following Cisplatin treatment of A549 cells

A549 cells were treated with 10µg/ml Cisplatin. Immunofluorescence was performed after 0, 2, 4, 8, 12, 16, 20, 24 hours post-treatment. Images were taken under NIBA mirror unit at 100×magnification.

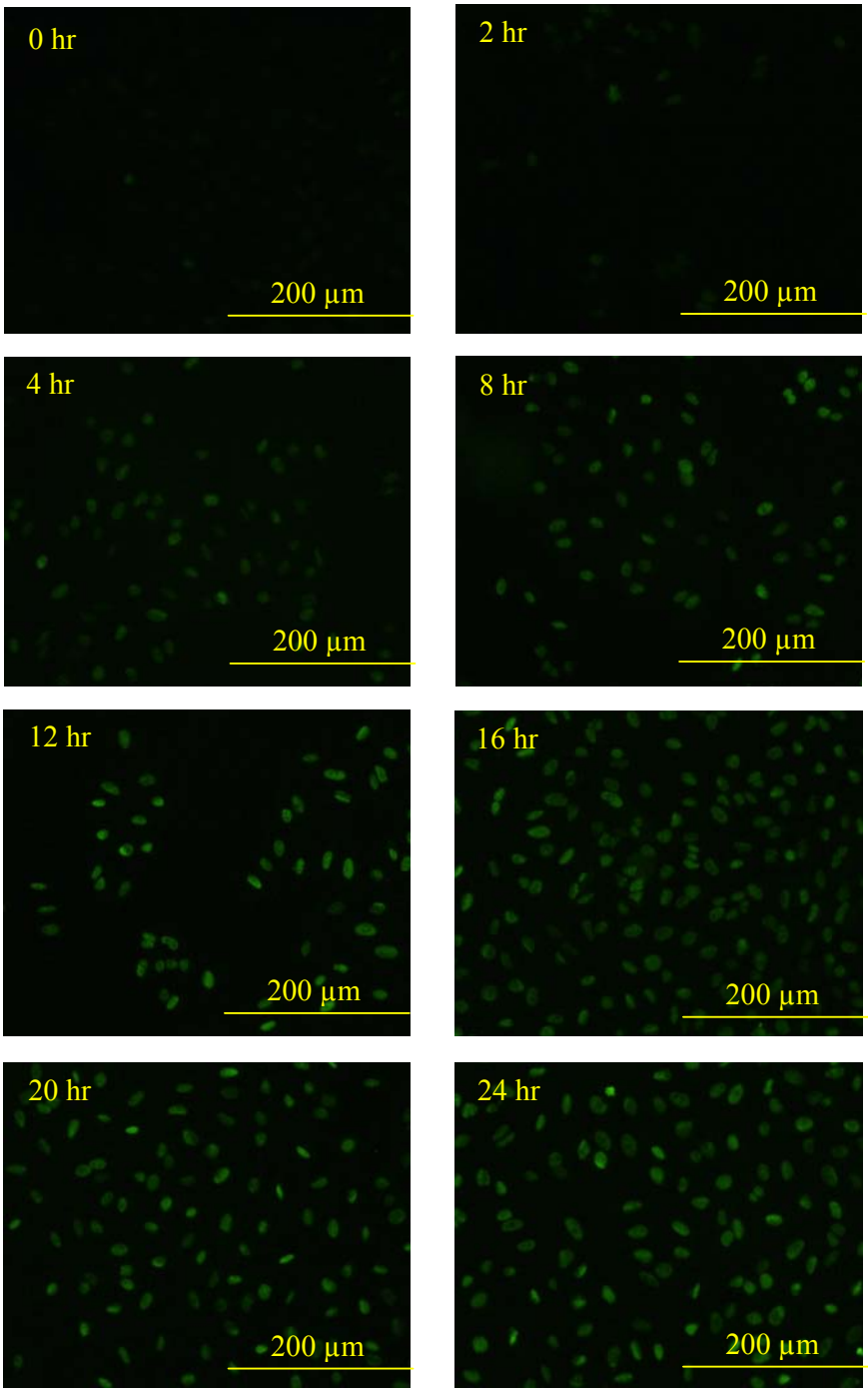

Fig 3.7: Identifying optimal time for maximal p53 accumulation following Nutlin-3 treatment of A549 cells

A549 cells were treated with 10µM Nutlin-3. Immunofluorescence was performed after 0, 2, 4, 8, 12, 16, 20, 24 hours post-treatment. Images were taken under NIBA mirror unit at 100×magnification.

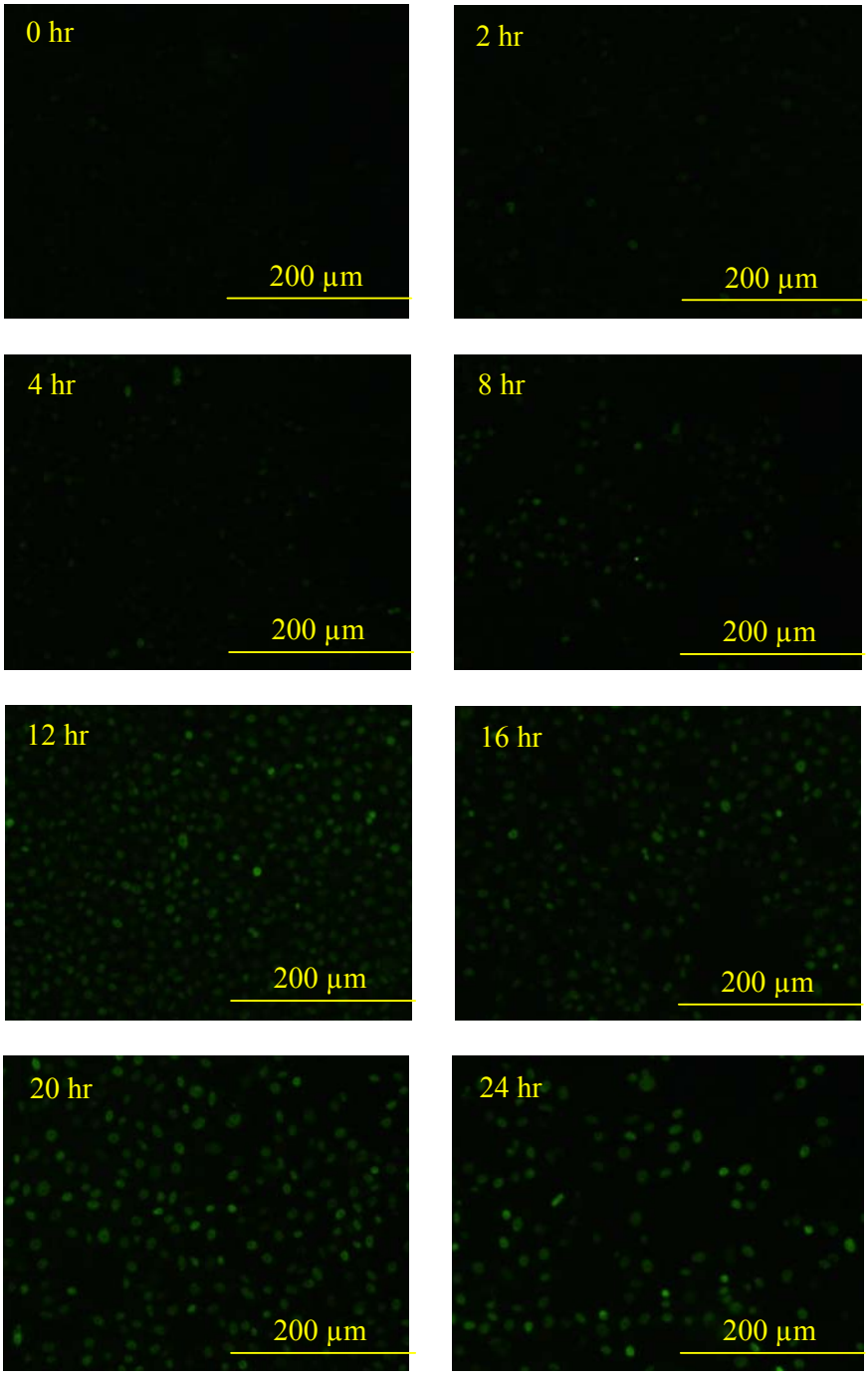

Fig 3.8: Identifying optimal time for maximal p53 accumulation following Cisplatin treatment of RKO cells

RKO cells were treated with 10µg/ml Cisplatin. Immunofluorescence was performed after 0, 2, 4, 8, 12, 16, 20, 24 hours post-treatment. Images were taken under NIBA mirror unit at 100×magnification.

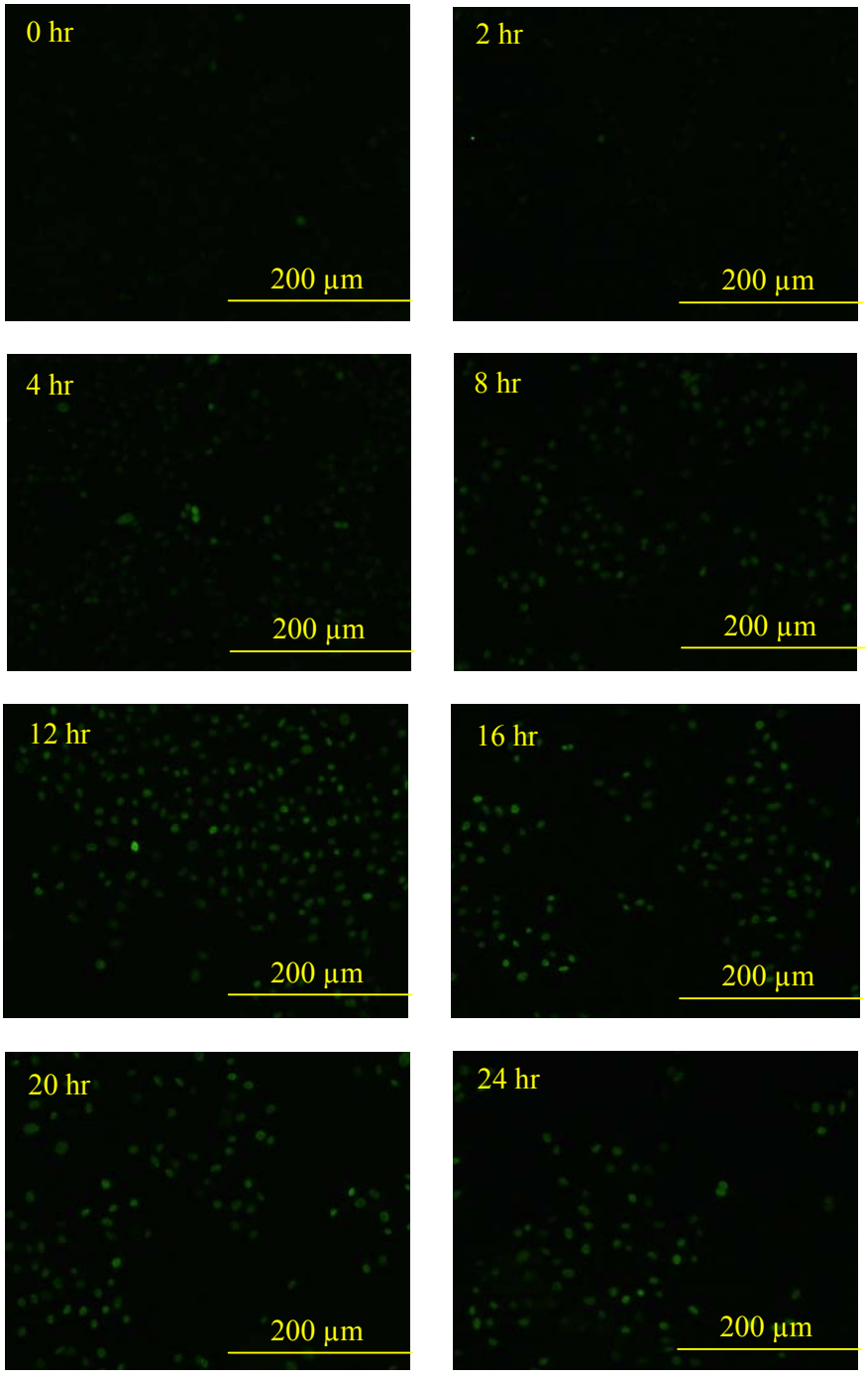

Fig 3.9: Identifying optimal time for maximal p53 accumulation following Nutlin-3 treatment of RKO cells

RKO cells were treated with 10µM Nutlin-3. Immunofluorescence was performed after 0, 2, 4, 8, 12, 16, 20, 24 hours post-treatment. Images were taken under NIBA mirror unit at 100×magnification.

3.4 Localisation of accumulated p53

As demonstrated in 3.2 and 3.3, maximal p53 expression was observed in A549 and RKO cells following treatment with 10µg/ml Cisplatin and 10µM Nutlin-3 after 24 hours. To investigate where p53 protein is located in the cell, bright field images were taken and compared to those taken via fluorescent filter. The two images were overlaid to identify the localization of p53. Slides were prepared following 24hr of 10µg/ml Cisplatin treatment and 10µM Nutlin-3 treatment. An identical volume of the drug solvent Ethanol was added to A549 cells as a control for normal p53 levels (***Fig 3.10***). As demonstrated in these images, p53 protein levels were very low under normal condition, but when cells were exposed to Cisplatin and Nutlin-3, p53 protein levels increased dramatically and were mainly located in the nucleus as would be expected of a transcription factor. Additionally, almost no p53 was observed in the cytoplasm in both Cisplatin and Nutlin-3 treated samples (***Fig 3.11-Fig 3.14***).

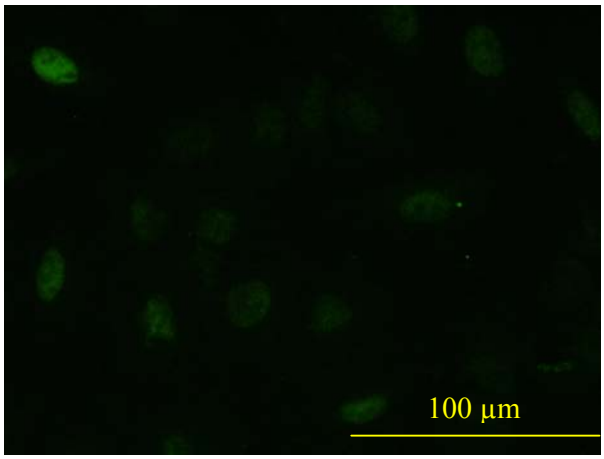

Fig 3.10: p53 level under normal circumstances
A549 cells were treated with Ethanol for 24 hours. Immunofluorescence images were taken under NIBA mirror unit at 400×magnification.

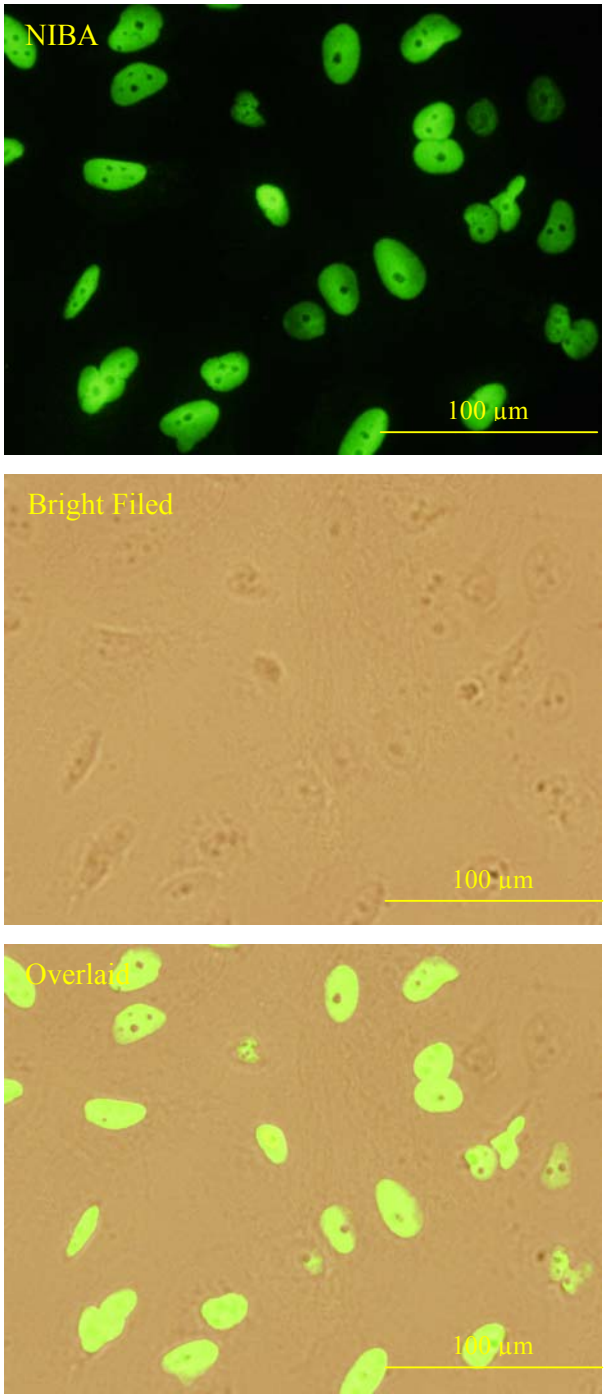

Fig 3.11: Identifying the localisation of accumulated p53 following Cisplatin treatment of A549 cells.

A549 cells were treated with 10µg/ml Cisplatin for 24 hours. Immunofluorescence images were at 400×magnification.

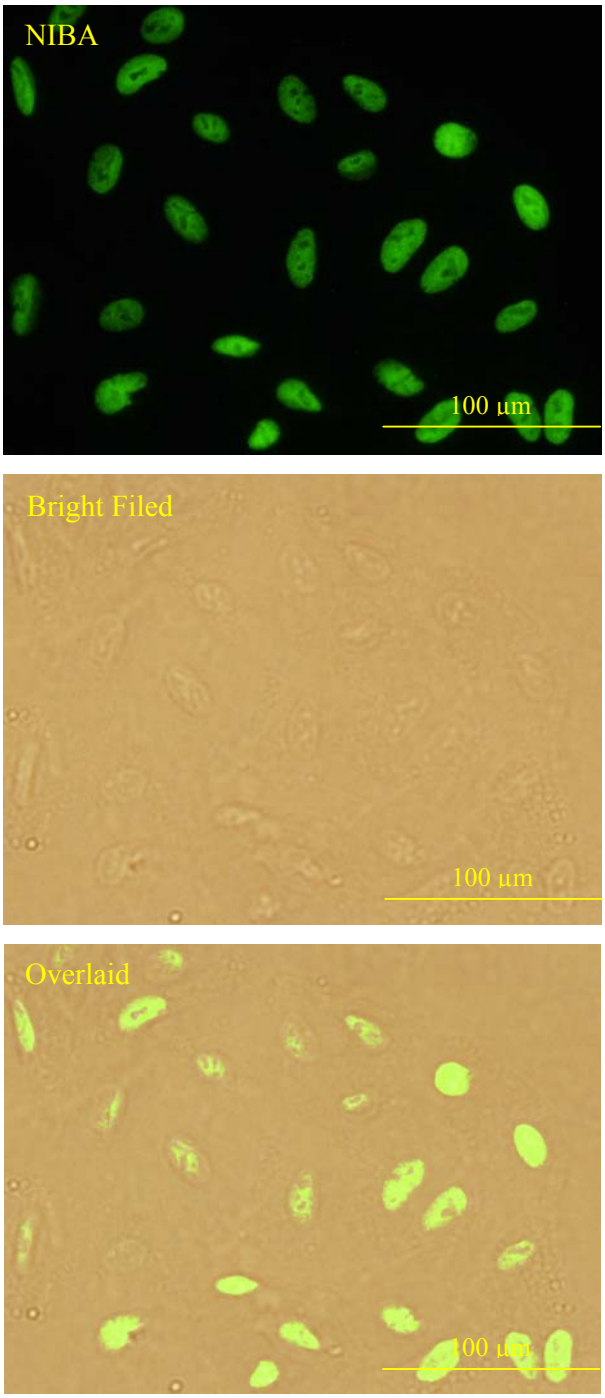

Fig 3.12: Identifying the localisation of accumulated p53 following Nutlin-3 treatment of A549 cells.

A549 cells were treated with 10µM Nutlin-3 for 24 hours. Immunofluorescence images were at 400×magnification.

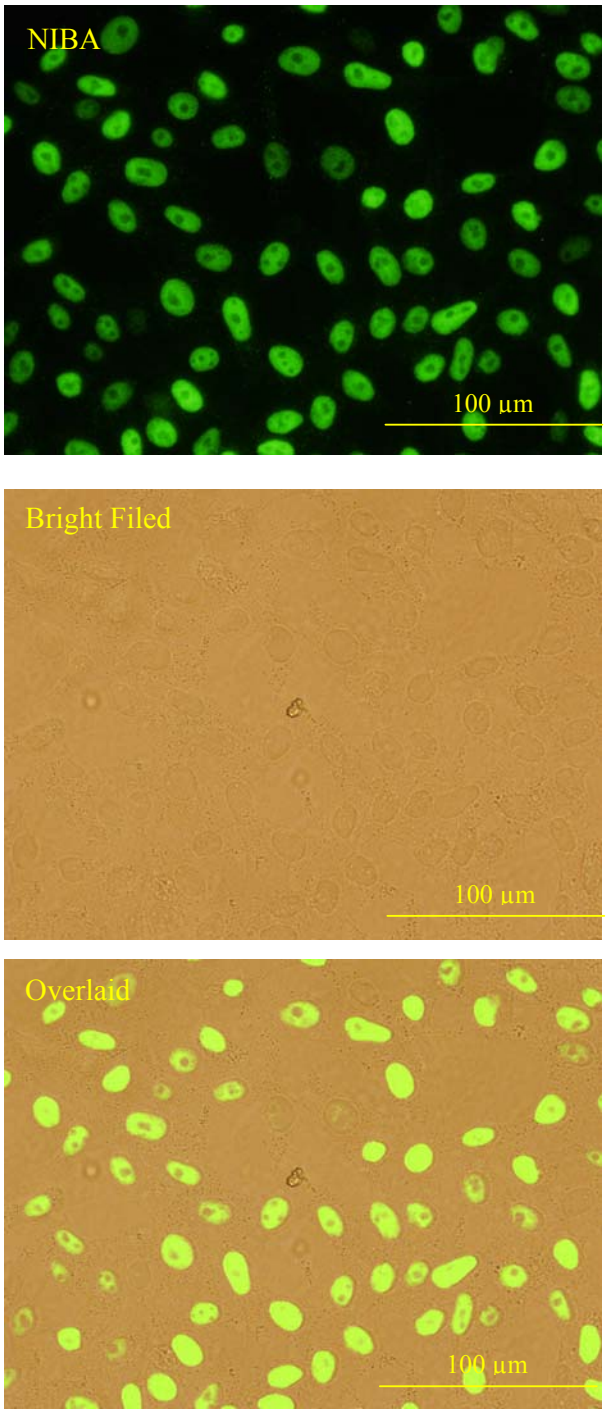

Fig 3.13: Identifying the localisation of accumulated p53 following Cisplatin treatment of RKO cells.

RKO cells were treated with 10µg/ml Cisplatin for 24 hours. Immunofluorescence images were at 400×magnification.

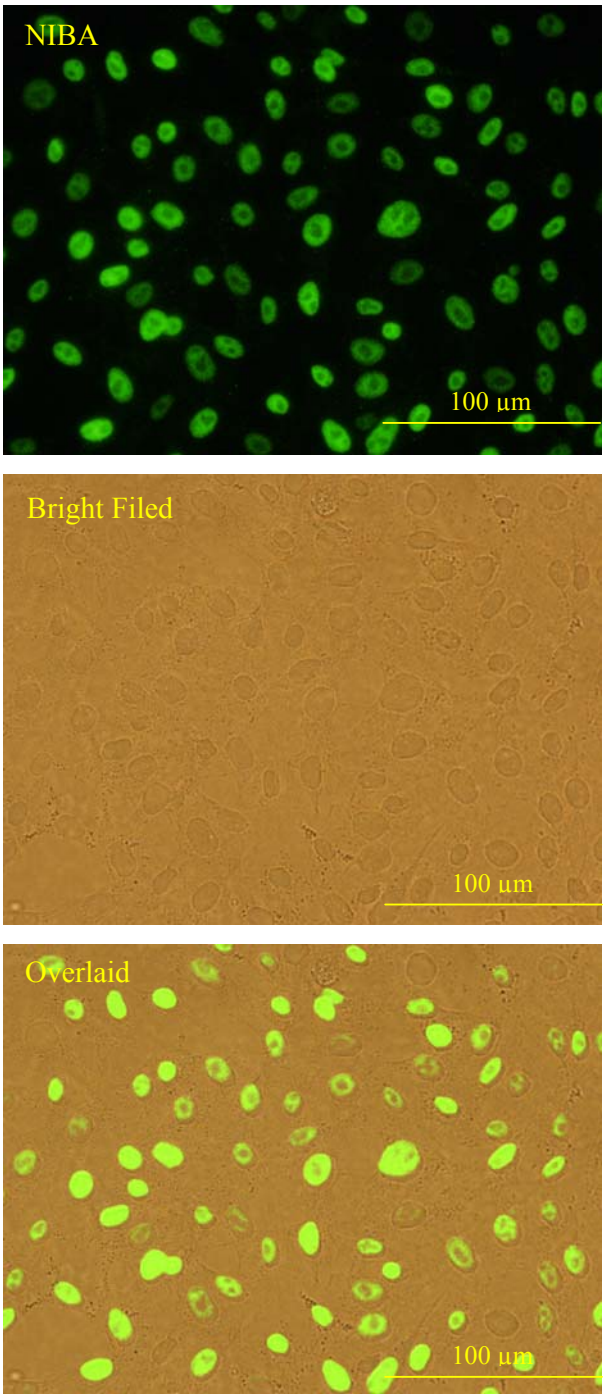

Fig 3.14: Identifying the localisation of accumulated p53 following Nutlin-3 treatment of RKO cells.

RKO cells were treated with 10µM Nutlin-3 for 24 hours. Immunofluorescence images were at 400×magnification.

CHAPTER IV

An investigation of the functional responses of p53 following treatment with Cisplatin or Nutlin-3

4.1 Viability of A549 and RKO cells following treatment with Cisplatin and Nutlin-3

To identify whether cells remained viable following treatment with Cisplatin or Nutlin-3, cell numbers were counted at 24, 48, and 72 hours after treatment using a haemocytometer. Viable cells were differentiated from dead or dying cells using a simple Trypan Blue staining assay. Control cells were incubated with an identical volume of Ethanol and cells were harvested as for the treated samples. ***Fig 4.1*** and ***Fig 4.3*** demonstrated that Nutlin-3 treated cell numbers remained almost unchanged indicative of cell cycle arrest or equivalence between dying and dividing cells while cell numbers were decreased significantly following Cisplatin treatment. Moreover, ***Fig 4.2*** and ***Fig 4.4*** showed Nutlin-treated cells were close to 100% viable up to 72hr after treatment. This suggests Nutlin-3 may trigger cell cycle arrest. However, the percentage of viable cells in Cisplatin-treated samples fell to 15%-20% after 48 hour. The decreased viable cells following Cisplatin treatment indicates that cell death was induced by Cisplatin.

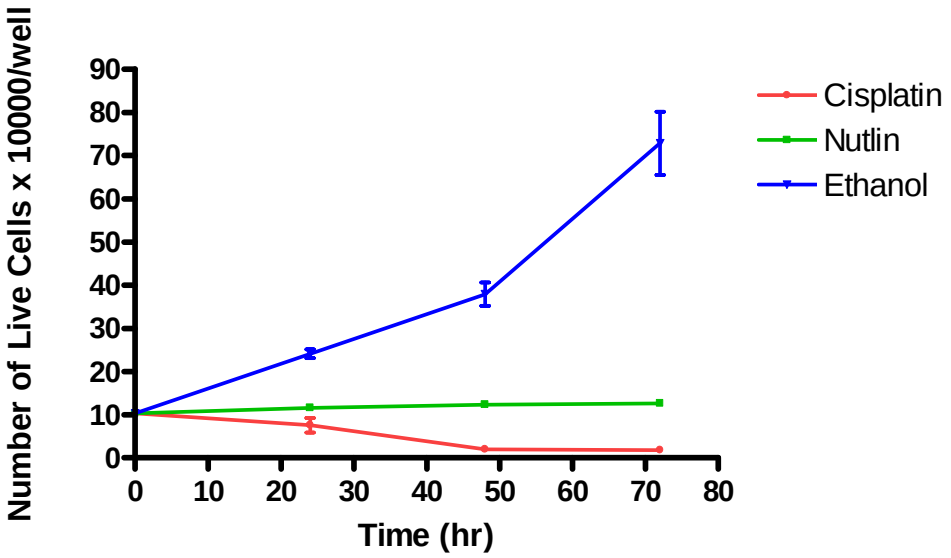

Fig 4.1: Total live cell number of A549 cells following treatment with Cisplatin and Nutlin-3

A549 cells treated with 10µg/ml of Cisplatin, 10µM Nutlin-3 and Ethanol respectively were counted after 24hr, 48hr, and 72hr. Data is presented as the total number of cells counted vs. time points Data points were typically represented as the mean of three identical experiments and the standard error of the mean (SEM).

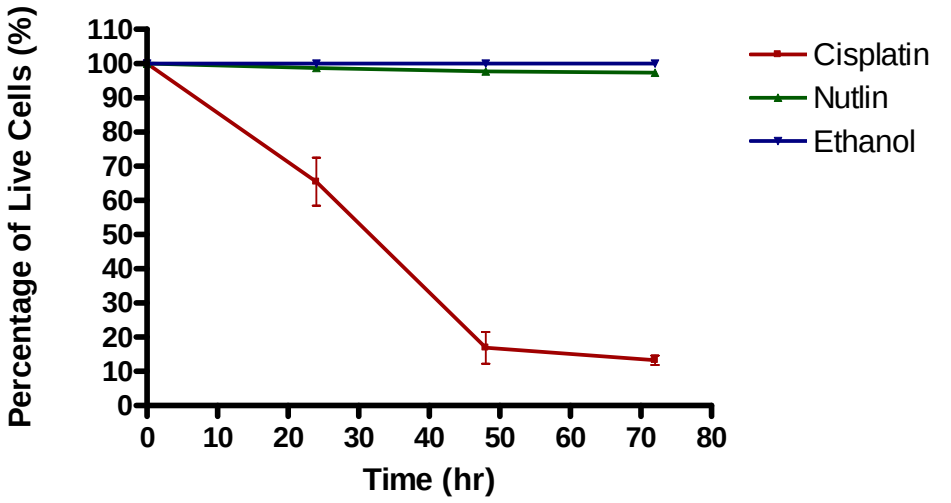

Fig 4.2: Total cell viability of A549 cells following treatment with Cisplatin and Nutlin-3

A549 cells treated with 10µg/ml of Cisplatin, 10µM Nutlin-3 and Ethanol respectively were counted after 24hr, 48hr, and 72hr. Data is presented as the percentage of live cells counted vs. time points. Data points were typically represented as the mean of three identical experiments and the standard error of the mean (SEM).

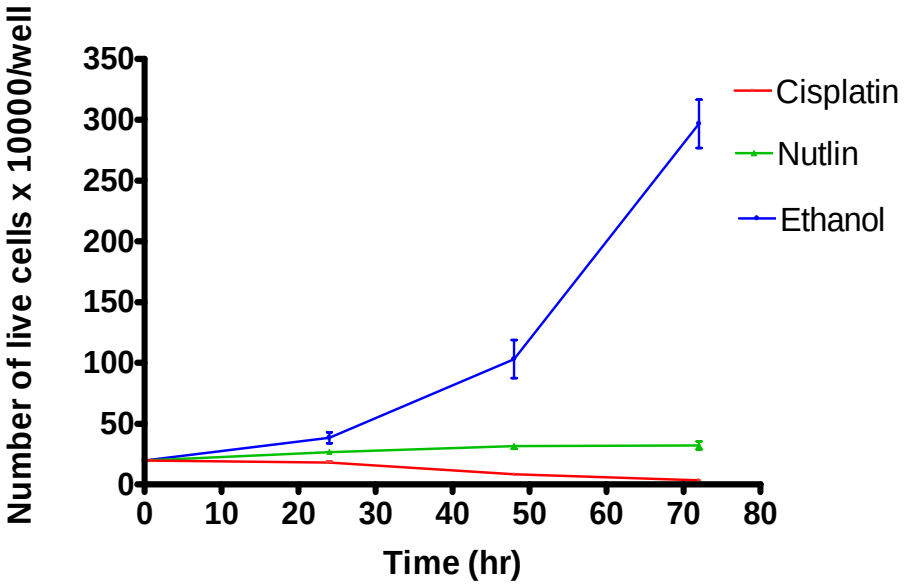

Fig 4.3: Total live cell number of RKO cells following treatment with Cisplatin and Nutlin-3

RKO cells treated with 10µg/ml of Cisplatin, 10µM Nutlin-3 and Ethanol respectively were counted after 24hr, 48hr, and 72hr. Data is presented as the total number of cells counted vs. time points. Data points were typically represented as the mean of three identical experiments and the standard error of the mean (SEM).

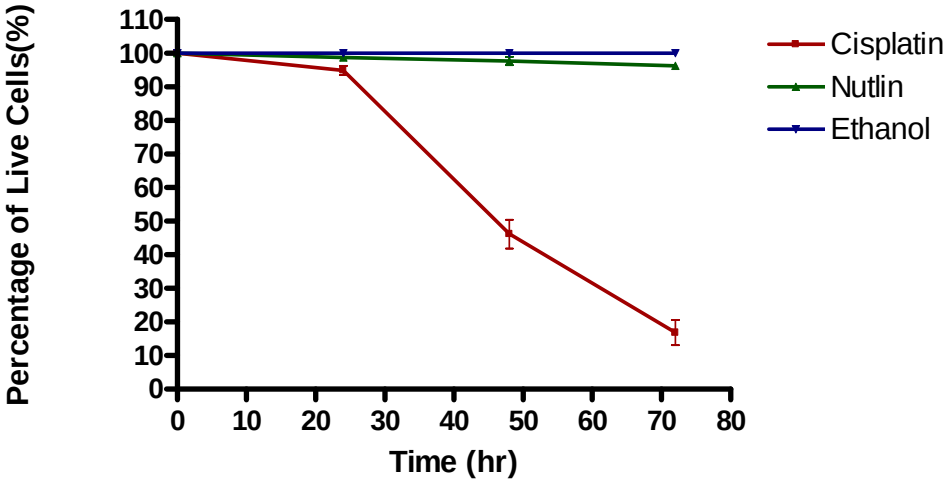

Fig 4.4: Total cell viability of RKO cells following treatment with Cisplatin and Nutlin-3

RKO cells treated with 10µg/ml of Cisplatin, 10µM Nutlin-3 and Ethanol respectively were counted after 24hr, 48hr, and 72hr. Data is presented as the percentage of live cells counted vs. time points. Data points were typically represented as the mean of three identical experiments and the standard error of the mean (SEM).

4.2 Morphological changes associated with Cisplatin and Nutlin-3 treatment

To identify whether the rapid cell death associated with Cisplatin treatment was due to apoptosis we investigated the morphological changes that took place following treatment with these two agents. Apoptosis has been shown to result in chromatin condensation, nuclear blebbing and disintegration of the nucleus into smaller fragments. Using a DNA staining agent DAPI we tracked the morphological changes taking place in Cisplatin and Nutlin-3 treated cells. A549 cells were treated with 10μg/ml Cisplatin and 10μM Nutlin-3 for 24 hours. After treatment with Cisplatin (***Fig 4.5***), there was evidence of intense staining in many nuclei indicating chromatin condensation and nuclear disintegration (arrows) indicative of an apoptotic response. The decreased cell number in Cisplatin-treated samples also indicated cells were dying. In contrast, Nutlin-3-treated cells showed no evidence of chromatin condensation or disintegration. However, there was no evidence of dividing cells which were clearly evident in ethanol treated controls (arrows) and it would appear that these cells have arrested in their growth.

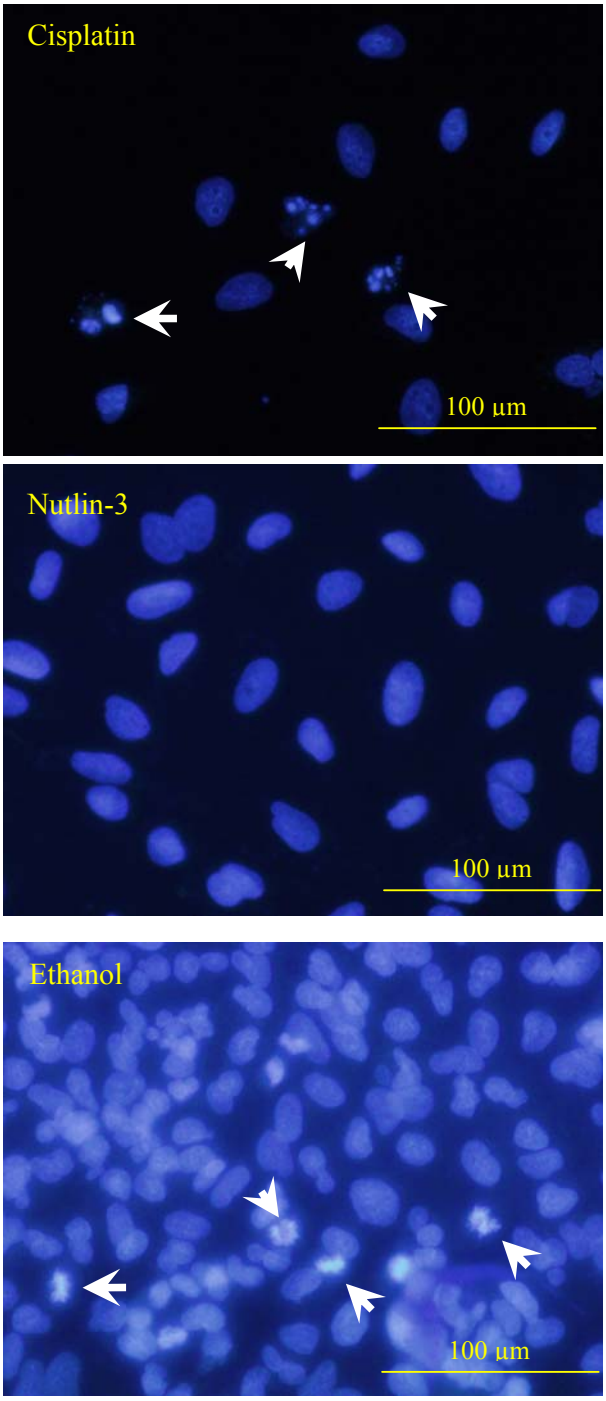

Fig 4.5: Morphological changes in A549 cells associated with Cisplatin and Nutlin-3 treatment

A549 cells were treated with 10µg/ml Cisplatin, 10µM Nutlin-3 and ethanol for 24hr respectively. Slides were stained with DAPI, and images were taken under a UV mirror unit at 400×magnification.

4.3 Cell cycle abnormalities associated with Cisplatin and Nutlin-3 treatment

To investigate whether the lack of dividing cells in our Nutlin-3 treated population was due to cell cycle arrest we stained both Nutlin-3 and Cisplatin treated cells with Propidium iodide and analysed their DNA content via flow cytometry. A549 cells and RKO cells were both treated with 10μg/ml Cisplatin and 10μM Nutlin-3 and fixed after 0 hour, 24 hours, 48 hours, and 72 hours treatment. As we can see from the data (***Fig 4.6*** and ***Fig 4.7***), in Cisplatin-treated cells, as supported by the morphological data, there was an evidence of a sub G_1 population indicative of disintegrating DNA and apoptosis. This sub G_1 population began to appear at 24 hours post treatment and had risen to a significant population by 48 hours in agreement with our Trypan blue staining (***Fig 4.1-Fig 4.4)***. Thus, Cisplatin initiates many of the classical features associated with apoptosis (i.e. nuclear condensation, disintegration, sub G_1 peak). Conversely, Nutlin-3 treated cells demonstrated a complete loss of replicating cells (S phase) and cells appeared to be arrested in both the G_1 and G_2 populations. As p53 was seen to be accumulated in the nucleus following Cisplatin or Nutlin-3 treatment, these differential responses might be initiated by p53.

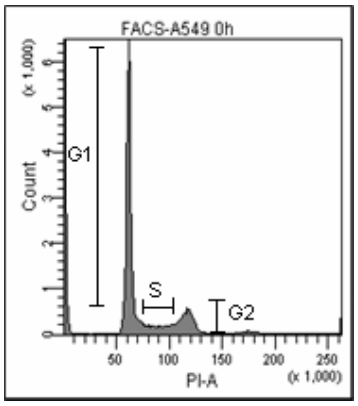
FACS-A549 0h
G1
S
G2
Count
PI-A
(x 1,000)

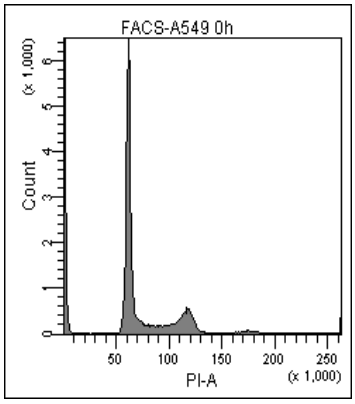
FACS-A549 0h
Count
PI-A
(x 1,000)

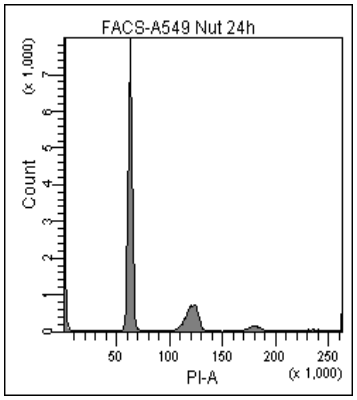
FACS-A549 Nut 24h
Count
PI-A
(x 1,000)

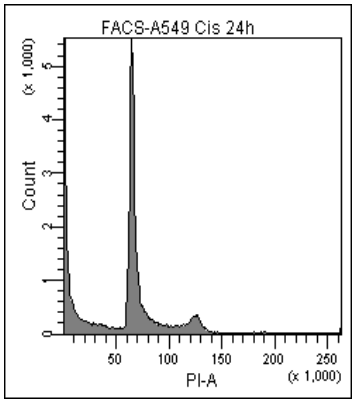
FACS-A549 Cis 24h
Count
PI-A
(x 1,000)

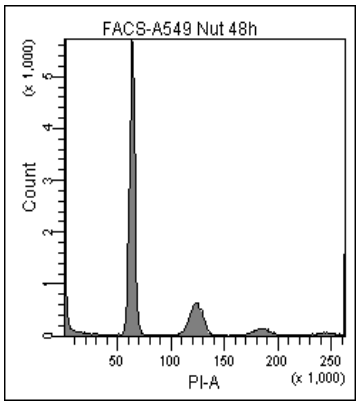
FACS-A549 Nut 48h
Count
PI-A
(x 1,000)

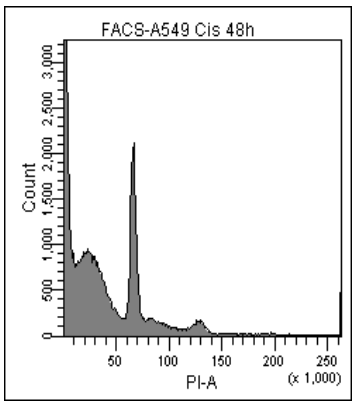
FACS-A549 Cis 48h
Count
PI-A
(x 1,000)

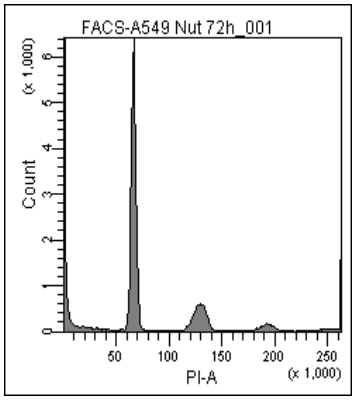
FACS-A549 Nut 72h_001
Count
PI-A
(x 1,000)

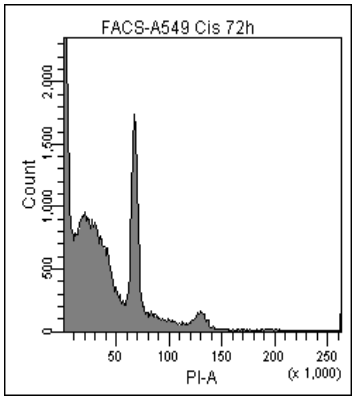
FACS-A549 Cis 72h
Count
PI-A
(x 1,000)

Fig 4.6: Cell cycle abnormalities associated with Cisplatin and Nutlin-3 treatment of A549 cells

A549 cells treated by 10μg/ml Cisplatin (right column), 10μM Nutlin-3 (left column) respectively were fixed for FACS after 0hr 24hr 48hr and 72hr. Cell cycle abnormalities were investigated using flow cytometry. Data was presented as fluorescence intensity (DNA content) vs. cell number. Proportions of the populations residing in each phase of the cell cycle are illustrated.

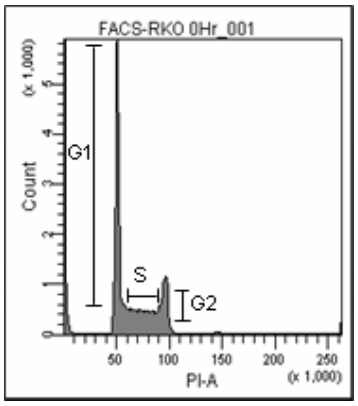
FACS-RKO 0Hr_001
G1
S
G2
Count
PI-A
(x 1,000)

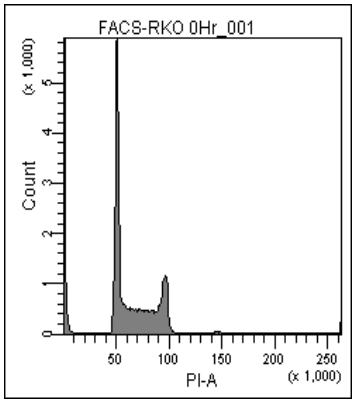
FACS-RKO 0Hr_001
Count
PI-A
(x 1,000)

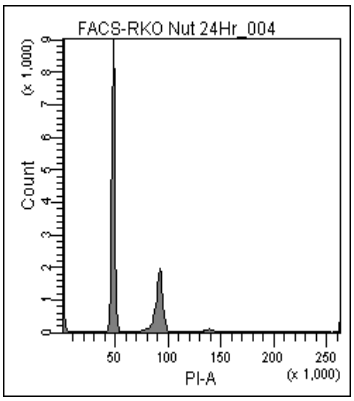
FACS-RKO Nut 24Hr_004
Count
PI-A
(x 1,000)

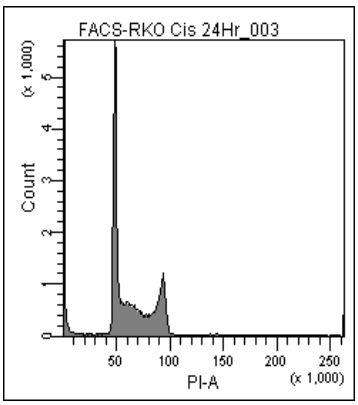
FACS-RKO Cis 24Hr_003
Count
PI-A
(x 1,000)

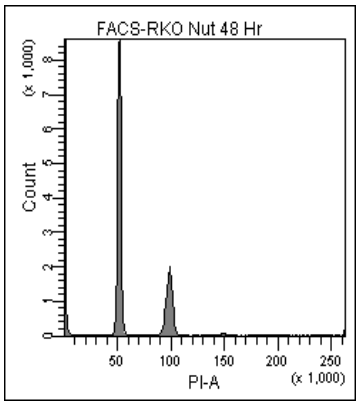
FACS-RKO Nut 48 Hr
Count
PI-A
(x 1,000)

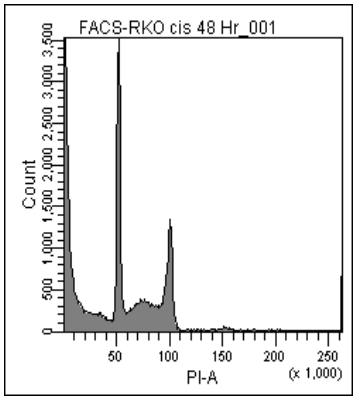
FACS-RKO cis 48 Hr_001
Count
PI-A
(x 1,000)

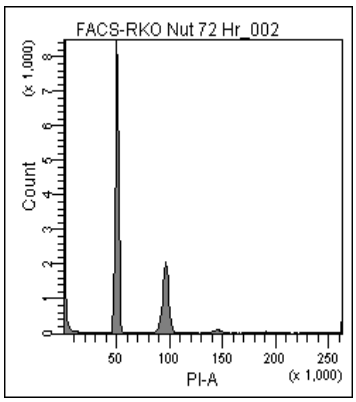
FACS-RKO Nut 72 Hr_002
Count
PI-A
(x 1,000)

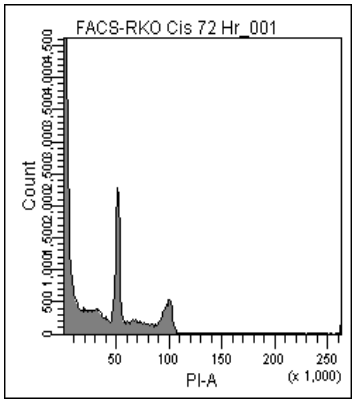
FACS-RKO Cis 72 Hr_001
Count
PI-A
(x 1,000)

Fig 4.7: Cell cycle abnormalities associated with Cisplatin and Nutlin-3 treatment of RKO cells
RKO cells treated by 10μg/ml Cisplatin (right column), 10μM Nutlin-3 (left column) respectively were fixed for FACS after 0hr 24hr 48hr and 72hr. Cell cycle abnormalities were investigated using flow cytometry. Data was presented as fluorescence intensity (DNA content) vs. cell number. Proportions of the populations residing in each phase of the cell cycle are illustrated.

4.4 Gene expression associated with Cisplatin and Nutlin-3 treatment

It has been suggested that the ability of p53 to differentially induce cell death or cell cycle arrest is achieved by activating different sets of genes. For example, $P21^{WAF1/CIP1}$, *GADD45*, *SFN* (14-3-3σ) are reported to be clearly involved in cell-cycle arrest while *BAX, BIK, BIM, PUMA, NOXA, DR4,* and *DR5* are involved in activating apoptosis via either the intrinsic or extrinsic pathways (22). Our data has demonstrated that Cisplatin induces apoptosis while Nutlin-3 leads to cell cycle arrest in RKO and A549 cells. To investigate whether distinct sets of genes are expressed in apoptotic cells as opposed to cells in cell-cycle arrest, several common genes involved in these processes were chosen for further analysis.

RKO cells were treated with 10μg/ml Cisplatin and 10μM Nutlin-3, and harvested for RNA extraction at 0 hour, 4 hours, 6 hours, and 8 hours post-treatment. *P21, GADD45A, NOXA, BAX, BIK* and *BIM* were chosen as examples of apoptotic and cell-cycle arrest genes for investigation of their expression patterns. *G3PDH* was used as a control gene to ensure similar loading. BAX plays a central role in mediating apoptosis, and a p53-dependent induction of *BAX* RNA was found following etoposide treatment in oncogene-expressing MEF cells (110). BIK and NOXA are recognized as the 'enablers' which bind to the pro-survival BCL-2 proteins thus freeing the pro-apoptotic members (52). P21 and GADD45 play an important role in regulating G_1/S and G_2/M cell cycle checkpoints in a p53-dependent manner. These genes were all effectively expressed in both treated cells and untreated cells as shown by RT-PCR (***Fig 4.8***).

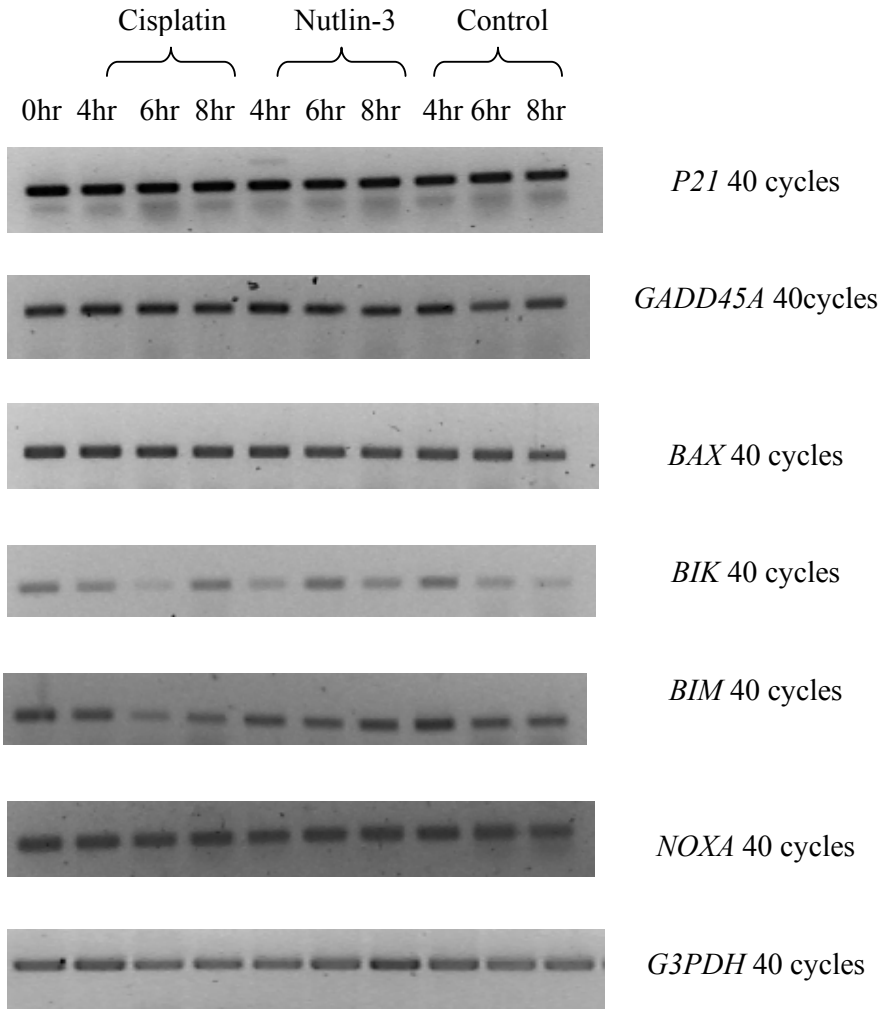

Fig 4.8: Gene expression investigated by Reverse-Transcription PCR

RKO cells were treated with 10μg/ml Cisplatin and 10μM Nutlin-3 and harvested for RT-PCR at regular interval between 4 and 8 hours. Untreated cells at different time point were used as a control. The common cell cycle arrest genes P21and GADD45 and some apoptotic genes including BAX, BIK, BIM, and NOXA were chosen, and G3PDH was used as a loading control.

However, traditional PCR is not precise enough to detect quantitative changes in gene expression, so real-time PCR is required to investigate the level of gene expression.

NOXA and *P21* were chosen for investigation by real-time RT-PCR as these demonstrated high expression levels at all time points and were representatives of apoptotic and cell cycle arrest genes. Their expression was normalized against the most stable housekeeping genes (*18S*, *UBC* and *HPRT1*). Both Cisplatin and Nutlin-3 were able to induce increase in p21 expression compared with their untreated

controls (***Fig 4.9***). Nutlin-3 demonstrated increases of between 4 and 8 fold while Cisplatin induced a 3-4 fold increase. Similarly, both Nutlin-3 and Cisplatin induced early increases in NOXA expression of 3-4 fold but these rapidly decreased to low levels by 8 hours. These results demonstrate that both the cell cycle arrest and apoptotic genes are increased by Nutlin-3 and Cisplatin but do not appear to be differentially activated by either treatment.

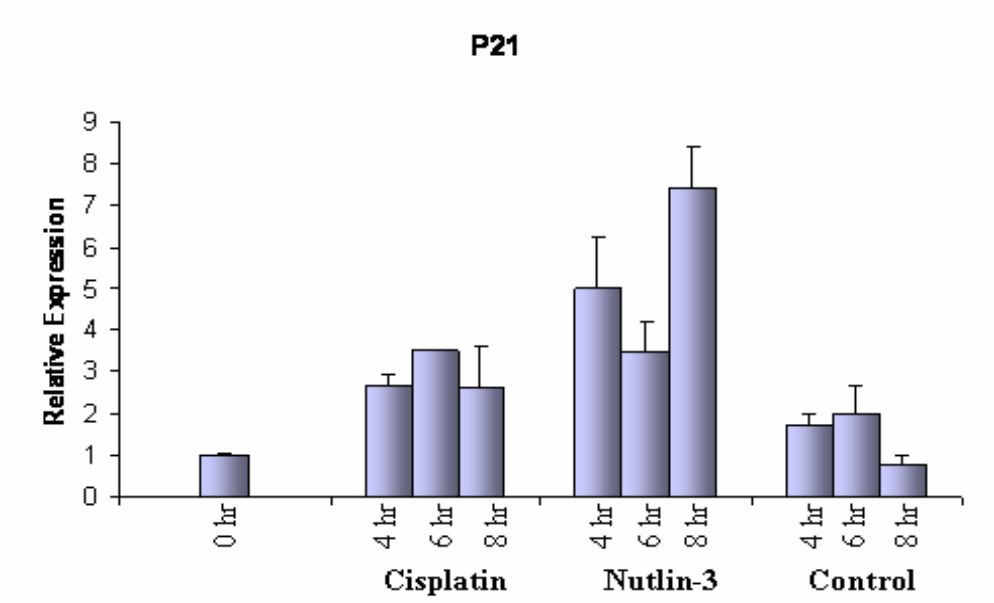

Fig 4.9: P21 expression investigated by Real Time RT-PCR

RKO cells were treated with 10μg/ml Cisplatin and 10μM Nutlin-3 and harvested for Real time RT-PCR at regular interval between 1 and 8 hours. Untreated cells at different time point were used as a control. Gene expression was normalized against the most stable housekeeping genes including 18S, UBC and HPRT1. Values are presented as the mean mRNA level of duplicate samples.

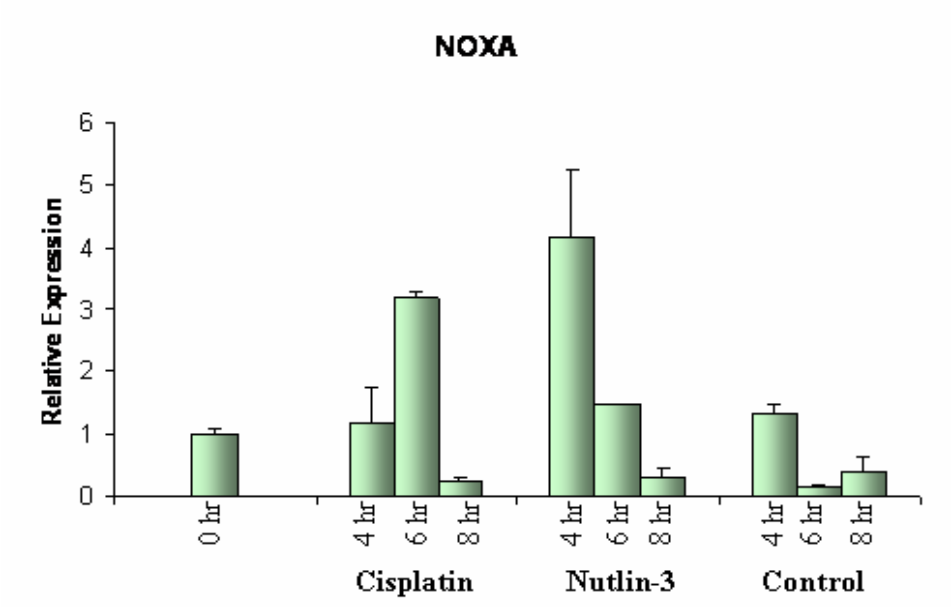

Fig 4.10: NOXA expression investigated by Real Time RT-PCR

RKO cells were treated with 10µg/ml Cisplatin and 10µM Nutlin-3 and harvested for Real time RT-PCR at regular interval between 1 and 8 hours. Untreated cells at different time point were used as a control. Gene expression was normalized against the most stable housekeeping genes including 18S, UBC and HPRT1. Values are presented as the mean mRNA level of duplicate samples.

CHAPTER V

Is localization of p53 or phosphorylation at Serine 392 responsible for the differing functional responses induced by treatment with Cisplatin and Nutlin-3?

5.1 Comparison of p53 and p53 phosphorylated at Ser392 (phospho-Ser392-p53) following treatment with Cisplatin and Nutlin-3

We have demonstrated earlier that treatment with Cisplatin and Nutlin-3 induces similar high levels of p53 accumulation in the nucleus (Chapter III). However, despite these similar expression patterns, both treatments demonstrated distinctly different functional responses but these did not appear to be transcriptionally driven (Chapter IV). p53's translocation to the mitochondria and subsequent induction of the transcription-independent pathway of apoptosis could be one mechanism for these differing responses. Phosphorylation of p53 at Ser392 is suggested to be related to p53's nucleocytoplasmic shuttling ability (72, 73, 111). However, whether phospho-Ser392-p53 is associated with mitochondrial localization remains unclear. In this section, we compared the localization of p53 and phospho-Ser392-p53 at different time points following Cisplatin and Nutlin-3 treatment. A double staining immunofluorescence technique was used to simultaneously detect p53 and phospho-Ser392-p53. A549 cells and RKO cells were treated with 10μM Nutlin-3 and 10μg/ml Cisplatin, and samples were fixed at regular intervals between 1 and 48 hours post exposure.

Our results demonstrated that p53 gradually accumulated in the nucleus reaching a maximum at approximately 16 hours post-treatment (***Fig 5.1-Fig 5.4***). On the contrary, maximal phospho-Ser392-p53 staining appeared after 2 hours treatment, and was clearly located outside the nucleus. From 4 hours to 8 hours, the phospho-Ser392-p53 gradually moved to the nucleus and from 16 to 48 hours, most of

Phospho-Ser392-p53 appeared in the nucleus with only a small fraction outside (***Fig 5.1-Fig 5.4***). No major difference was identified between Cisplatin-treated cells and Nutlin-treated cells suggesting that phosphorylation of Serine392 was not involved in the different functional responses to these treatments.

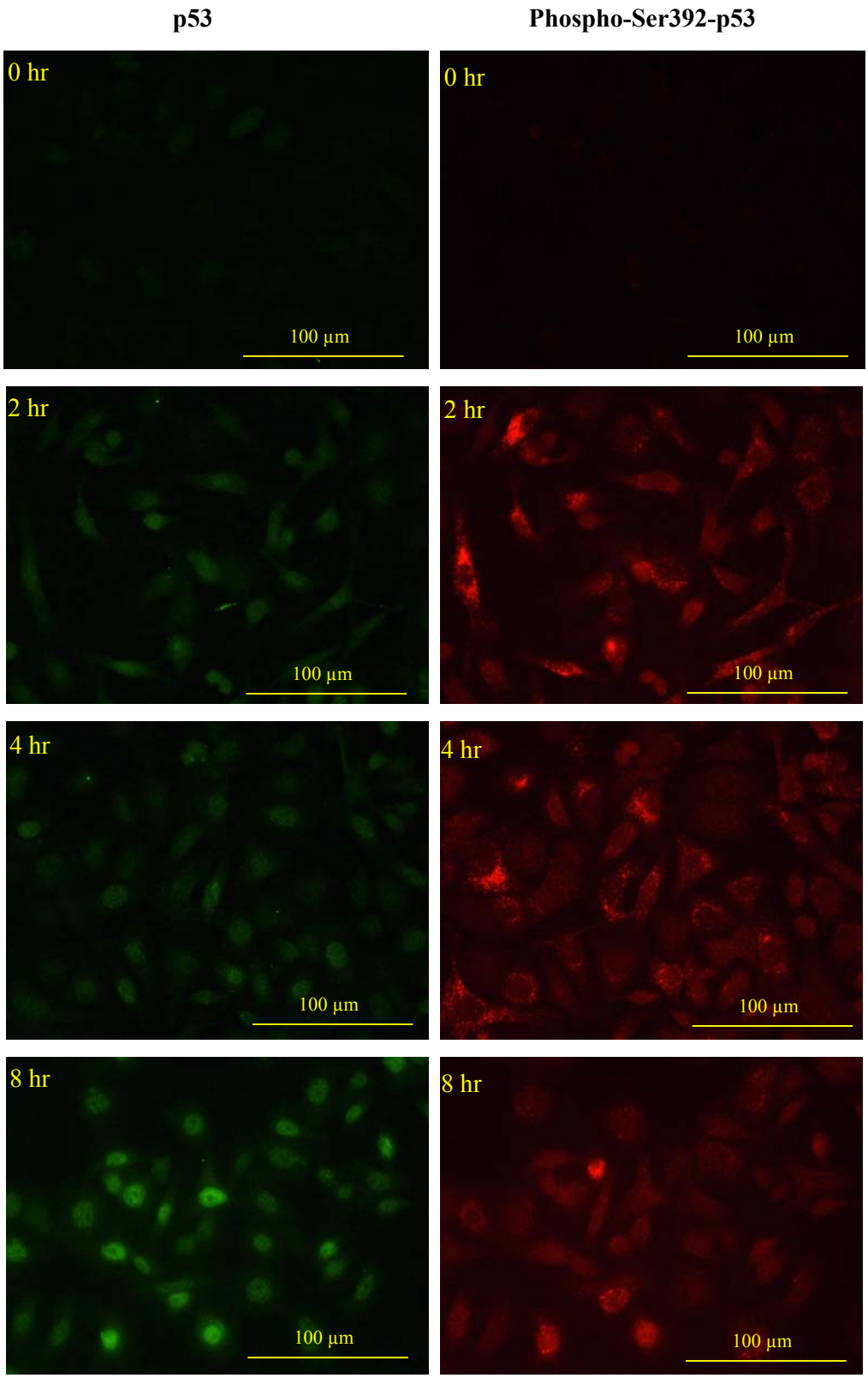
p53
Phospho-Ser392-p53
0 hr
0 hr
100 µm
100 µm
2 hr
2 hr
100 µm
100 µm
4 hr
4 hr
100 µm
100 µm
8 hr
8 hr
100 µm
100 µm

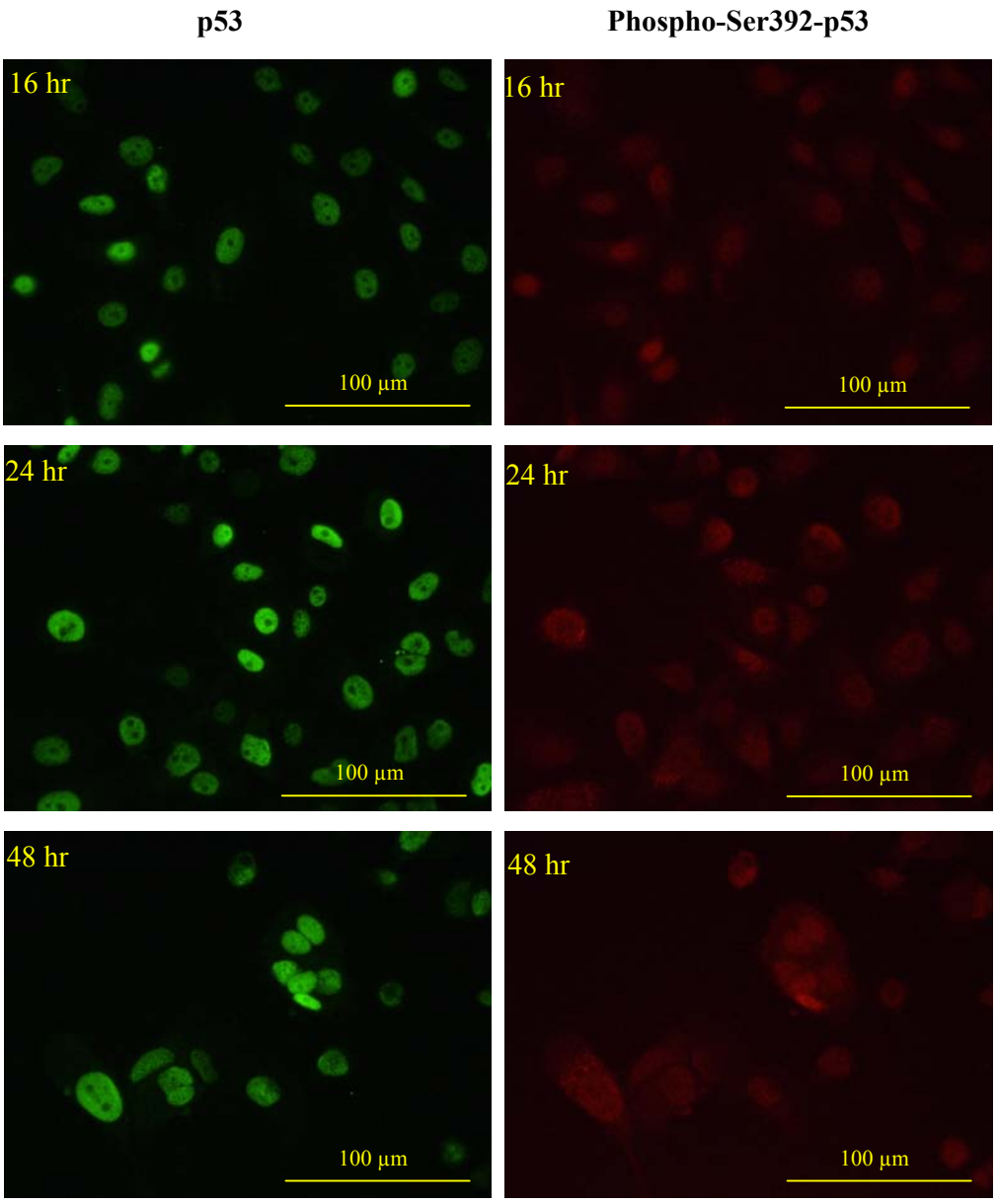

Fig 5.1: Comparison of p53 and phospho-Ser392-p53 following Cisplatin treatment of A549 cells

A549 cells were treated with 10µg/ml Cisplatin. Immunofluorescence was performed after 0, 2, 4, 8, 16, 24, 48 treatment and images were taken using NIBA mirror unit for p53 and WG mirror unit for phospho-Ser392-p53 at 400× magnification.

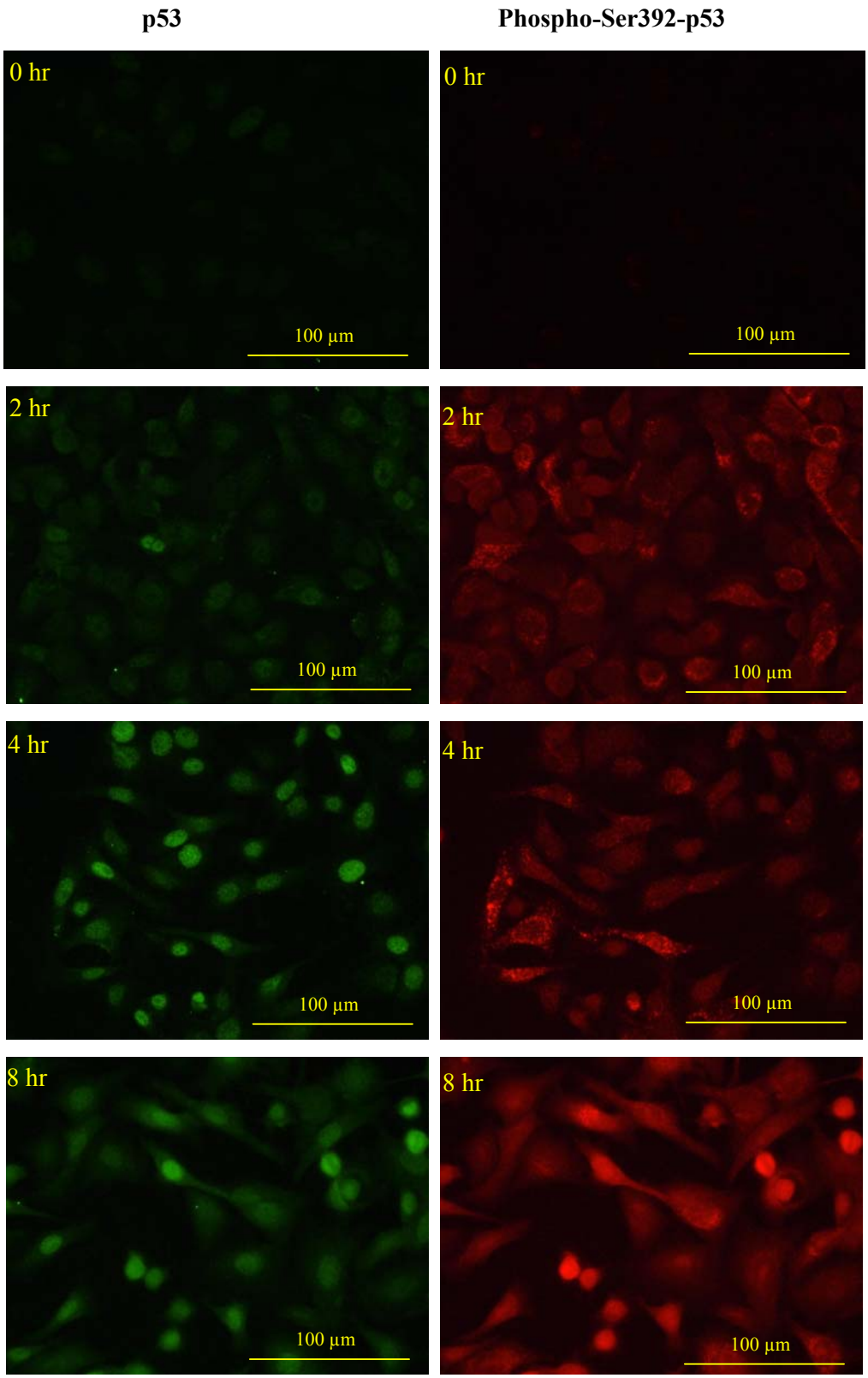
p53
Phospho-Ser392-p53
0 hr
0 hr
100 µm
100 µm
2 hr
2 hr
100 µm
100 µm
4 hr
4 hr
100 µm
100 µm
8 hr
8 hr
100 µm
100 µm

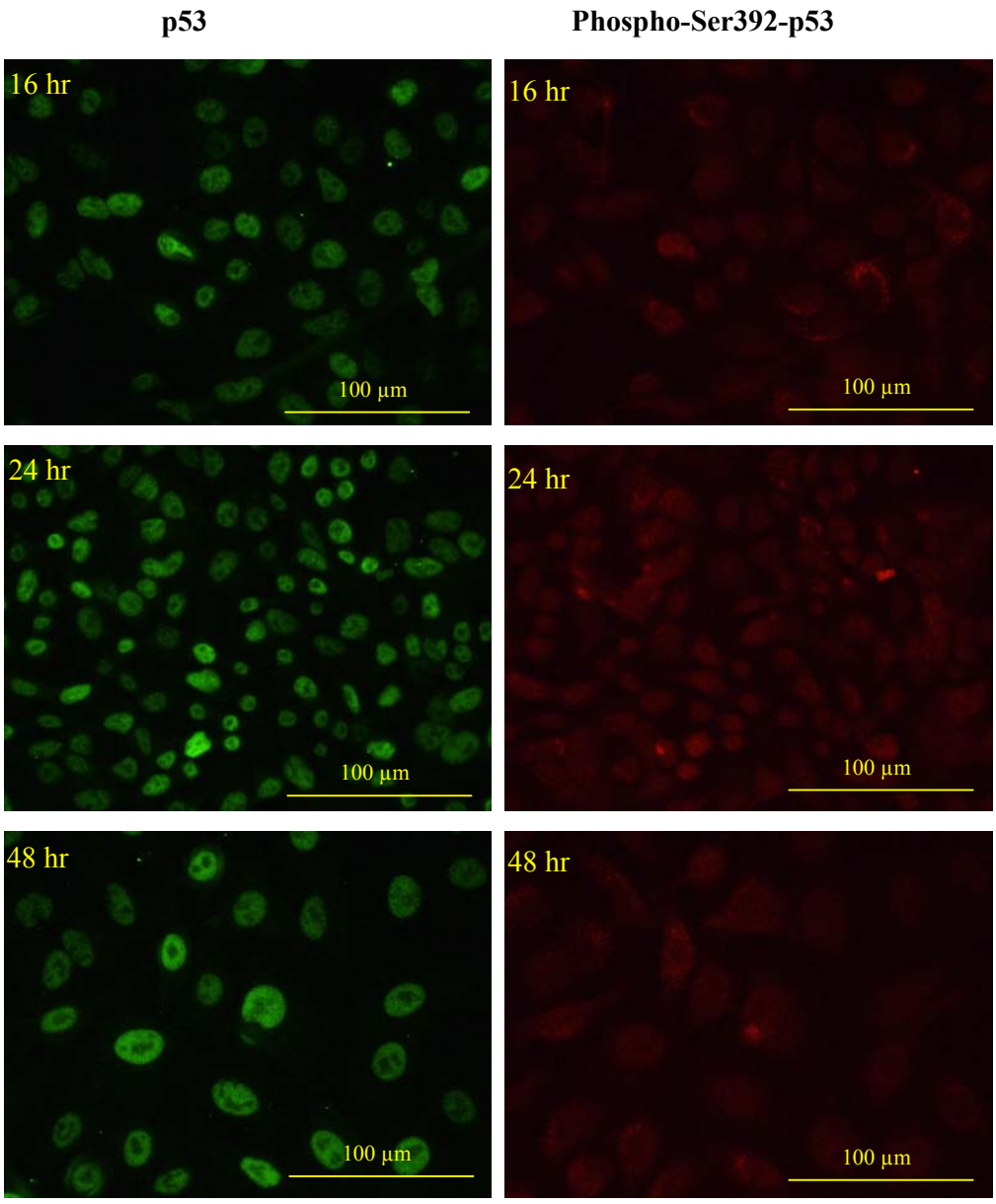

Fig 5.2: Comparison of p53 and phospho-Ser392-p53 following Nutlin-3 treatment of A549 cells

A549 cells were treated with 10µM Nutlin-3. Immunofluorescence was performed after 0, 2, 4, 8, 16, 24, 48 treatment and images were taken using NIBA mirror unit for p53 and WG mirror unit for phospho-Ser392-p53 at 400× magnification.

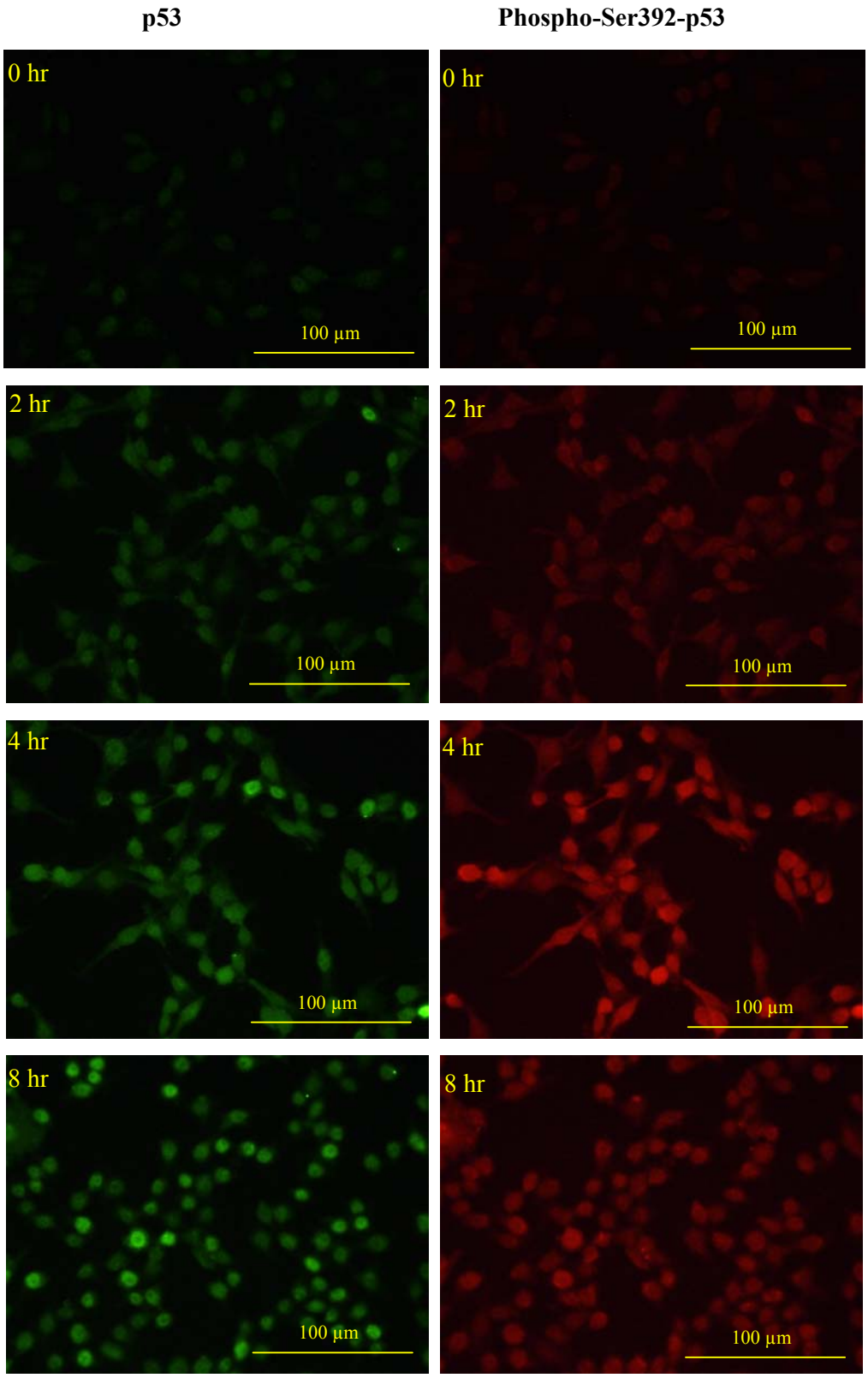
p53
Phospho-Ser392-p53
0 hr
100 µm
0 hr
100 µm
2 hr
100 µm
2 hr
100 µm
4 hr
100 µm
4 hr
100 µm
8 hr
100 µm
8 hr
100 µm

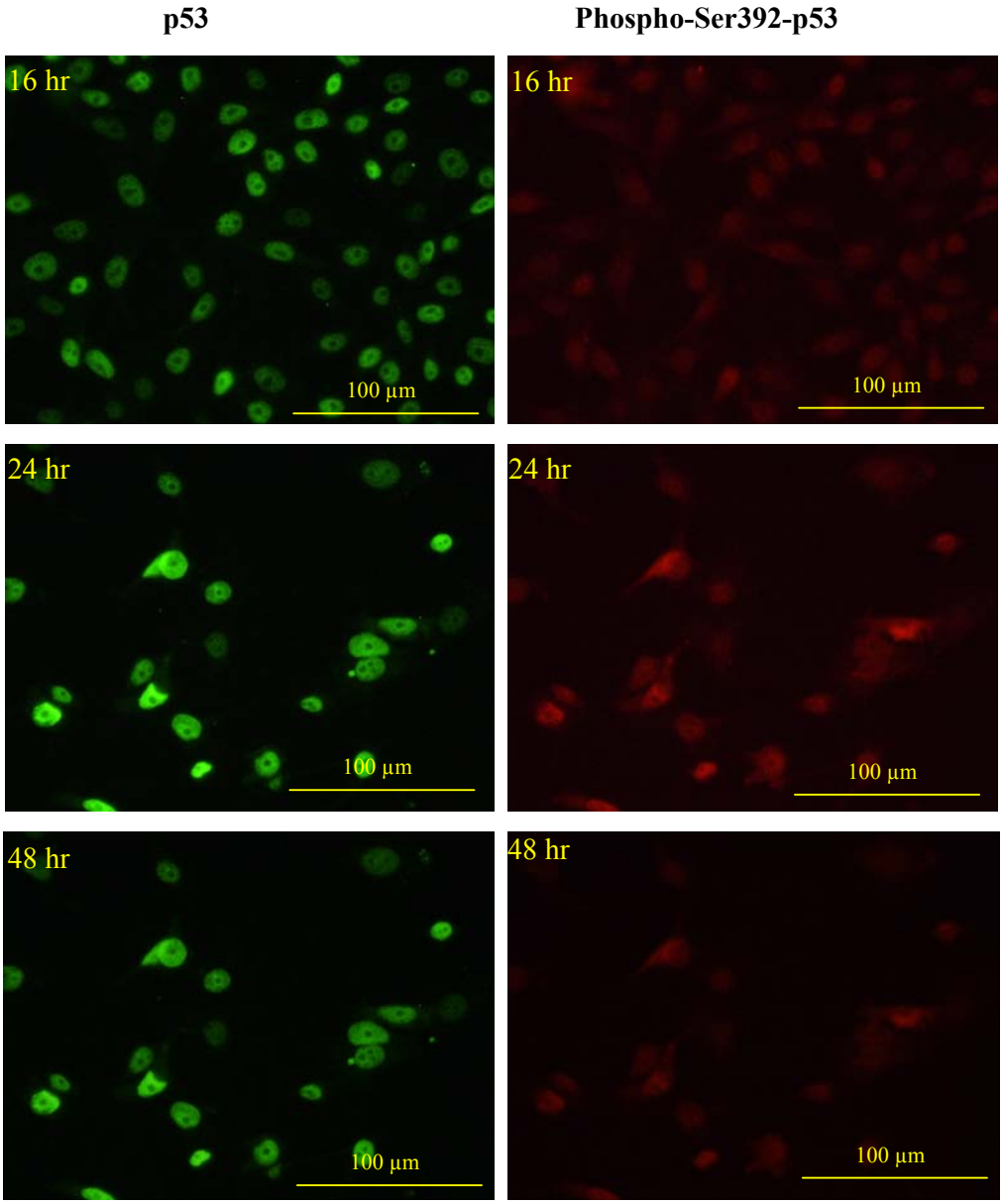

Fig 5.3: Comparison of p53 and phospho-Ser392-p53 following Cisplatin treatment of RKO cells

RKO cells were treated with 10µg/ml Cisplatin. Immunofluorescence was performed after 0, 2, 4, 8, 16, 24, 48 treatment and images were taken using NIBA mirror unit for p53 and WG mirror unit for phospho-Ser392-p53 at 400× magnification.

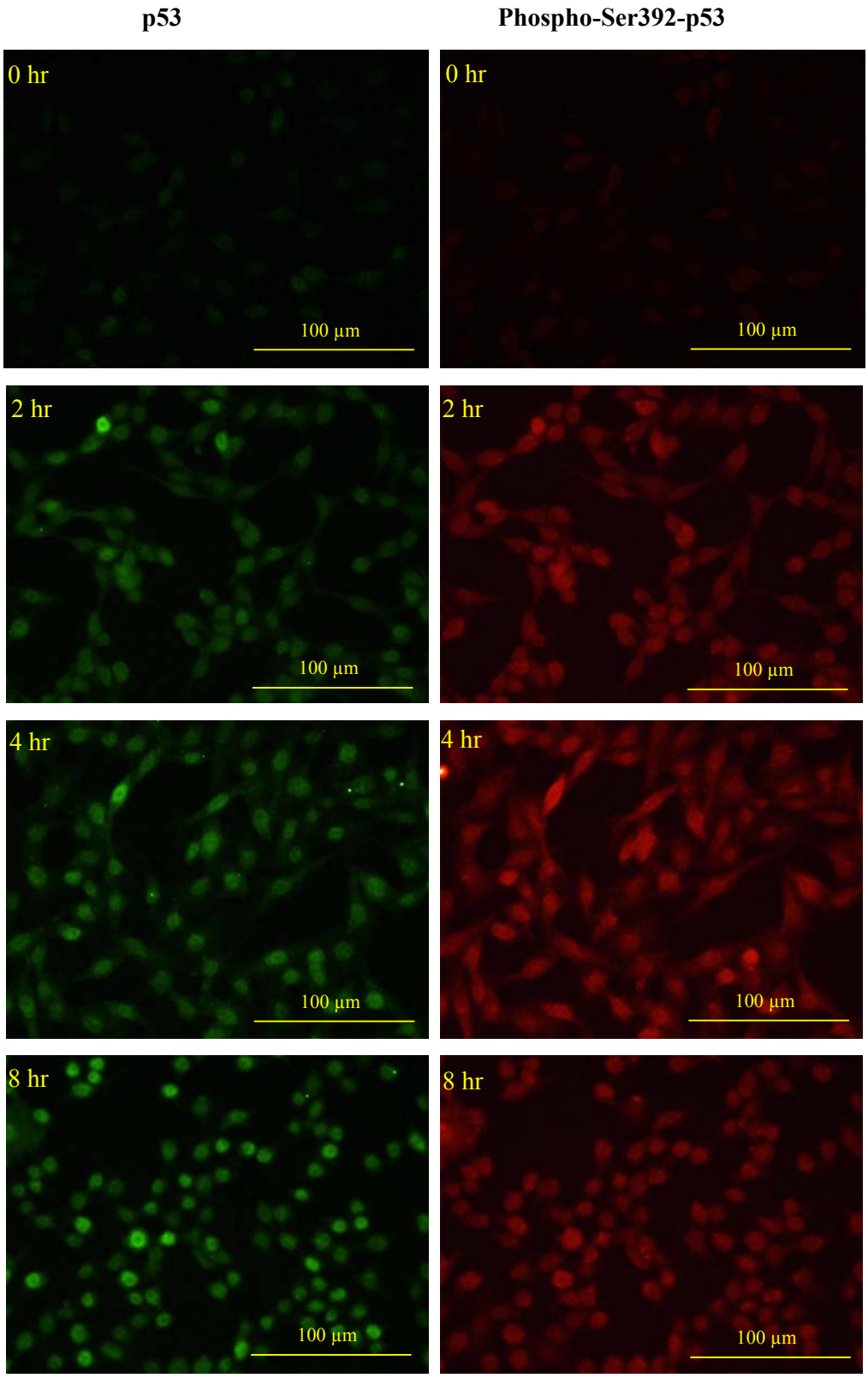
p53
Phospho-Ser392-p53
0 hr
100 µm
0 hr
100 µm
2 hr
100 µm
2 hr
100 µm
4 hr
100 µm
4 hr
100 µm
8 hr
100 µm
8 hr
100 µm

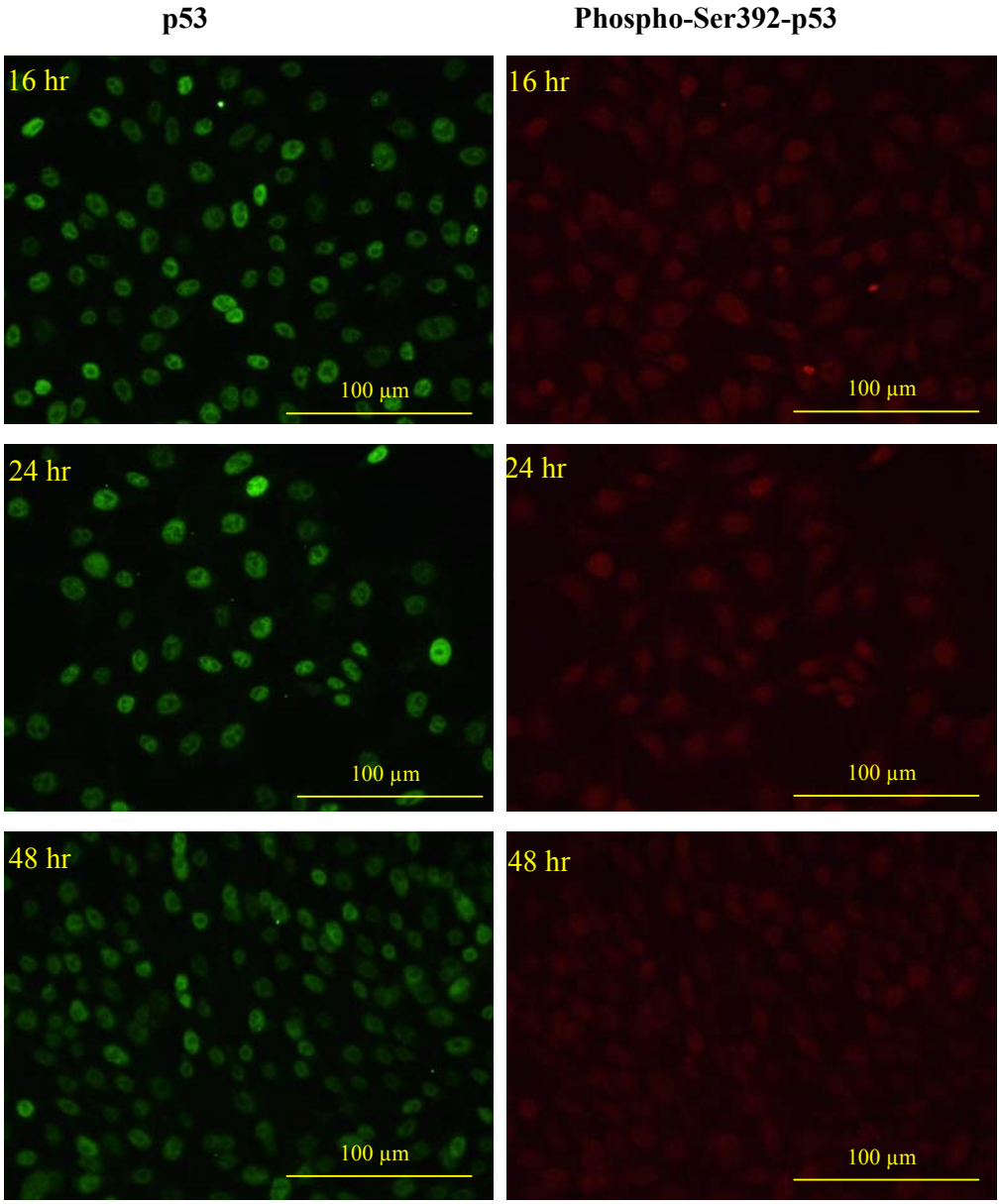

Fig 5.4: Comparison of p53 and phospho-Ser392-p53 following Nutlin-3 treatment of RKO cells

RKO cells were treated with 10µM Nutlin-3. Immunofluorescence was performed after 0, 2, 4, 8, 16, 24, 48 treatment and images were taken using NIBA mirror unit for p53 and WG mirror unit for phospho-Ser392-p53 at 400× magnification.

To confirm the localization of p53 and phospho-Ser392-p53, 1000× Images were taken and overlaid. The images below show that phospho-Ser392-p53 and p53 were clearly separate at 2 hours and 8 hours post-treatment with Cisplatin and Nutlin-3. Of note, although very little p53 accumulation was observed in most cells after 2 hours treatment, some dividing cells displayed higher expression of p53 due to the fact that p53 is a cell cycle checkpoint protein. In addition, as clearly demonstrated in the overlaid images, most phospho-Ser392-p53 appeared in the nucleus after 24 and 48 hours treatment with only a small part outside the nucleus (***Fig 5.5-Fig 5.20***).

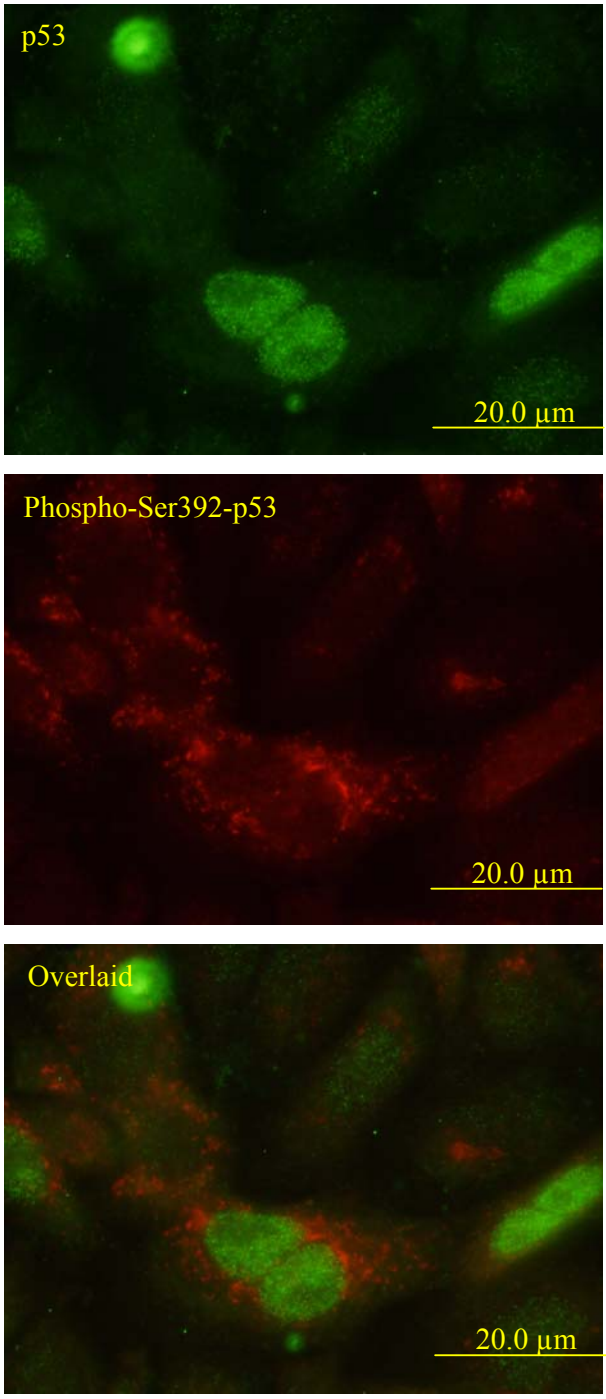

Fig 5.5: Co-localisation of p53 and phospho-Ser392-p53 in A549 cells 2 hr after Cisplatin treatment

Slides viewed under narrow blue wavelength (Green) indicate p53 while slides viewed under WG wavelength (Red) indicate phospho-Ser392-p53.

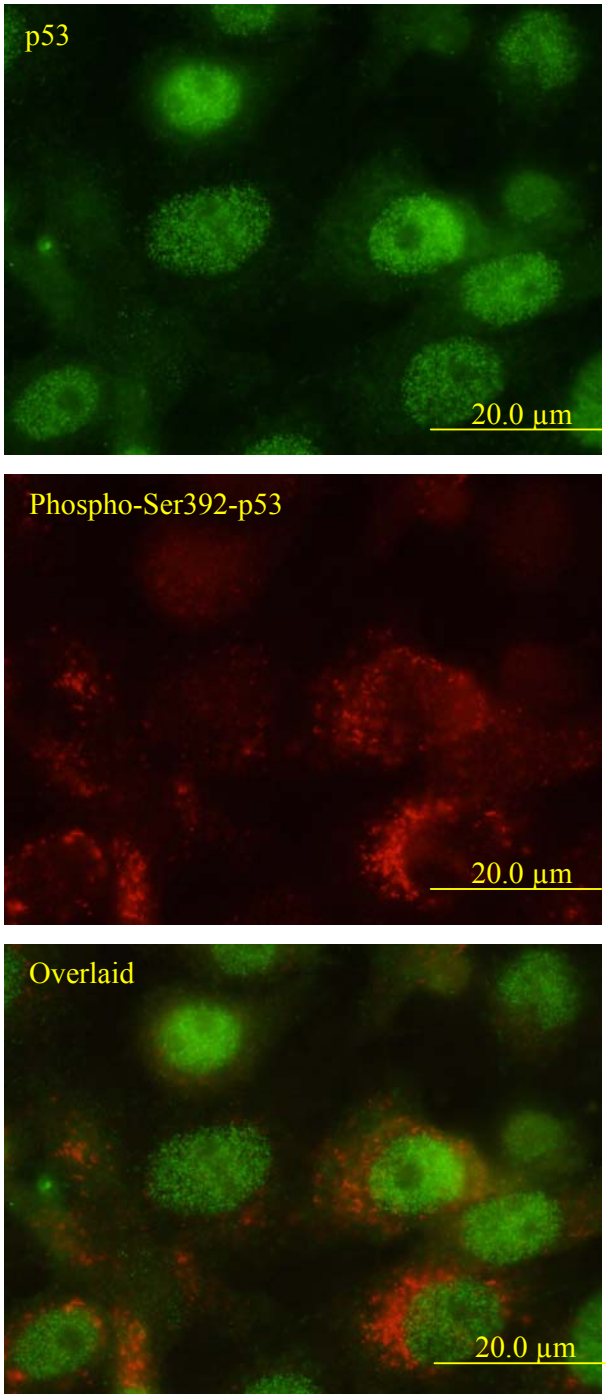

Fig 5.6: Co-localisation of p53 and phospho-Ser392-p53 in A549 cells 8 hr after Cisplatin treatment

Slides viewed under narrow blue wavelength (Green) indicate p53 while slides viewed under WG wavelength (Red) indicate phospho-Ser392-p53.

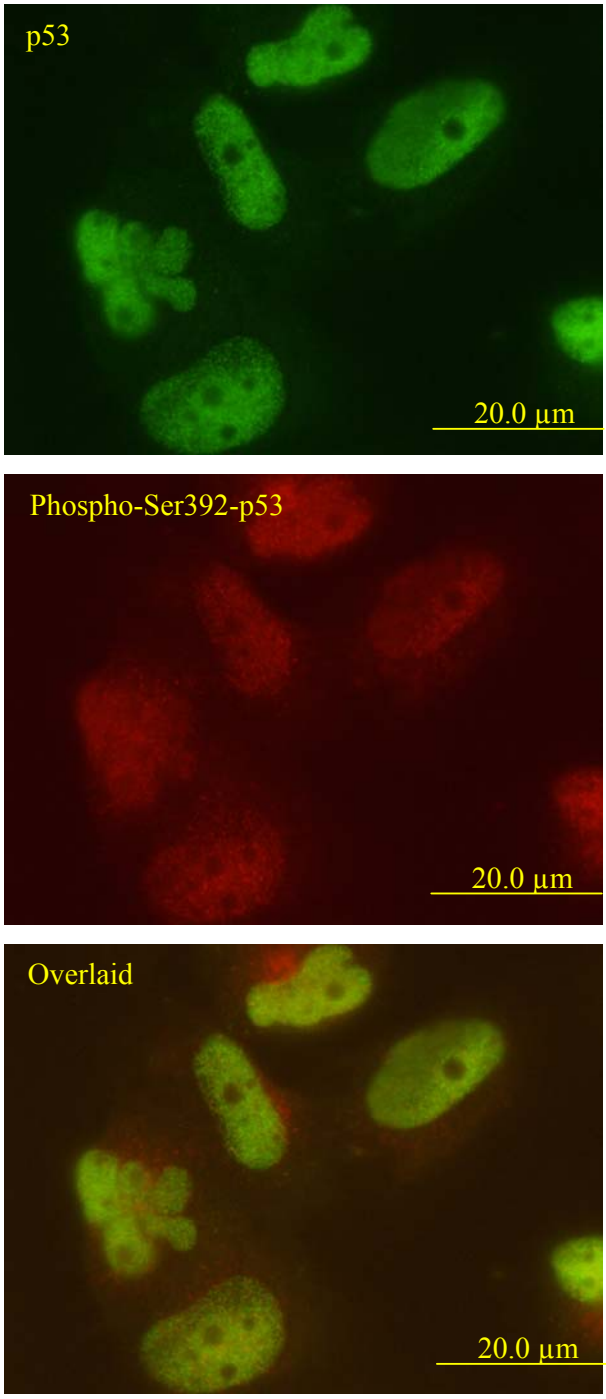

Fig 5.7: Co-localisation of p53 and phospho-Ser392-p53 in A549 cells 24 hr after Cisplatin treatment

Slides viewed under narrow blue wavelength (Green) indicate p53 while slides viewed under WG wavelength (Red) indicate phospho-Ser392-p53.

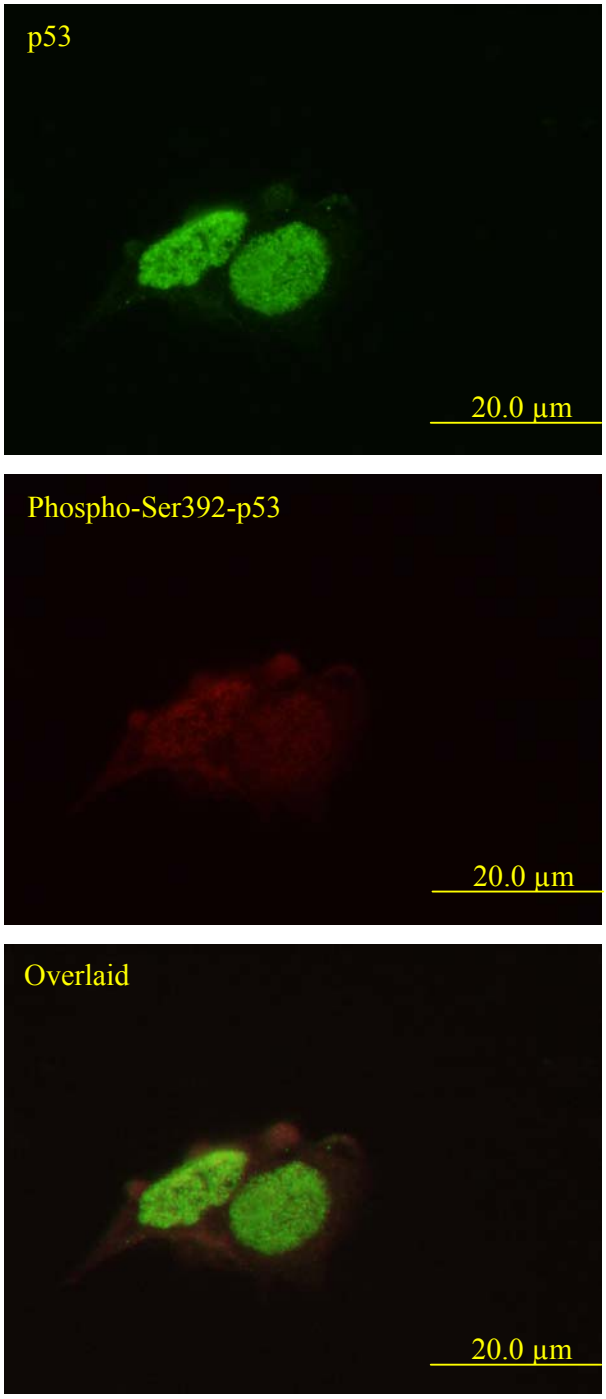

Fig 5.8: Co-localisation of p53 and phospho-Ser392-p53 in A549 cells 48 hr after Cisplatin treatment

Slides viewed under narrow blue wavelength (Green) indicate p53 while slides viewed under WG wavelength (Red) indicate phospho-Ser392-p53.

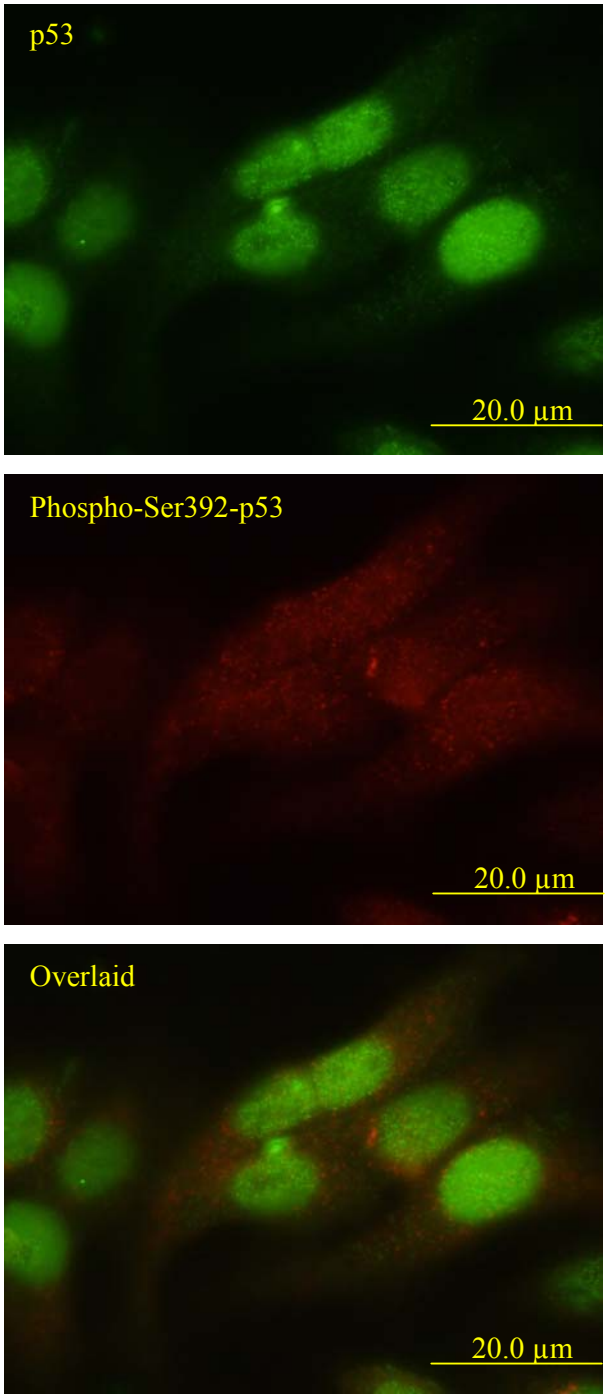

Fig 5.9: Co-localisation of p53 and phospho-Ser392-p53 in A549 cells 2 hr after Nutlin-3 treatment

Slides viewed under narrow blue wavelength (Green) indicate p53 while slides viewed under WG wavelength (Red) indicate phospho-Ser392-p53.

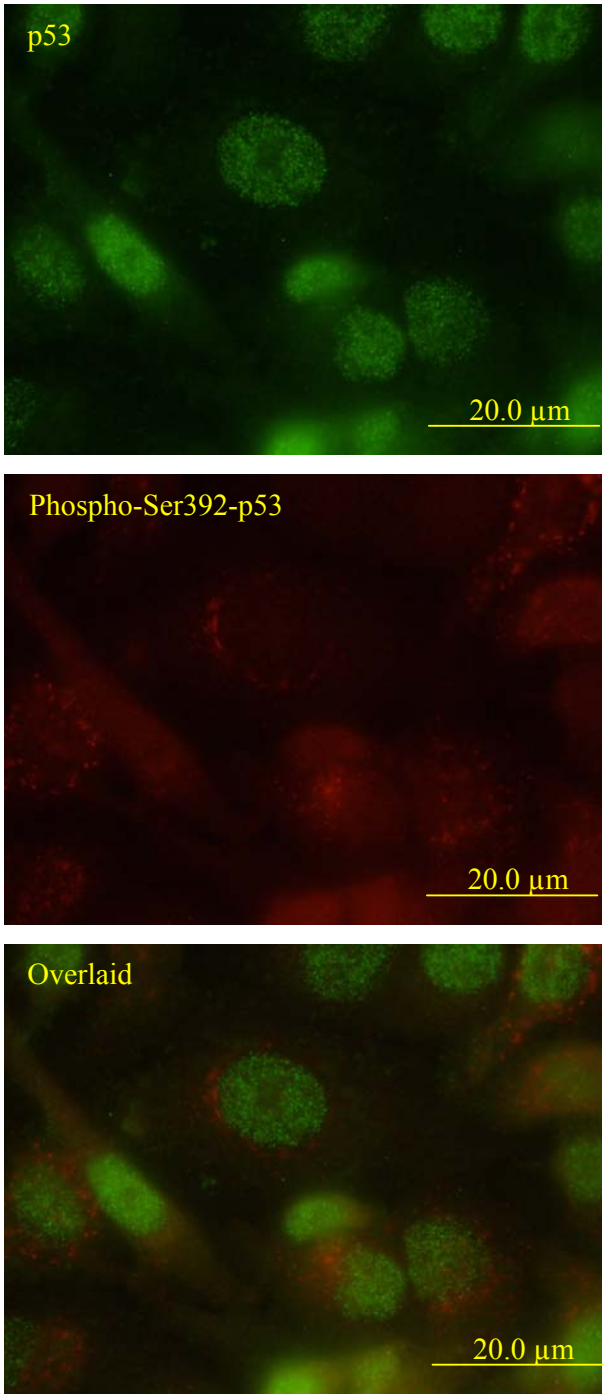

Fig 5.10: Co-localisation of p53 and phospho-Ser392-p53 in A549 cells 8 hr after Nutlin-3 treatment

Slides viewed under narrow blue wavelength (Green) indicate p53 while slides viewed under WG wavelength (Red) indicate phospho-Ser392-p53.

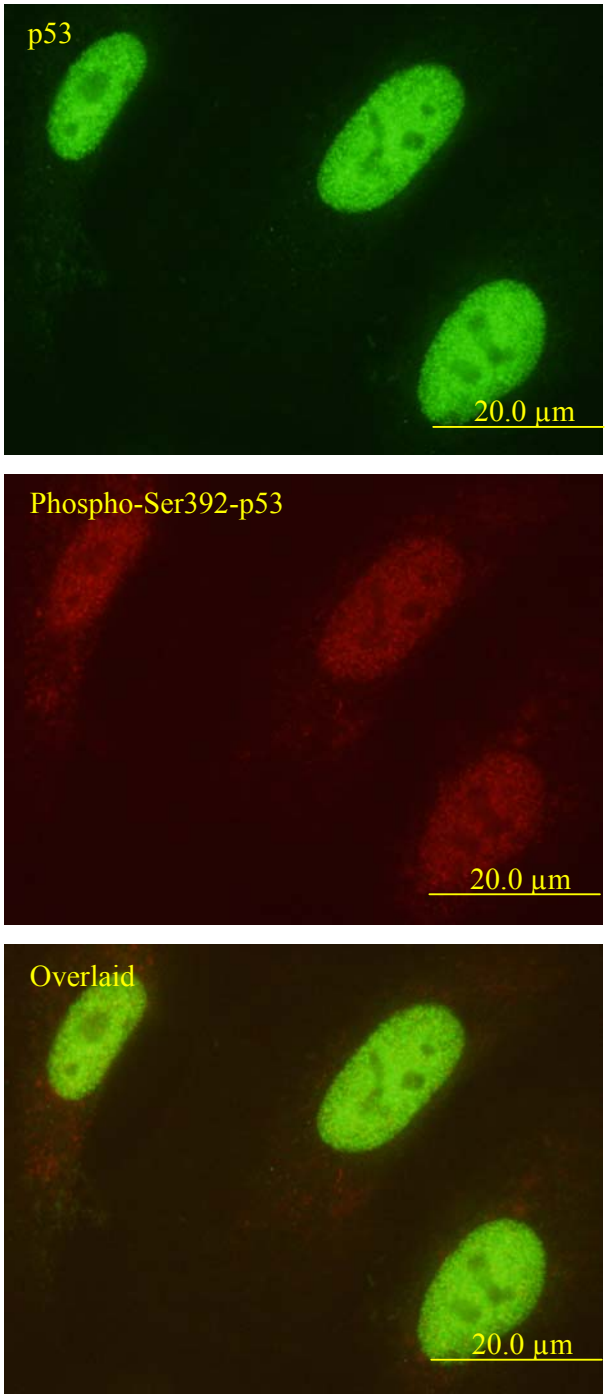

Fig 5.11: Co-localisation of p53 and phospho-Ser392-p53 in A549 cells 24 hr after Nutlin-3 treatment

Slides viewed under narrow blue wavelength (Green) indicate p53 while slides viewed under WG wavelength (Red) indicate phospho-Ser392-p53.

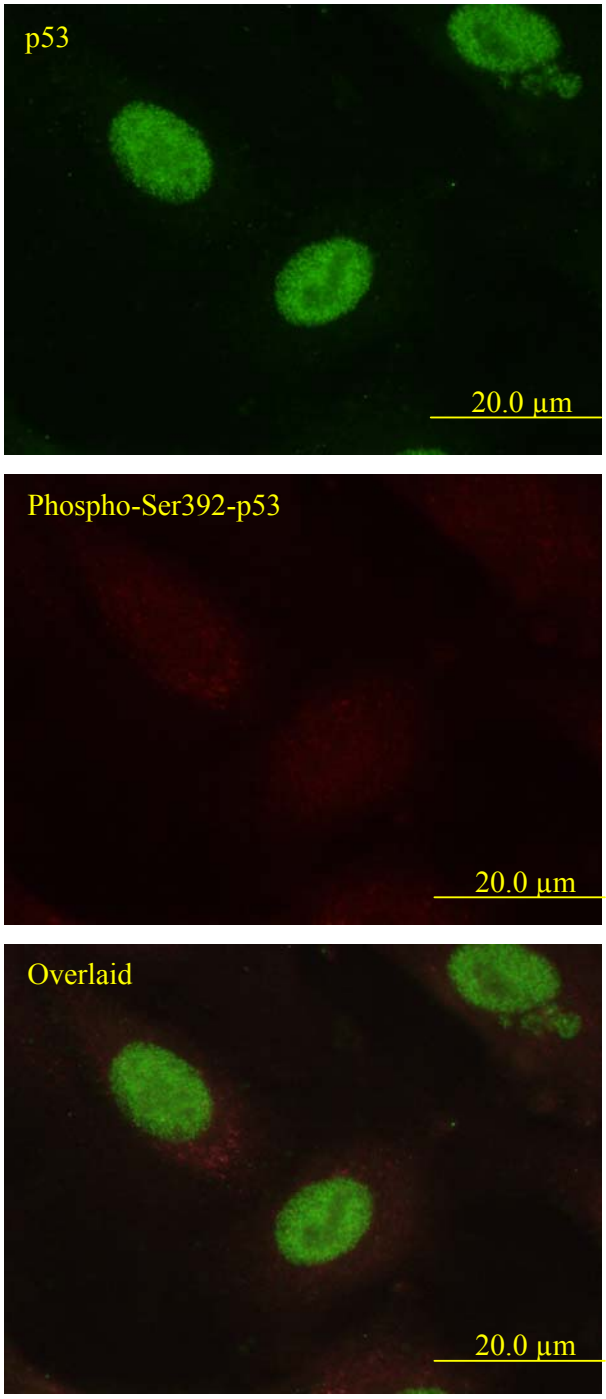

Fig 5.12: Co-localisation of p53 and phospho-Ser392-p53 in A549 48 hr after Nutlin-3 treatment

Slides viewed under narrow blue wavelength (Green) indicate p53 while slides viewed under WG wavelength (Red) indicate phospho-Ser392-p53.

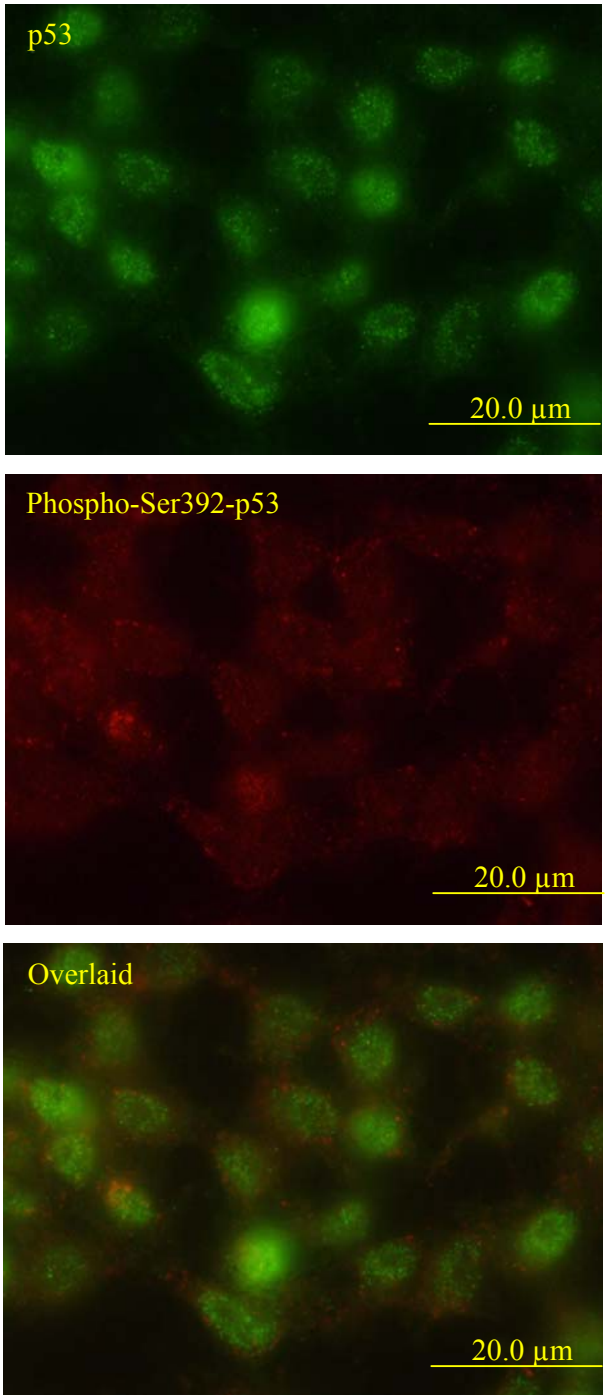

Fig 5.13: Co-localisation of p53 and phospho-Ser392-p53 in RKO cells 2hr after Cisplatin treatment

Slides viewed under narrow blue wavelength (Green) indicate p53 while slides viewed under WG wavelength (Red) indicate phospho-Ser392-p53.

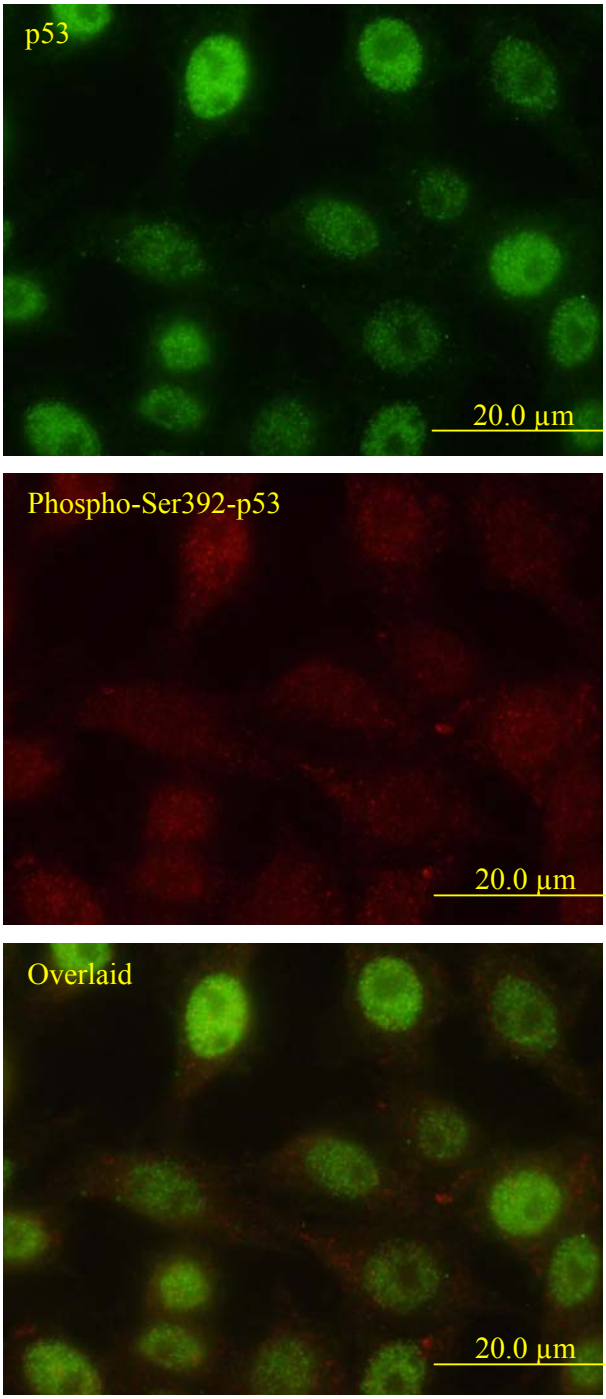

Fig 5.14: Co-localisation of p53 and phospho-Ser392-p53 in RKO cells 8hr after Cisplatin treatment

Slides viewed under narrow blue wavelength (Green) indicate p53 while slides viewed under WG wavelength (Red) indicate phospho-Ser392-p53.

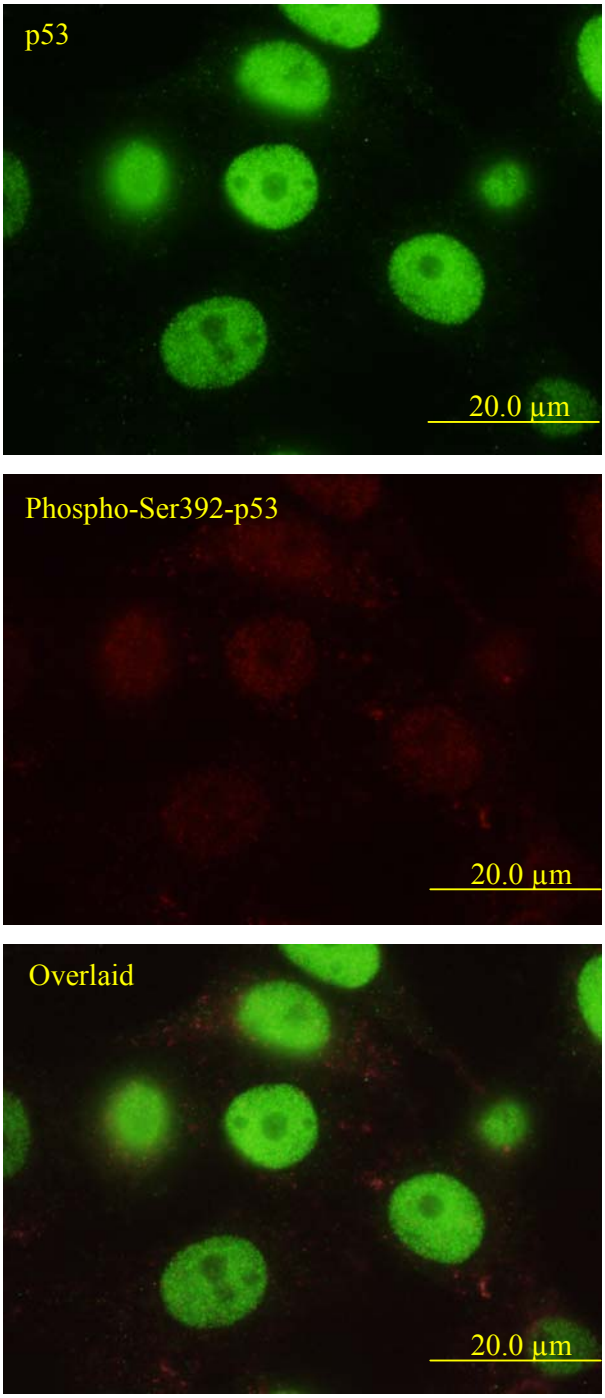

Fig 5.15: Co-localisation of p53 and phospho-Ser392-p53 in RKO cells 24hr after Cisplatin treatment

Slides viewed under narrow blue wavelength (Green) indicate p53 while slides viewed under WG wavelength (Red) indicate phospho-Ser392-p53.

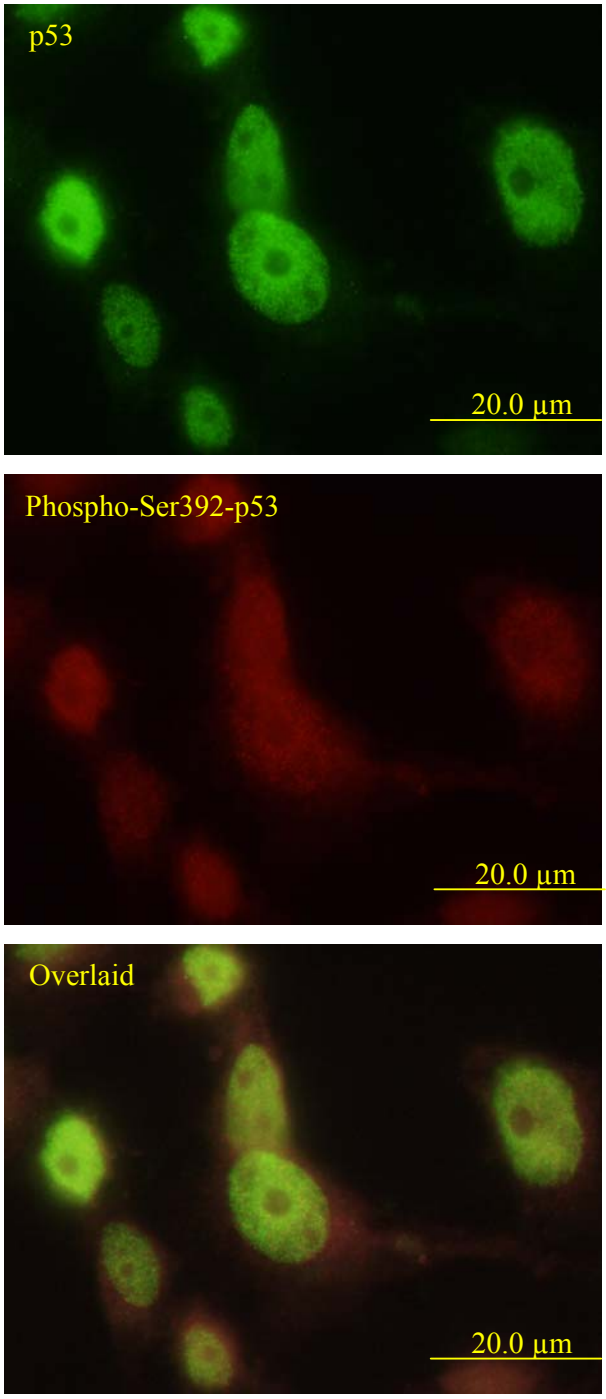

Fig 5.16: Co-localisation of p53 and phospho-Ser392-p53 in RKO cells 48hr after Cisplatin treatment

Slides viewed under narrow blue wavelength (Green) indicate p53 while slides viewed under WG wavelength (Red) indicate phospho-Ser392-p53.

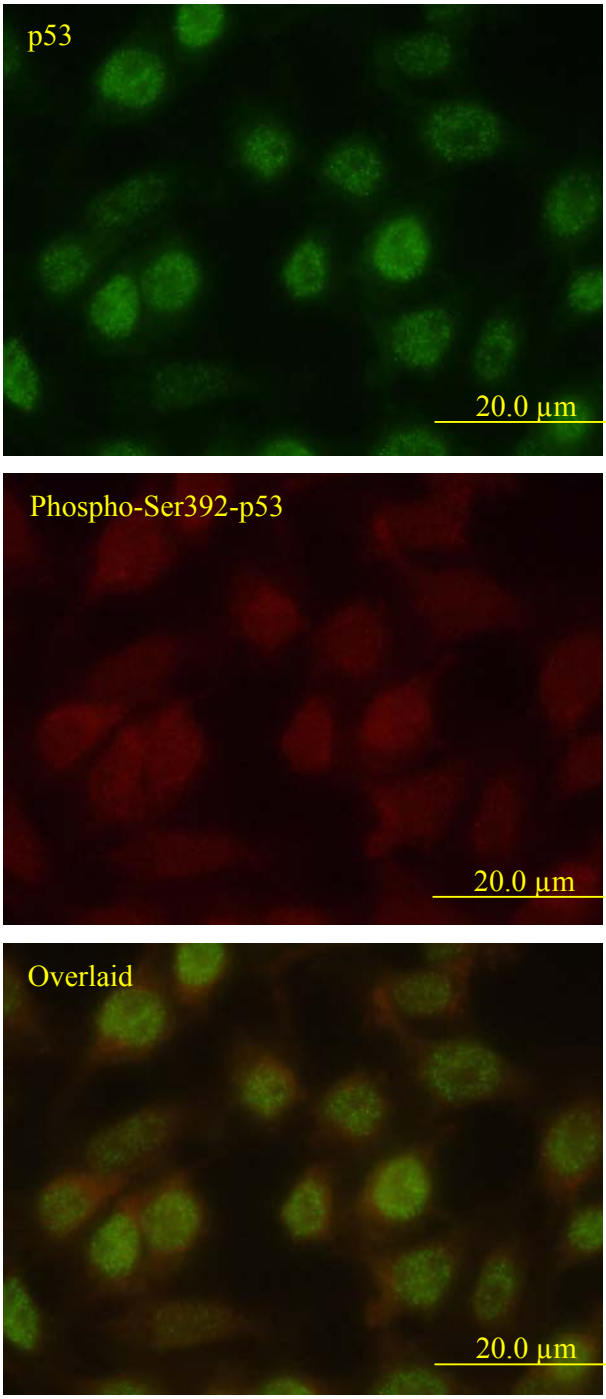

Fig 5.17: Co-localisation of p53 and phospho-Ser392-p53 in RKO cells 2hr after Nutlin-3 treatment

Slides viewed under narrow blue wavelength (Green) indicate p53 while slides viewed under WG wavelength (Red) indicate phospho-Ser392-p53.

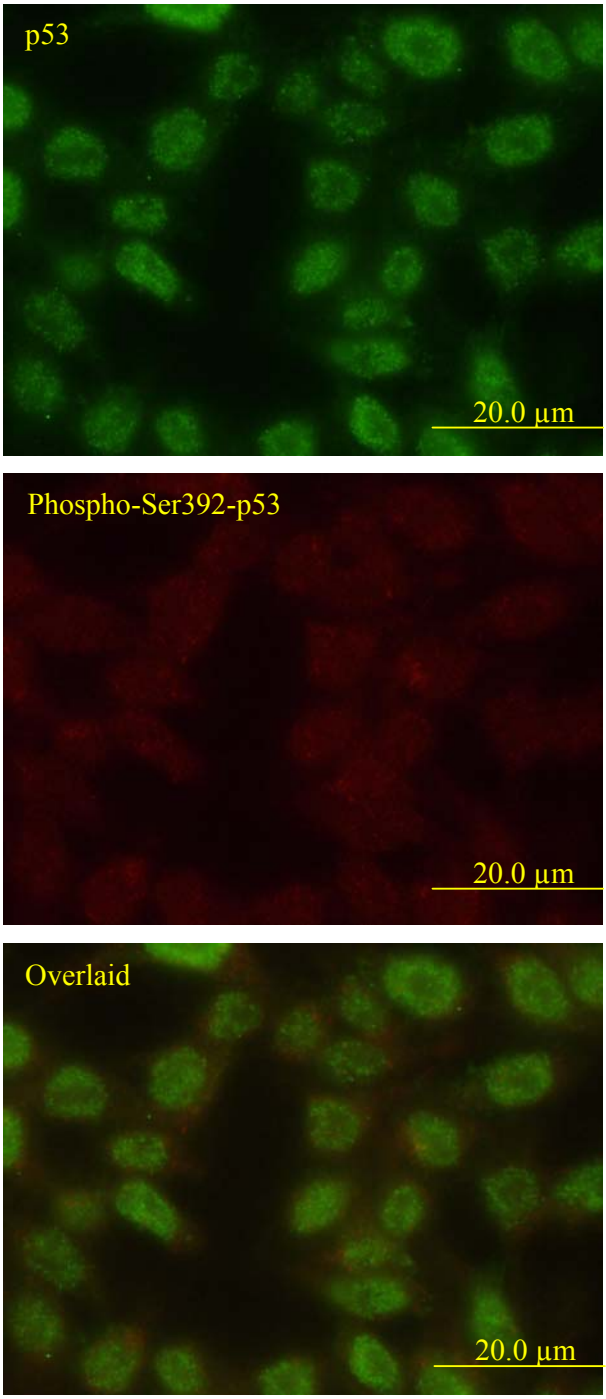

Fig 5.18: Co-localisation of p53 and phospho-Ser392-p53 in RKO cells 8hr after Nutlin-3 treatment

Slides viewed under narrow blue wavelength (Green) indicate p53 while slides viewed under WG wavelength (Red) indicate phospho-Ser392-p53.

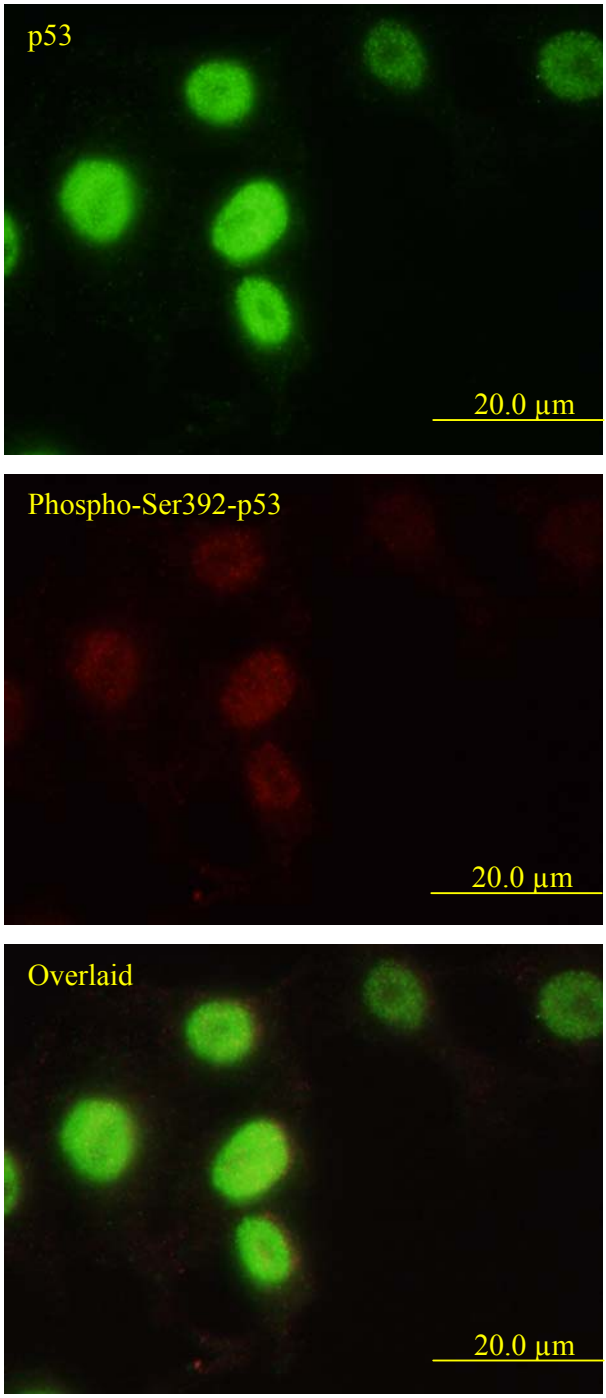

Fig 5.19: Co-localisation of p53 and phospho-Ser392-p53 in RKO cells 24hr after Nutlin-3 treatment

Slides viewed under narrow blue wavelength (Green) indicate p53 while slides viewed under WG wavelength (Red) indicate phospho-Ser392-p53.

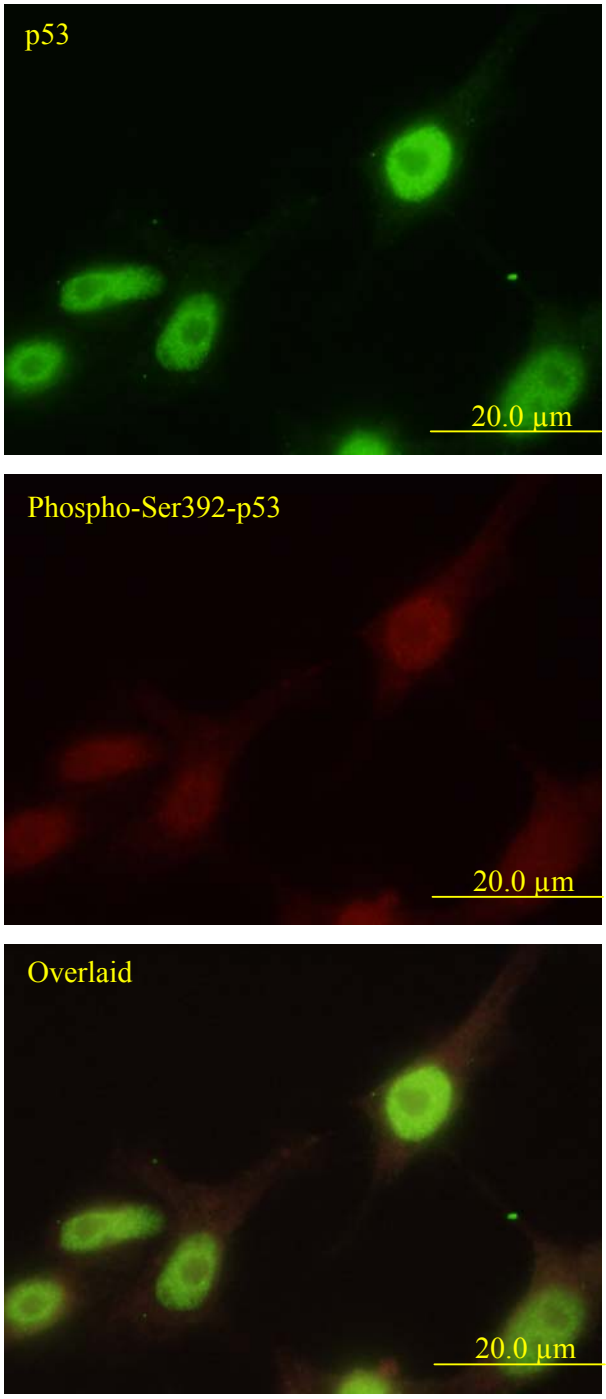

Fig 5.20: Co-localisation of p53 and phospho-Ser392-p53 in RKO cells 48hr after Nutlin-3 treatment

Slides viewed under narrow blue wavelength (Green) indicate p53 while slides viewed under WG wavelength (Red) indicate phospho-Ser392-p53.

An issue in this experiment needs to be pointed out. The antibodies used for p53 was expected to identify all the p53 proteins. However, when the p53 primary antibodies were mixed with phospho-Ser392-p53 primary antibodies, it appeared only to identify the p53 proteins which were not phosphorylated at Ser392 due to the distinct staining patterns displayed in these images (***Fig 5.5-Fig 5.20***). A possible explanation is that the phospho-Ser392-p53 primary antibodies have higher affinity to the phospho-Ser392-p53 and prevent the binding of p53 primary antibodies when used simultaneously.

5.2 Co-localisation of p53 and phospho-Ser392-p53 at differing doses of Cisplatin and Nutlin-3

Studies suggest that increasing the concentration of chemotherapeutic drugs leads to increased cell death via apoptosis while increasing Nutlin-3 concentration showed no induction of apoptosis (112, 113). The data from our lab confirms that increasing Cisplatin concentration leads to increased cell death while high concentrations of Nutlin-3 induce cell-cycle arrest but not cell death. If phosphorylation of p53 at Ser392 were associated with induction of apoptosis, we would expect to see increased levels of Ser392 phosphorylated p53 in Cisplatin treated cells. However, this would not be the case for Nutlin treated cells.

The accumulation of p53 and phospho-Ser392-p53 in response to various doses of treatment were investigated using a double staining immunofluorescence technique. This aims to further identify whether phosphorylation at Ser392 is associated with p53's translocation to the mitochondria thereby inducing transcription-independent apoptosis. A549 and RKO cells were treated with 0, 1, 2, 5, 10μg/ml Cisplatin and 0, 1, 2, 5, 10μM Nutlin-3 for 24 hours. The samples treated with 1μg/ml, 2μg/ml of Cisplatin and 1μM, 2μM of Nutlin-3 showed low levels of p53 in the nucleus while phospho-Ser392-p53 mostly accumulated in the cytoplasm. The intensity of p53 staining increased with increasing dosage while the level of phospho-Ser392-p53

seemed almost unchanged after treatment (***Fig 5.21-Fig 5.24***). In addition, there was no difference between Cisplatin treated samples and Nutlin treated samples suggesting that phosphorylation of Serine 392 is not associated with p53's ability to induce apoptosis via the transcription-independent pathway (***Fig 5.21-Fig 5.24***).

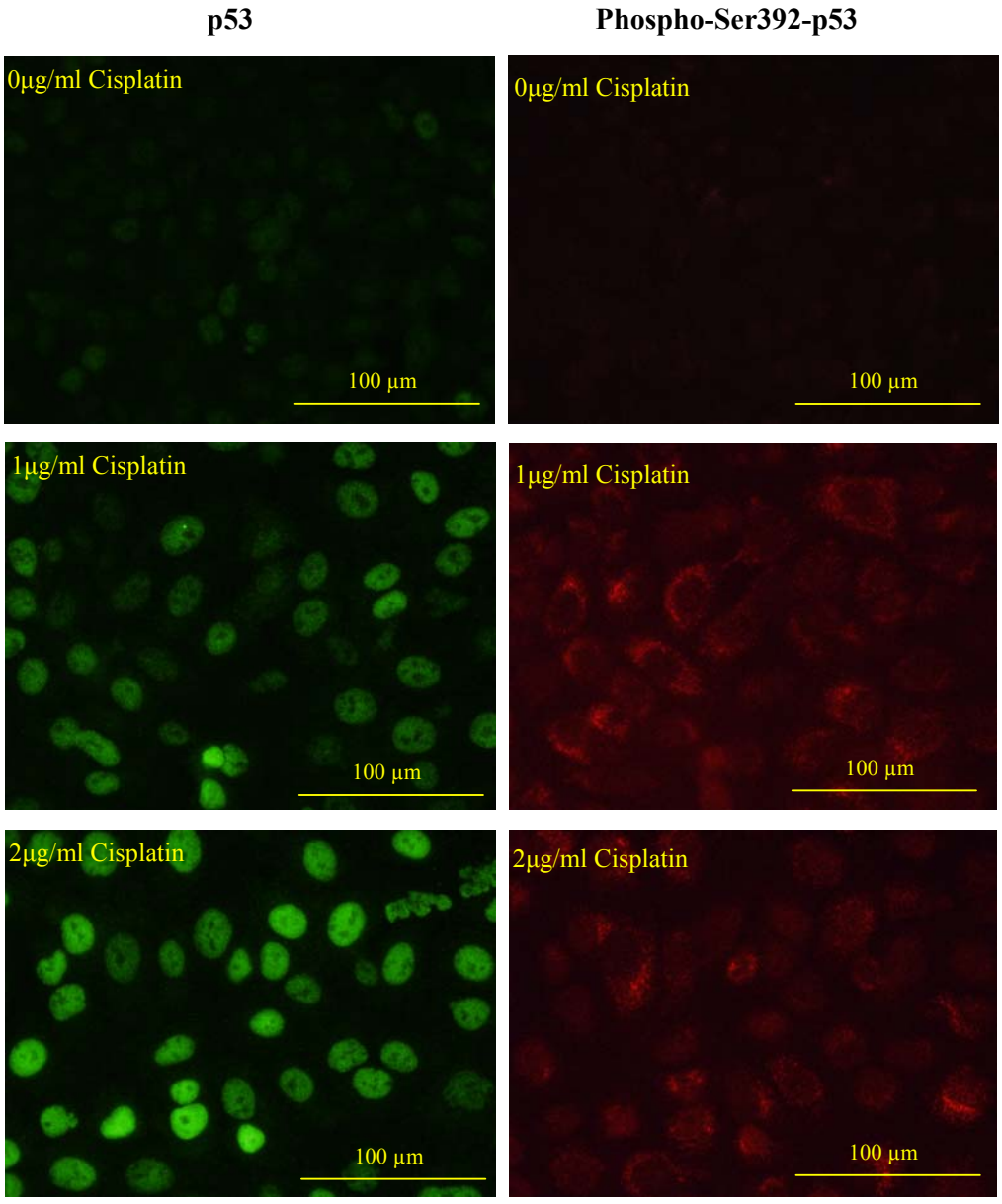

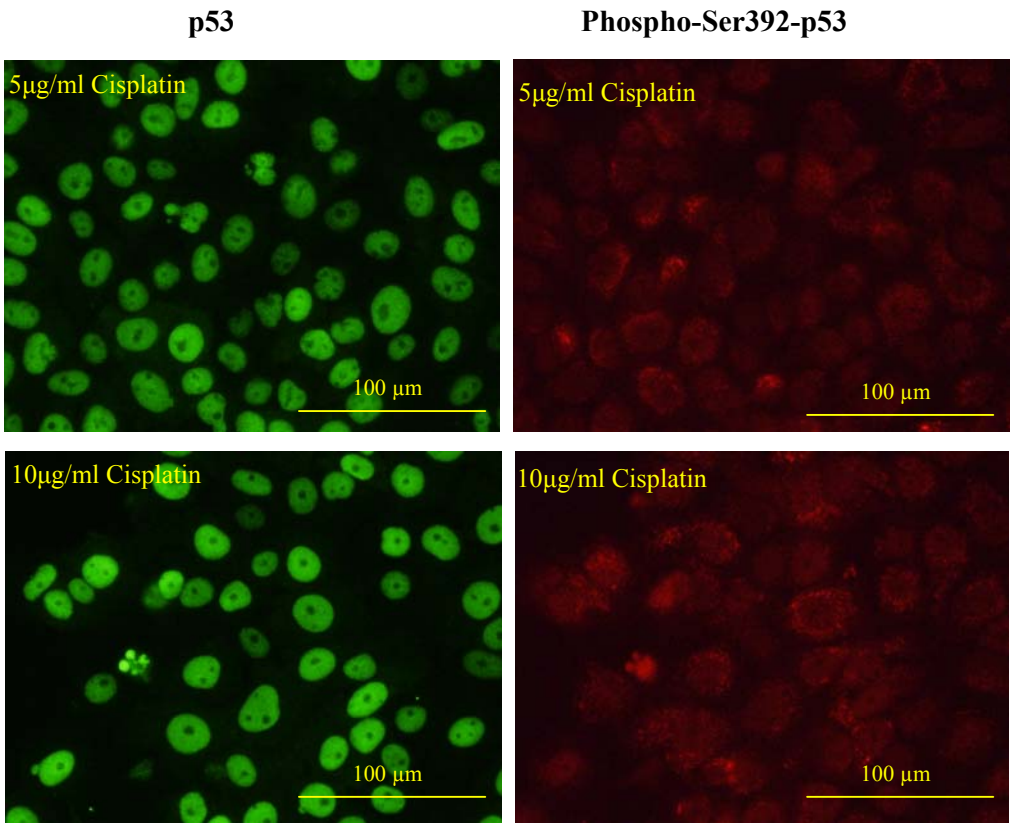

Fig 5.21: Co-localisation of p53 and phospho-Ser392-p53 in A549 cells at different doses of Cisplatin

A549 cells were treated with various doses of Cisplatin. Immunofluorescence was performed after 24 hr. Images were taken using NIBA mirror unit for p53 and WG mirror unit for phospho-Ser392-p53 at 400× magnification.

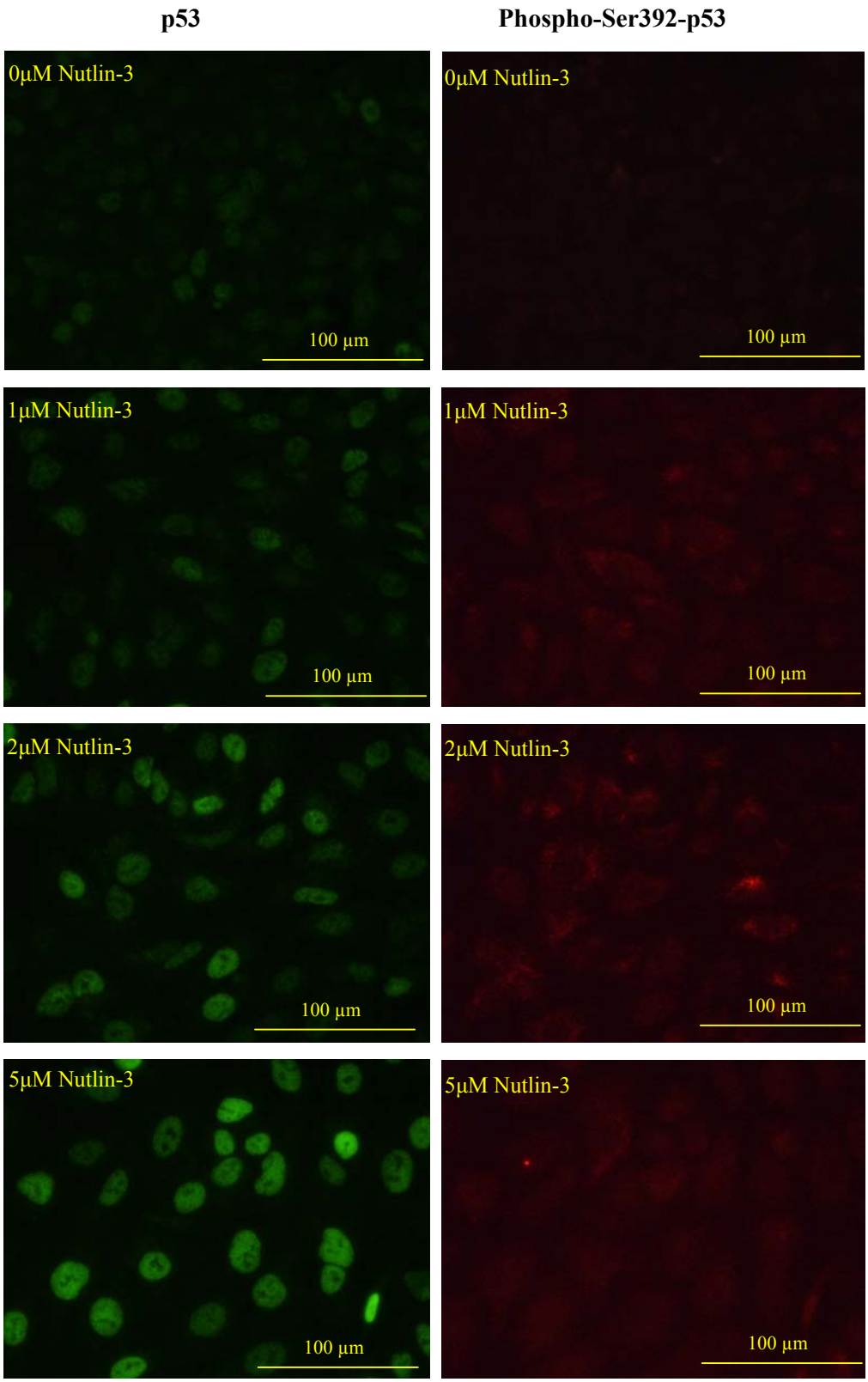
p53
Phospho-Ser392-p53
0μM Nutlin-3
0μM Nutlin-3
100 μm
100 μm
1μM Nutlin-3
1μM Nutlin-3
100 μm
100 μm
2μM Nutlin-3
2μM Nutlin-3
100 μm
100 μm
5μM Nutlin-3
5μM Nutlin-3
100 μm
100 μm

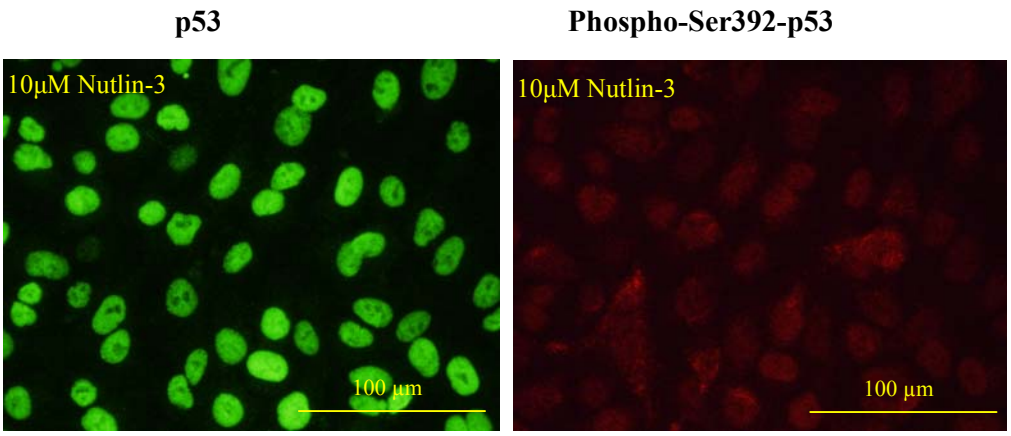

Fig 5.22: Co-localisation of p53 and phospho-Ser392-p53 in A549 cells at different doses of Nutlin-3

A549 cells were treated with various doses of Nutlin-3. Immunofluorescence was performed after 24 hr. Images were taken using NIBA mirror unit for p53 and WG mirror unit for phospho-Ser392-p53 at 400× magnification.

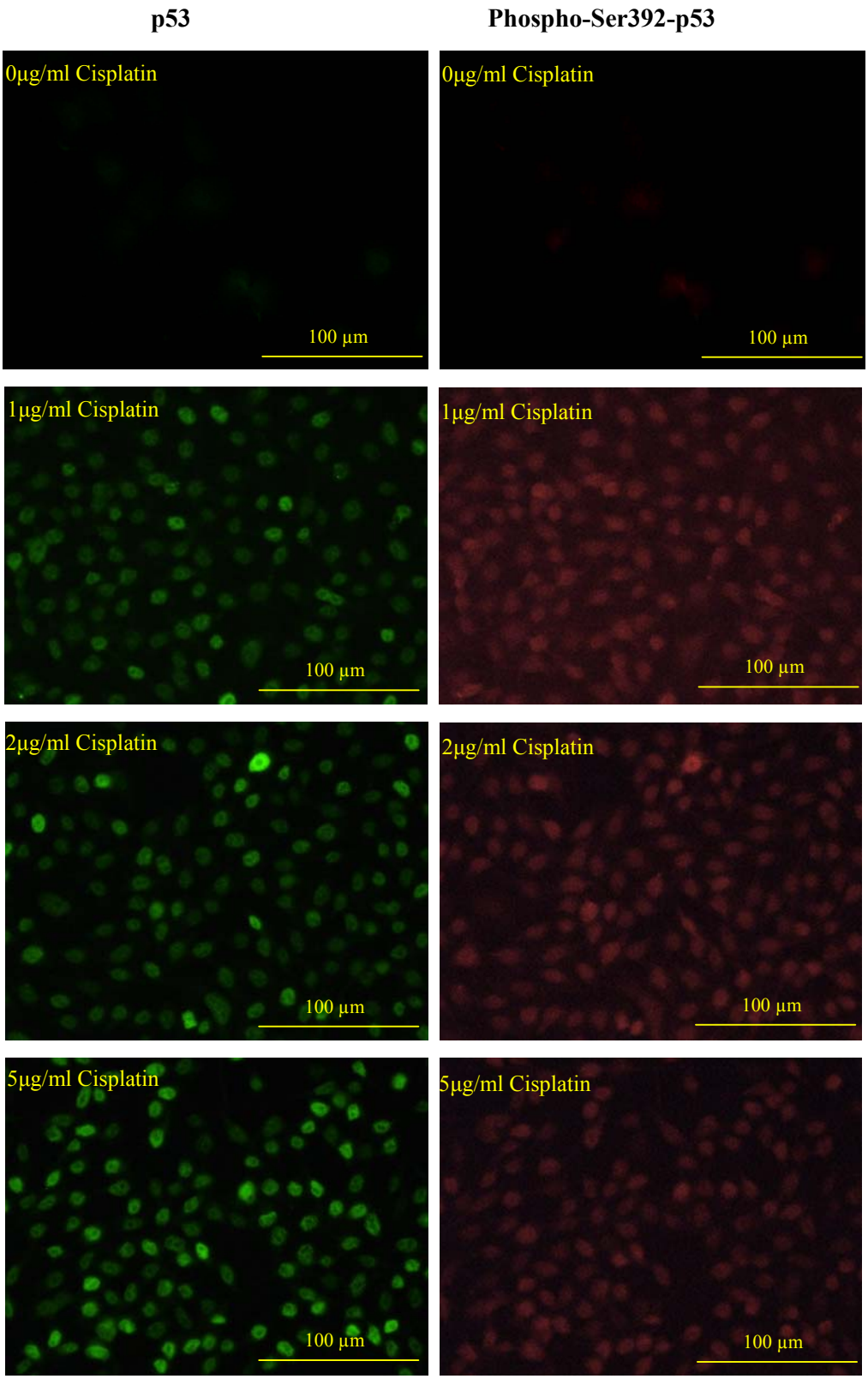
p53
Phospho-Ser392-p53
0μg/ml Cisplatin
0μg/ml Cisplatin
100 μm
100 μm
1μg/ml Cisplatin
1μg/ml Cisplatin
100 μm
100 μm
2μg/ml Cisplatin
2μg/ml Cisplatin
100 μm
100 μm
5μg/ml Cisplatin
5μg/ml Cisplatin
100 μm
100 μm

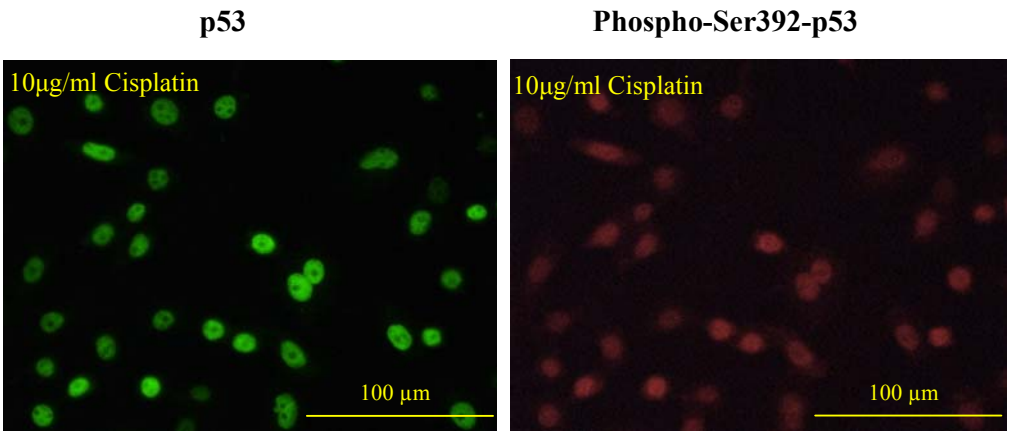

Fig 5.23: Co-localisation of p53 and phospho-Ser392-p53 in RKO cells at differing doses of Cisplatin

RKO cells were treated with various doses of Cisplatin. Immunofluorescence was performed after 24 hr. Images were taken using NIBA mirror unit for p53 and WG mirror unit for phospho-Ser392-p53 at 400× magnification.

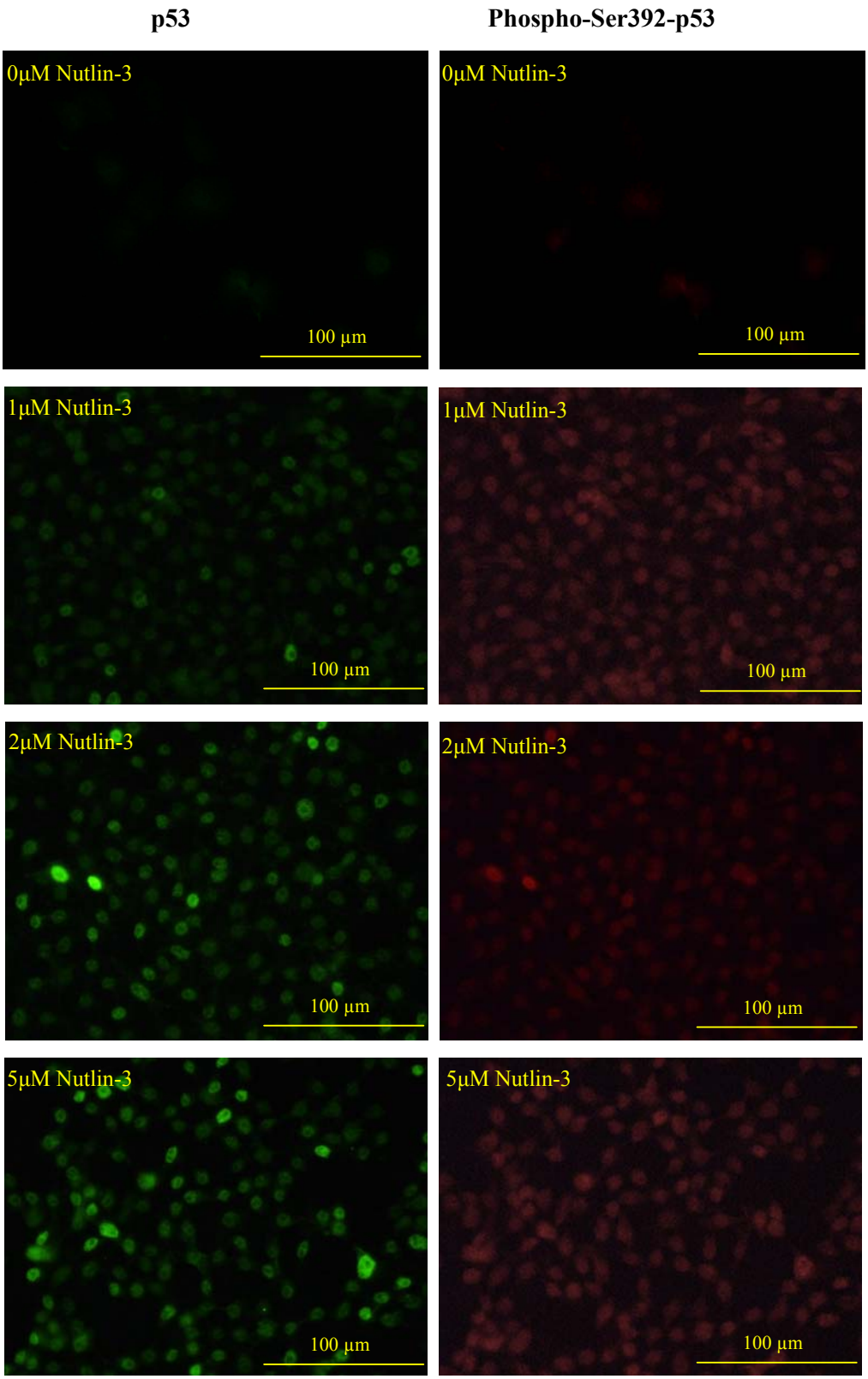
p53
Phospho-Ser392-p53
0μM Nutlin-3
0μM Nutlin-3
100 μm
100 μm
1μM Nutlin-3
1μM Nutlin-3
100 μm
100 μm
2μM Nutlin-3
2μM Nutlin-3
100 μm
100 μm
5μM Nutlin-3
5μM Nutlin-3
100 μm
100 μm

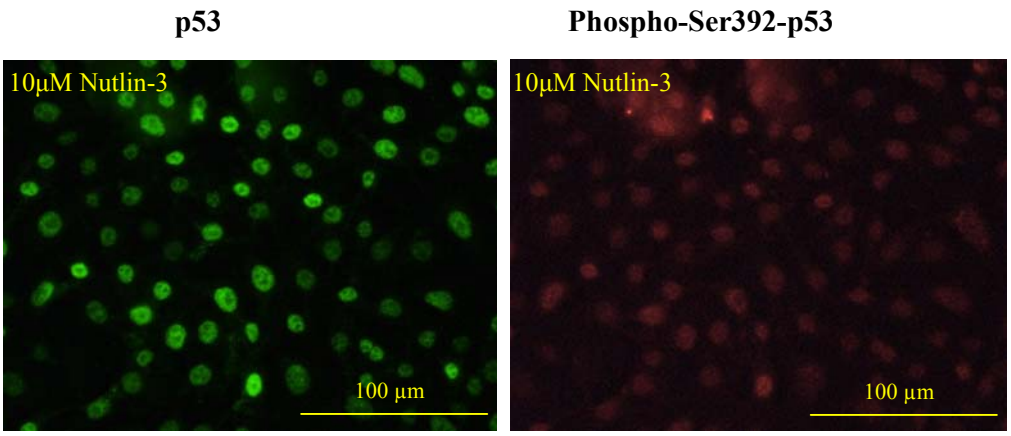

Fig 5.24: Co-localisation of p53 and phospho-Ser392-p53 in RKO cells at differing doses of Nutlin-3

RKO cells were treated with various doses of Nutlin-3.Immunofluorescence was performed after 24 hr. Images were taken using NIBA mirror unit for p53 and WG mirror unit for phospho-Ser392-p53 at 400× magnification.

5.3 Co-localization of phospho-Ser392-p53 and mitochondria

Phosphorylation at Serine392 is suggested to be related to p53's nucleocytoplasmic shuttling ability (111), but whether it is related to p53's translocation to the mitochondria remains unclear. To identify whether phospho-Ser392-p53 is localized to the mitochondria, an immunofluorescence double staining procedure simultaneously staining phospho-Ser392-p53 and mitochondria was used. A549 cells and RKO cells were treated with 10μg/ml Cisplatin and 10μM Nutlin-3, and fixed after 0 hour, 2 hours and 24hours. Images were viewed at 1000× magnification.

From our data, although the phospho-Ser392-p53 was distributed in the cytoplasm after 2 hours treatment, it was not exclusively associated with mitochondria. After 24 hours treatment, p53 phoshorylated at Ser392 appeared in the nucleus. Additionally, Nutlin-3 treated cells displayed similar patterns to Cisplatin treated cells suggesting phosphorylation of p53 at Ser392 is not associated with the transcription-independent pathway of apoptosis (***Fig 5.25- Fig 5.32***).

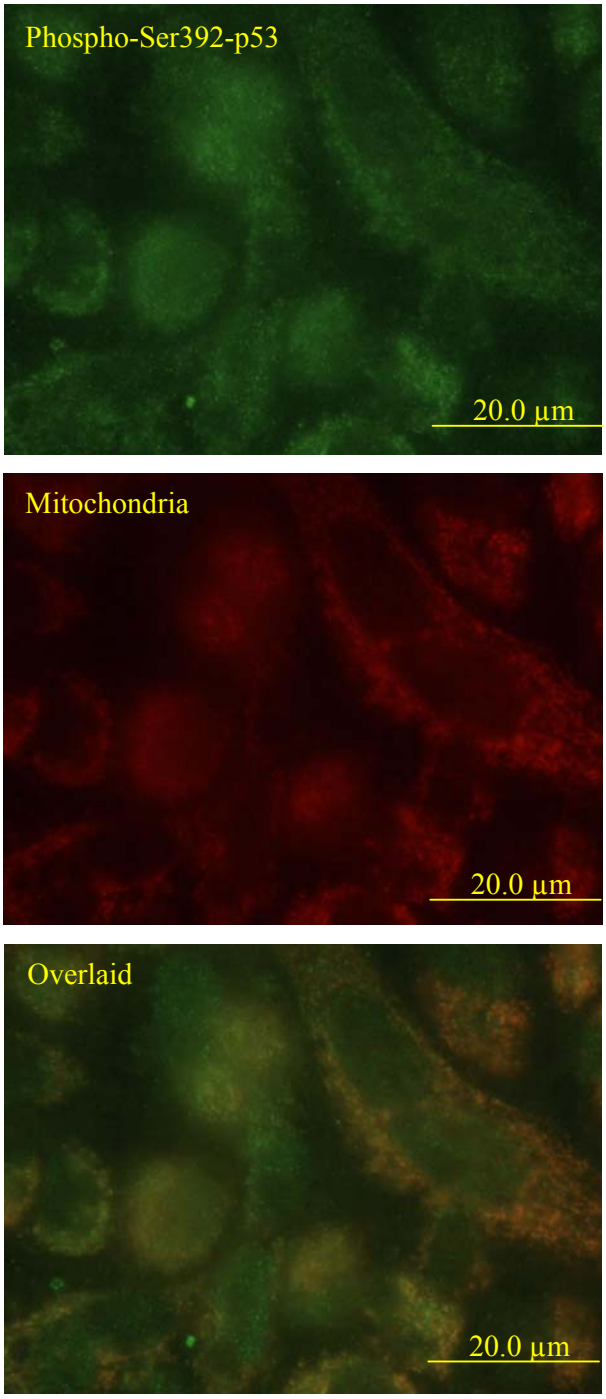

Fig 5.25: Co-localization of phospho-Ser392-p53 and mitochondria in A549 cells 2hr after Cisplatin treatment

Slides viewed under narrow blue wavelength (Green) indicate phospho-Ser392-p53 while slides viewed under WG wavelength (Red) indicate mitochondria.

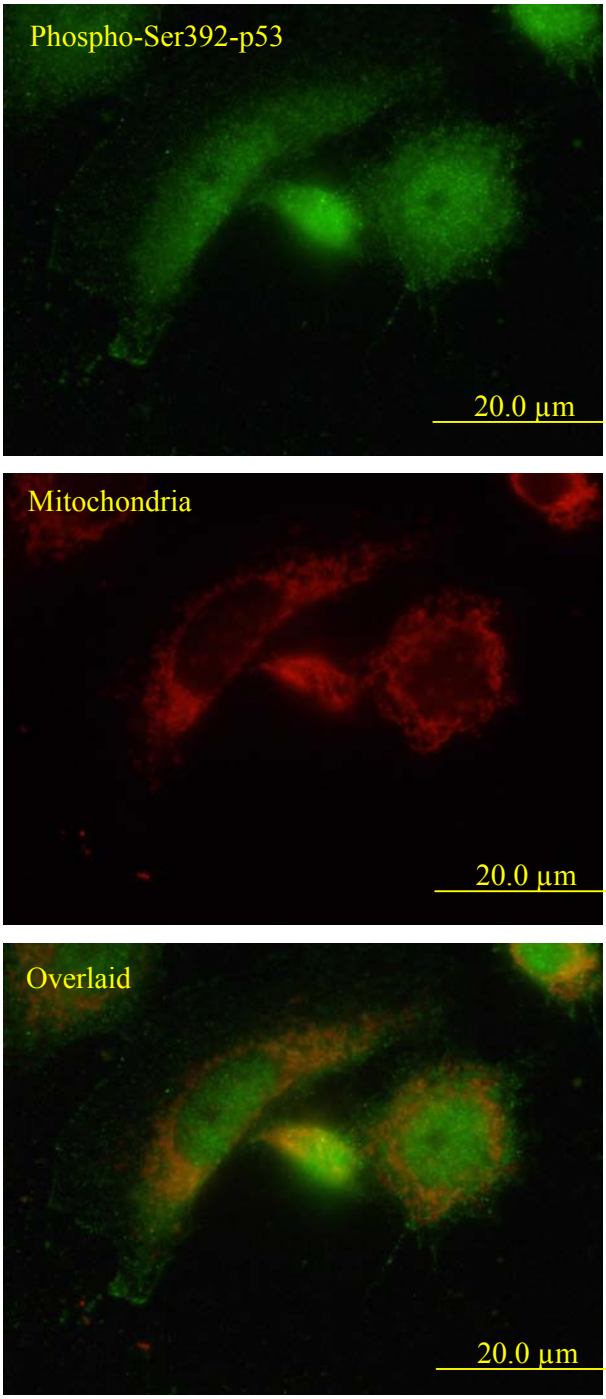

Fig 5.26: Co-localization of phospho-Ser392-p53 and mitochondria in A549 cells 24hr after Cisplatin treatment

Slides viewed under narrow blue wavelength (Green) indicate phospho-Ser392-p53 while slides viewed under WG wavelength (Red) indicate mitochondria.

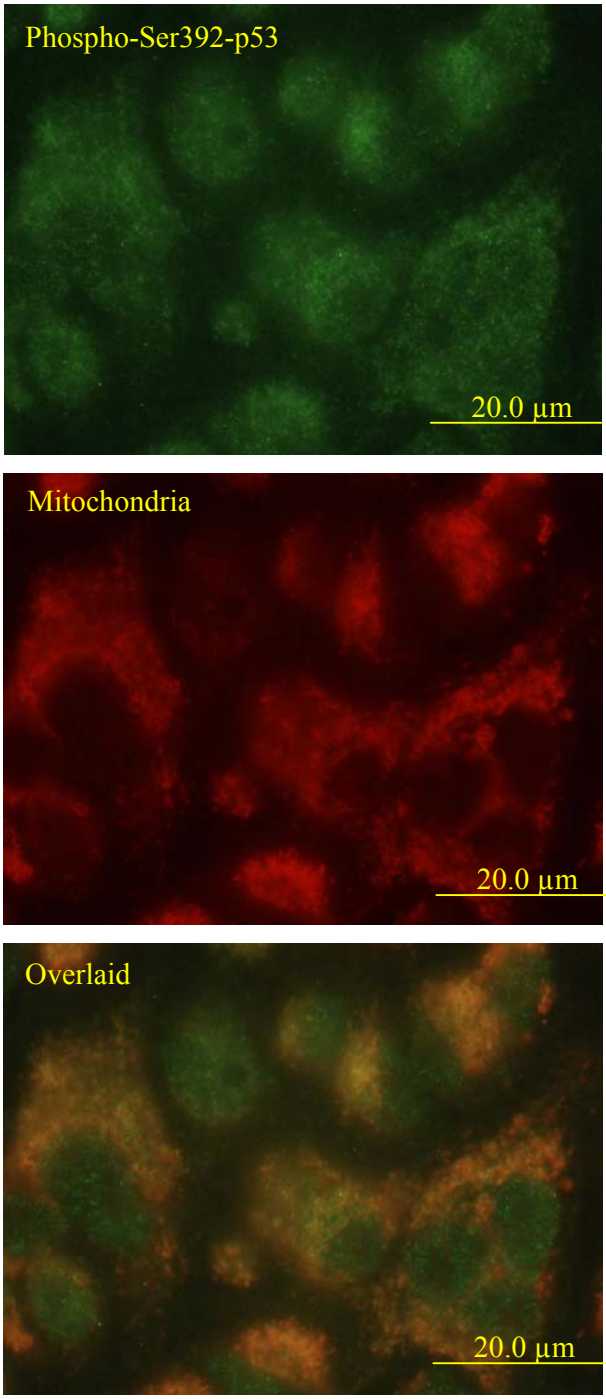

Fig 5.27: Co-localization of phospho-Ser392-p53 and mitochondria in A549 cells 2hr after Nutlin-3 treatment

Slides viewed under narrow blue wavelength (Green) indicate phospho-Ser392-p53 while slides viewed under WG wavelength (Red) indicate mitochondria.

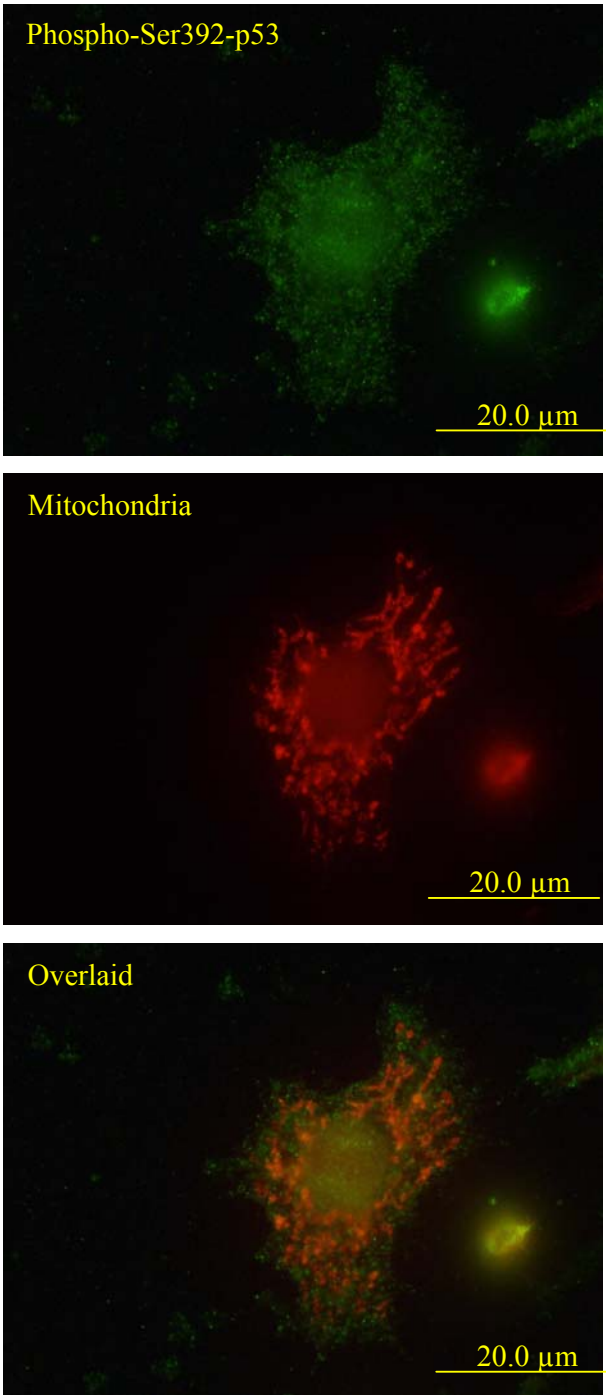

Fig 5.28: Co-localization of phospho-Ser392-p53 and mitochondria in A549 cells 24hr after Nutlin-3 treatment

Slides viewed under narrow blue wavelength (Green) indicate phospho-Ser392-p53 while slides viewed under WG wavelength (Red) indicate mitochondria.

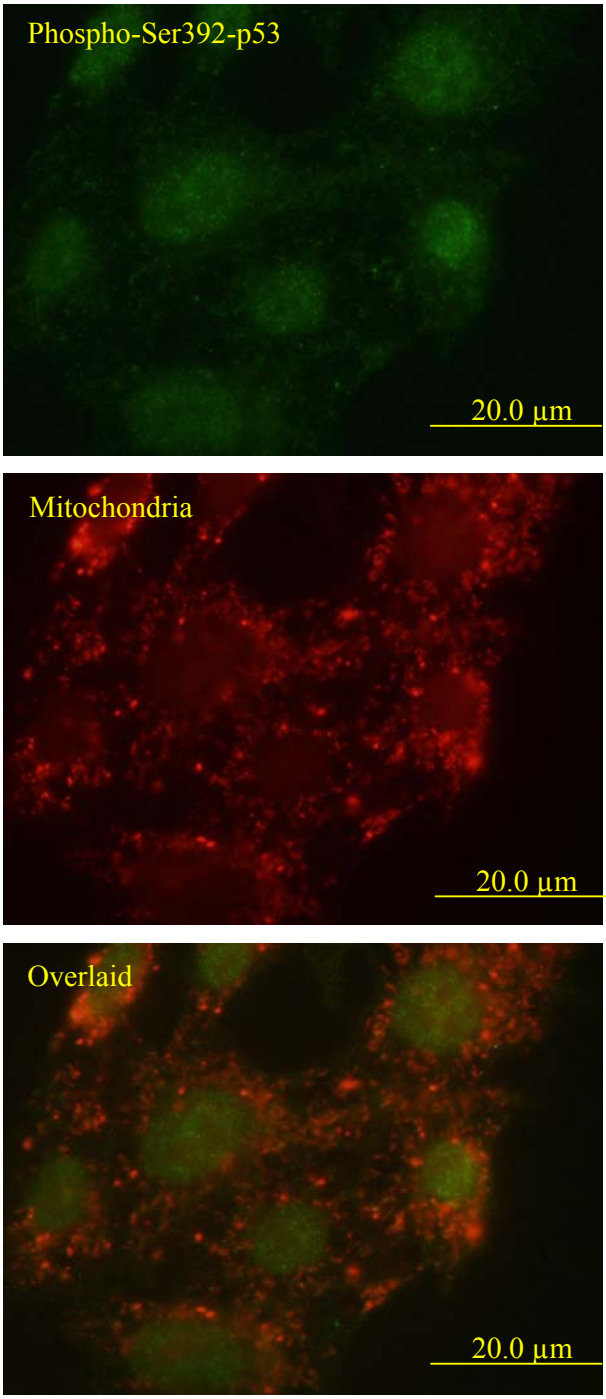

Fig 5.29: Co-localization of phospho-Ser392-p53 and mitochondria in RKO cells 2hr after Cisplatin treatment

Slides viewed under narrow blue wavelength (Green) indicate phospho-Ser392-p53 while slides viewed under WG wavelength (Red) indicate mitochondria.

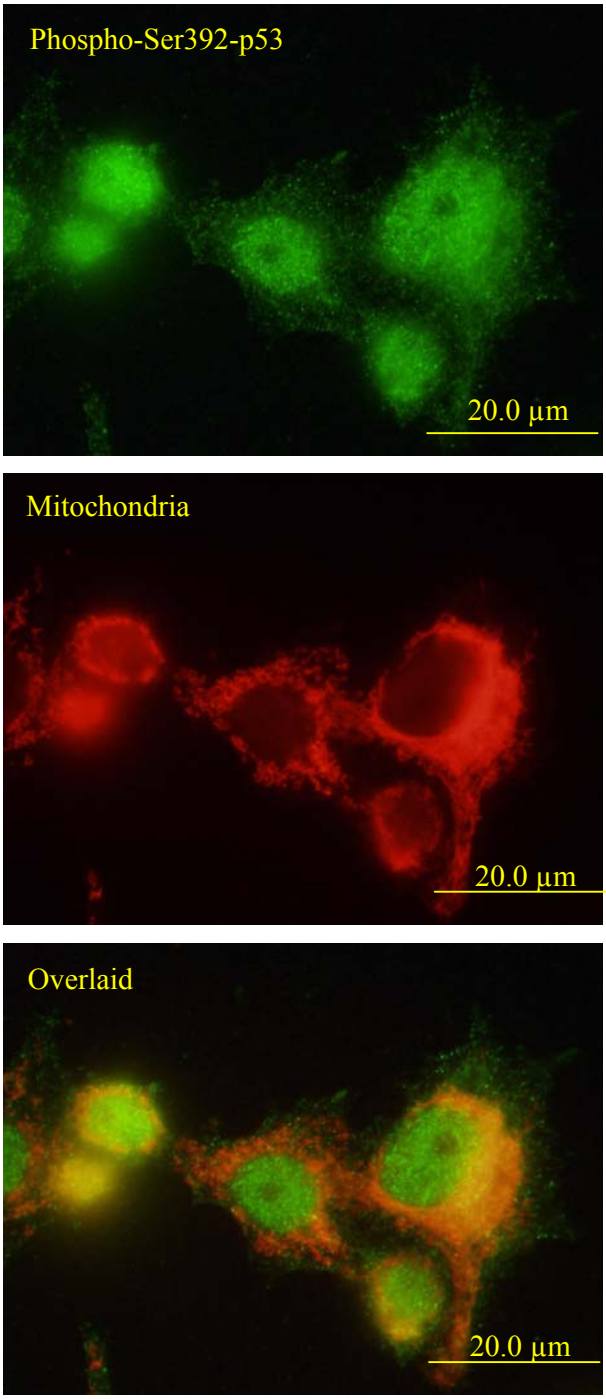

Fig 5.30: Co-localization of phospho-Ser392-p53 and mitochondria in RKO cells 24hr after Cisplatin treatment

Slides viewed under narrow blue wavelength (Green) indicate phospho-Ser392-p53 while slides viewed under WG wavelength (Red) indicate mitochondria.

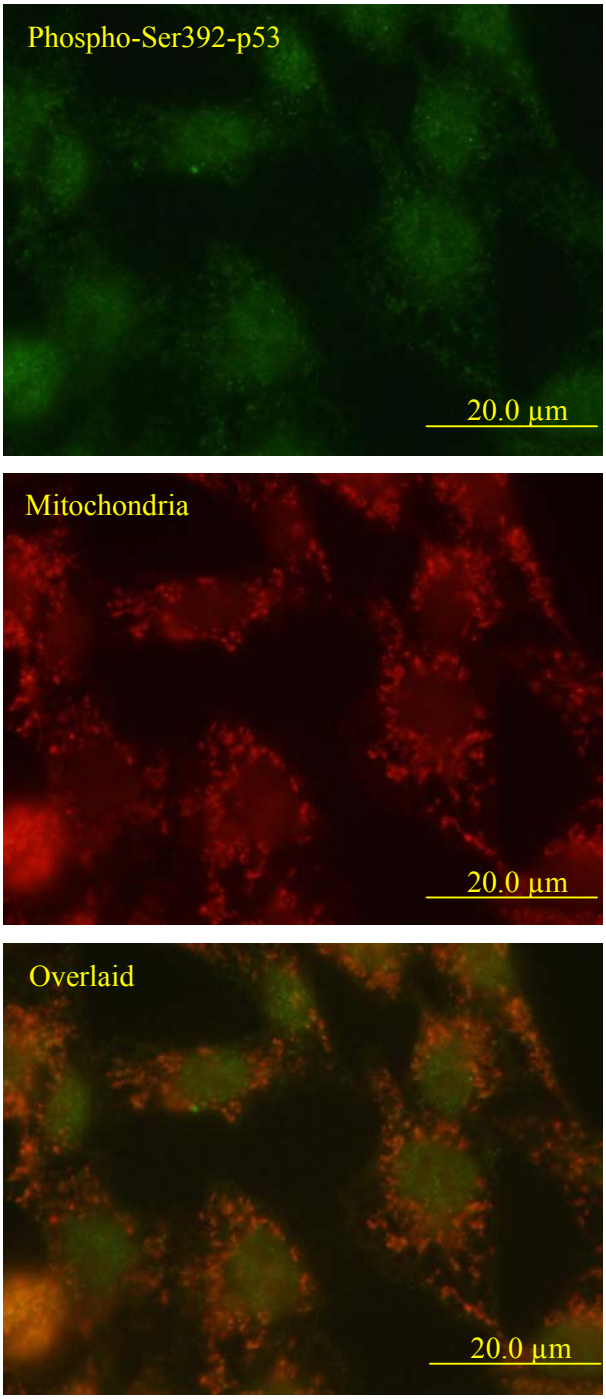

Fig 5.31: Co-localization of phospho-Ser392-p53 and mitochondria in RKO cells 2hr after Nutlin-3 treatment

Slides viewed under narrow blue wavelength (Green) indicate phospho-Ser392-p53 while slides viewed under WG wavelength (Red) indicate mitochondria.

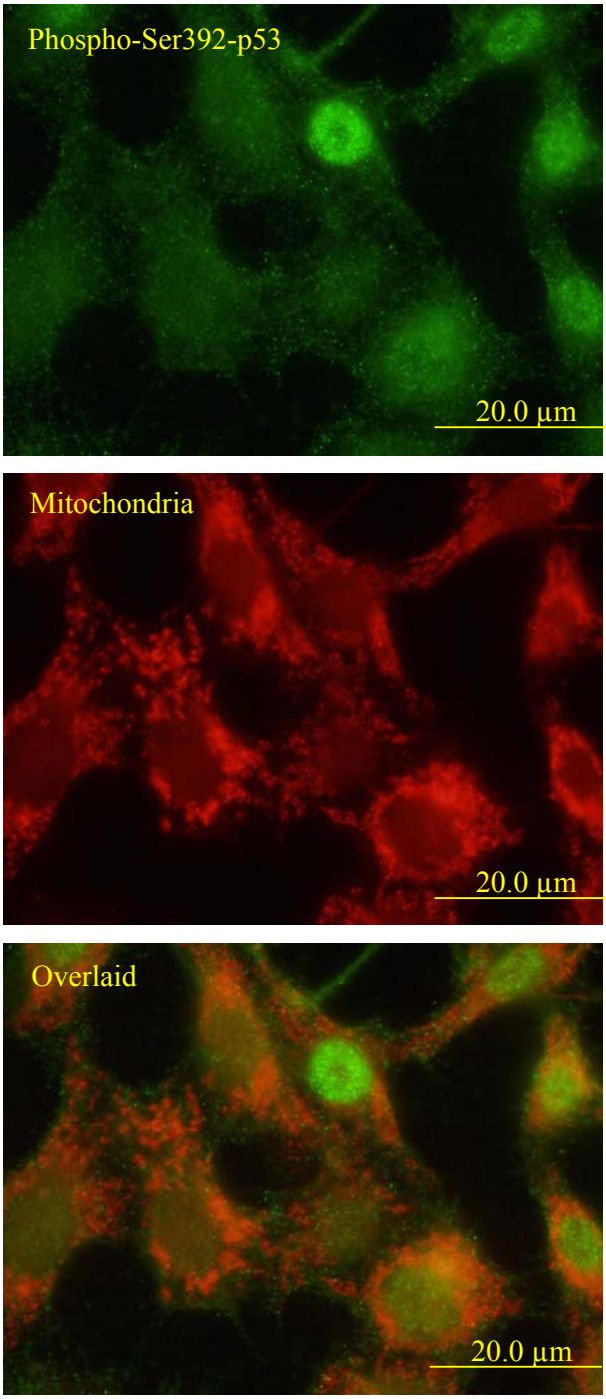

Fig 5.32: Co-localization of phospho-Ser392-p53 and mitochondria in RKO cells 24hr after Nutlin-3 treatment

Slides viewed under narrow blue wavelength (Green) indicate phospho-Ser392-p53 while slides viewed under WG wavelength (Red) indicate mitochondria.

CHAPTER VI

Discussion

While it is clear that p53 can regulate entry into either the cell cycle arrest or apoptotic pathway, it is less clear how it is able to differentiate between these disparate events. There are several possible theories to explain p53's differential ability. Some studies have suggested that p53 needs to reach a threshold prior to transactivation of apoptotic genes (22) while others suggested post-translational modifications are responsible for conformational changes of p53 which may affect the preference to the promoters of its target genes (65). Another theory has suggested that p53's interaction with proteins involved in apoptosis or cell cycle arrest might be a possible strategy to induce these different responses (86). Moreover, p53's translocation to the mitochondria thereby initializing transcription-independent pathway of apoptosis may be critical to p53's differential function (114). In our project, we constructed a model that demonstrated similar high level p53 accumulation in the nucleus but with very different functional responses. We used this model to examine how p53 is able to differentiate between cell cycle arrest and apoptosis and in particular studied the localization of p53 and phosphorylation at Ser392 which is speculated to be associated with p53's nucleocytoplasmic shuttling ability (111).

6.1 Cisplatin and Nutlin-3 induce similar high level nuclear p53 accumulation

6.1.1 p53 accumulates to high levels following Cisplatin and Nutlin-3 treatment

In Chapter III, we demonstrated that Cisplatin and Nutlin both induce high levels of p53 accumulation in the nucleus. However, this p53 accumulation elicits very

different functional responses with Cisplatin inducing apoptosis and Nutlin-3 inducing cell cycle arrest (Chapter IV). Previous studies have suggested that this differential ability of p53 is due to transactivation of different sets of genes involved in apoptosis or cell cycle arrest, and this transactivation may depend on the level of p53 (22). This theory also suggests that cell cycle arrest genes have a high affinity for p53 and thus are activated at low levels while apoptotic genes have a lower affinity thereby requiring higher levels of p53 for transactivation (22). Our results would not support this theory as we demonstrated cell cycle arrest in the presence of high levels of p53 accumulation with no evidence of apoptosis.

6.1.2 p53 accumulates in the nucleus following Cisplatin and Nutlin-3 treatment

Recent studies have found that a proportion of p53 translocates to the mitochondria and initiates the apoptotic cascade through interaction with mitochondrial membrane proteins (114). However, in our results presented in Chapter III and IV, p53 gradually localized in the nucleus with maximal nuclear accumulation occurring between 12-24 hours following either Cisplatin or Nutlin-3 treatment. This may suggest that p53's activity is most likely transcriptionally driven. However, there remains the possibility that low levels of p53 may still reside outside of the nucleus and possibly associate with cytoplasmic organelles such as the mitochondria.

Another theory has suggested that p53 might be associated with different sets of proteins which play particular roles in apoptosis or cell cycle arrest (82-84). Although similar patterns of p53 accumulation were observed following Cisplatin and Nutlin-3 treatment, it is unclear whether p53 interacts with the same proteins in apoptotic cells or those in cell cycle arrest. Therefore, it may be interesting to investigate the protein-protein interaction between p53 and other proteins involved in our model.

6.1.3 Nutlin-3 and Cisplatin treatment induce similar transactivation of p53 dependent cell cycle arrest and apoptotic genes

Previous studies suggest that apoptotic genes possess lower affinity p53-binding sites and require higher levels of p53 to turn them on (22). In order to investigate whether there is any difference in gene expression pattern between cells undergoing apoptosis and cell-cycle arrest, two p53-targeted genes were chosen for quantitative investigation using real time RT-PCR. *P21* and *NOXA* were chosen as indicative of genes transactivated in apoptosis and cell cycle arrest.

P21 is the most likely candidate for the cell cycle abnormalities demonstrated in Nutlin-treated cells because it has been clearly associated with p53 dependent cell cycle arrest (30). Interestingly, *P21* is elevated in both Nutlin-3 and Cisplatin treated cells although the level of transactivation appears higher in Nutlin-treated cells (***Fig 4.9***). There may be two explanations for this anomaly. Firstly, expression of *P21* may need to achieve a threshold before it becomes functionally significant. Thus, while *P21* is elevated in Cisplatin treated cells this is insufficient to activate the necessary functional effects. Secondly, other transcriptional targets may override the cell cycle arrest driven by *P21*. For example, although cell cycle arrest was initiated in Cisplatin-treated cells, this may have been overridden by similar activation of apoptotic genes. Clearly, if these were true, the apoptotic genes would not be activated in Nutlin treated cells.

In an attempt to see whether apoptotic genes were activated by Cisplatin but not by Nultin-3, we investigated the expression of a common apoptotic gene *NOXA*. The results showed a similar activation following both Cisplatin and Nutlin-3 treatment with expression levels elevated between 3 and 4 fold at 4 and 6 hours after treatment but falling to pre-treatment levels by 8 hours (***Fig 4.10***). The similar activation of

this apoptotic gene does not support the conclusion that Cisplatin activates apoptotic genes while Nutlin-3 does not. In fact, the similar transactivation of both cell cycle arrest and apoptotic genes by both treatments would suggest that differentiation between cell cycle arrest and apoptosis is not purely driven by a different transcriptional activation profile for the two drugs. These findings do not support the suggestion that apoptotic signals would override cell cycle arrest signals. If this were the case then the high level p53 expression induced by Cisplatin and Nutlin-3 would result in apoptosis for both treatments.

It is possible that post-translational modification of various apoptotic proteins may lead to different protein-protein interactions or translocation to different sites and these alterations may be critical for the differential activation of apoptotic pathways following treatment with Cisplatin and Nutlin-3.

Although this investigation of gene expression is limited, our results are inconsistent with previous suggestions that activation of different suites of genes is responsible for p53's differential ability to activate cell cycle arrest and apoptosis. However, an investigation of other apoptotic genes including *PUMA, BAX*, *BCL-2, BCL-XL* etc needs to be performed to confirm these findings and to ensure that similar expression patterns exist in disparate cell lines.

6.2 Phospho-Ser392-p53 is localised to the cytoplasm immediately after treatment with Cisplatin and Nutlin-3

6.2.1 Cisplatin and Nutlin-3 induce phosphorylation of p53 at Ser392

Post-translational modifications generally result in stabilization, accumulation and activation of p53 (115). We have demonstrated previously that p53 accumulation is efficiently induced by Cisplatin and Nutlin-3. Following DNA damage induced by

Cisplatin, p53 is rapidly stabilized by post-translational modifications to the MDM-2 binding domain thus preventing its binding to MDM-2 (22). However, whether Nutlin-3 induces similar patterns of post-translational modifications remains uncertain. The results in Chapter V showed that Cisplatin and Nutlin-3 both induce phosphorylation at Serine 392. This is not in agreement with the findings showing Nutlin-3 failed to induce phosphorylation at several key residues including Serine 6, Serine 15, Serine 20, Serine 37, Serine 46 and Serine 392 using western blotting after 24 hours in RKO cells (62). This disagreement may be due to the different methods used or the increased sensitivity of immunofluorescence.

6.2.2 Phosphorylation of p53 at Ser392 is not associated with its translocation to the mitochondria

Previous studies suggest p53's translocation to the mitochondria thereby inducing transcriptional independent pathway of apoptosis is one of the possible mechanisms for its differential ability to induce cell cycle arrest and apoptosis. Phosphorylation at Ser392 is suggested to influence the nucleocytoplasmic shuttling ability of p53, thus might be involved in targeting p53 to the mitochondria (77, 111). In Chapter V, we showed that phospho-Ser392-p53 is distributed outside the nucleus but not exclusively localized with mitochondria after 2 hours treatment and there was no major difference between Cisplatin-treated samples and Nutlin-treated samples. Our results are in agreement with some recent findings suggesting the C terminus is not necessary for mitochondrial p53 function (114) and posttranslational modifications are dispensable for targeting p53 to the mitochondria (57). However, a significant portion of phospho-Ser392-p53 was clearly evident in the cytoplasm following treatments at early time points. These phenomena suggest that the phospho-Ser392-p53 might have a function in the cytoplasm which is not associated with differentiation between cell death or cell survival.

Further investigation of the localisation of phospho-Ser392-p53 is warranted. The use of confocal microscopy and its ability to optically slice specimens will enable a more accurate detection of the localisation of this protein and its interaction with other cellular organelles.

In addition, it would also be interesting to compare Ser392 phosphorylated p53 with mono-ubiquitinated p53 as this is thought to be associated with its translocation to the nucleus (14).

6.2.3 p53 phosphorylated at Ser392 may influence the nucleocytoplasmic shuttling ability of p53

Phosphorylation of p53 at Ser392 has been suggested to stabilize tetramer formation, leading to enhancement of site-specific DNA binding (72). In our research, we have shown that Cisplatin and Nutlin-3 are both effective at inducing phosphorylation at Serine392 and therefore, it is possible that these treatments may enhance tetramerization of p53. Additionally, our results showed phospho-Ser392-p53 is mainly located outside the nucleus at 2, 4 and 8 hours post-treatment suggesting p53 may play a part in the cytoplasm in addition to its traditional role as a transcription factor. However, after 24 hours, instead of remaining in the cytoplasm, the majority of phospho-Ser392-p53 now appeared in the nucleus. One possibility is that phosphorylation at Ser392 may affect the nucleocytoplasmic shuttling ability of p53. Phosphorylation at Serine 392 purportedly stabilizes tetramer formation, which may subsequently influence the nucleocytoplasmic shuttling ability of p53 (111) but the mechanism involved remains unclear. Some people suggest modification at Ser392 may influence p53's nuclear export signal based on the fact that substitution of Ser392 with Alanine and Glutamic acid has shown enormous influence on p53's localization to the nucleus (73). However, whether phosphorylation at this site has the same effect remains uncertain. In our results, the fact that p53 phosphorylated at

Serine 392 gradually appeared in the nucleus suggests phosphorylation at this site may influence several NLS or NES localized closely to Ser392 (***Fig 1.1***).

There are two scenarios for our findings that phosphorylated p53 at Ser392 accumulates in the cytoplasm early after treatment.

Firstly, initial transport of p53 to the nucleus could conceivably be interfered with by phosphorylation at Ser392 as this is adjacent to several NLS. Thus, phospho-Ser392-p53 would accumulate in the cytoplasm and gradually be degraded over time. It is known that kinase activity leading to phosphorylation of p53 at Ser392 can be active in both the cytoplasm and nucleus. Our data would suggest that phosphorylation in the cytoplasm may restrict movement into the nucleus whereas previous studies have shown that phosphorylation in the nucleus can increase tetramerization and eventual transcriptional activity.

Secondly, phosphorylated p53 at Ser392 appears to be present in both Cisplatin and Nutlin-3 treated cells at early time points and thus is not associated with the different functional outcomes attributed to these treatments. In addition, the amount of phosphorylated p53 in the cytoplasm does not increase with increasing dosage suggesting that the response may be secondary to treatment effects rather than a response to the treatment itself.

Moreover, it has been reported that p53 can only be active as a transcription factor in a tetrameric form (9) and phosphorylation at Serine 392 is suggested to be associated with stabilization of tetramerization (72). If this were the case, then active p53 in the nucleus would be expected to be phosphorylated at Serine 392. However, our findings showed that the majority of p53 in the nucleus is not phosphorylated on Serine 392 despite being transcriptionally active. Thus, our finings do not agree with

those of our predecessors (22, 72). Alternatively, it could also be possible that our Ser392-phosphorylated primary antibody does not bind to the tetramarized p53.

6.3 Conclusions

Our observations demonstrate that high levels of p53 accumulate in the nucleus in response to Cisplatin and Nutlin-3 treatment. Although the expression pattern of p53 is similar for both treatments, Cisplatin induces apoptosis while Nutlin-3 leads to cell cycle arrest.

As p53 is known to transactivate genes involved in apoptosis and cell cycle arrest we examined the expression patterns of the *P21* and *NOXA* genes. Our data demonstrates that *P21* which regulates cell cycle arrest, was elevated in Nutlin-3 treated cells and less so in Cisplatin treated cells. Thus, induction of cell cycle arrest may be due to increases in p53 expression. However, our data also shows *NOXA*, a pro-apoptotic regulator, was up-regulated in both Nutlin-3 and Cisplatin treated cells suggesting that apoptosis is not purely driven by transactivation of p53 responsive apoptotic genes but could conceivably be overridden by expression of cell cycle arrest genes.

Phosphorylation of Serine 392 is thought to be associated with p53 translocation to the mitochondria where the transcriptional-independent pathway might be activated. However, our data have shown phosphorylation of p53 at Serine 392 occurs in both cell cycle arrested and apoptotic cells. Further, our data demonstrates that phospho-Ser392-p53 is not exclusively associated with the mitochondria. These phenomena suggest that phosphorylation of p53 at Serine 392 is not responsible for p53's ability to induce apoptosis through interaction with the mitochondria but may instead be involved in its nuclear-cytoplasmic shuttling capacity.

6.4 Future directions

Clearly, future research in this area has many questions to answer. For example, do post-translational modifications at other sites, such as Serine 46, contribute to p53's ability to differentially activate cell cycle arrest or apoptosis. Alternatively, this differentiation may be driven by regulation of other p53 dependent genes involved in apoptosis or cell cycle arrest including *BAX*, *PUMA* and *GADD45*.

As p53 responses to chemotherapeutic drugs has been suggested to be tissue specific, studies using a wider range of tissue types or cell lines should be performed to identify whether this response is tissue specific or not.

While we have identified that p53 phosphorylated at Ser 392 localises differently to unphosphorylated p53, higher definition studies using confocal microscopy may more clearly identify the localisation patterns and give clues as to its possible mechanism of action.

The data provided in this thesis begins to explain the complicated ways in which p53 differentially activates cell cycle arrest and apoptosis. Understanding these mechanisms provides us with new ways to regulate the fate of cells and new opportunities to establish therapeutic interventions that in the future may allow better health outcomes.

REFERENCE

1. Linzer DI, Maltzman W, Levine AJ. The SV40 A gene product is required for the production of a 54,000 MW cellular tumor antigen. Virology. 1979 Oct 30;98(2):308-18.
2. Tyner SD, Venkatachalam S, Choi J, Jones S, Ghebranious N, Igelmann H, et al. p53 mutant mice that display early ageing-associated phenotypes. Nature. 2002 Jan 3;415(6867):45-53.
3. Soussi T, Beroud C. Assessing TP53 status in human tumours to evaluate clinical outcome. Nature reviews. 2001 Dec;1(3):233-40.
4. Donehower LA, Harvey M, Slagle BL, McArthur MJ, Montgomery CA, Jr., Butel JS, et al. Mice deficient for p53 are developmentally normal but susceptible to spontaneous tumours. Nature. 1992 Mar 19;356(6366):215-21.
5. Boyle JM, Mitchell EL, Greaves MJ, Roberts SA, Tricker K, Burt E, et al. Chromosome instability is a predominant trait of fibroblasts from Li-Fraumeni families. Br J Cancer. 1998 Jun;77(12):2181-92.
6. Burns TF, El-Deiry WS. The p53 pathway and apoptosis. J Cell Physiol. 1999 Nov;181(2):231-9.
7. Resnick-Silverman L, Manfredi JJ. Gene-specific mechanisms of p53 transcriptional control and prospects for cancer therapy. J Cell Biochem. 2006 Oct 15;99(3):679-89.
8. Fisher DE. The p53 tumor suppressor: critical regulator of life & death in cancer. Apoptosis. 2001 Feb-Apr;6(1-2):7-15.
9. Lacroix M, Toillon RA, Leclercq G. p53 and breast cancer, an update. 2006 Jun;13(2):293-325.
10. Chen J, Lin J, Levine AJ. Regulation of transcription functions of the p53 tumor suppressor by the mdm-2 oncogene. Mol Med. 1995 Jan;1(2):142-52.
11. Momand J, Zambetti GP. Mdm-2: "big brother" of p53. J Cell Biochem. 1997 Mar 1;64(3):343-52.
12. Picksley SM, Lane DP. The p53-mdm2 autoregulatory feedback loop: a paradigm for the regulation of growth control by p53? Bioessays. 1993 Oct;15(10):689-90.
13. Kohn KW, Pommier Y. Molecular interaction map of the p53 and Mdm2 logic elements, which control the Off-On switch of p53 in response to DNA damage. Biochem Biophys Res Commun. 2005 Jun 10;331(3):816-27.
14. Marchenko ND, Wolff S, Erster S, Becker K, Moll UM. Monoubiquitylation promotes mitochondrial p53 translocation. Embo J. 2007 Feb 21;26(4):923-34.
15. Brooks CL, Gu W. Dynamics in the p53-Mdm2 ubiquitination pathway. Cell Cycle. 2004 Jul;3(7):895-9.
16. Marchenko ND, Moll UM. The Role of Ubiquitination in the Direct Mitochondrial Death Program of p53. Cell Cycle. 2007 May 25;6(14).

17. Brooks CL, Gu W. Ubiquitination, phosphorylation and acetylation: the molecular basis for p53 regulation. Curr Opin Cell Biol. 2003 Apr;15(2):164-71.
18. Buolamwini JK, Addo J, Kamath S, Patil S, Mason D, Ores M. Small molecule antagonists of the MDM2 oncoprotein as anticancer agents. Curr Cancer Drug Targets. 2005 Feb;5(1):57-68.
19. Faderl S, Kantarjian HM, Estey E, Manshouri T, Chan CY, Rahman Elsaied A, et al. The prognostic significance of p16(INK4a)/p14(ARF) locus deletion and MDM-2 protein expression in adult acute myelogenous leukemia. Cancer. 2000 Nov 1;89(9):1976-82.
20. Tokino T, Nakamura Y. The role of p53-target genes in human cancer. Critical reviews in oncology/hematology. 2000 Jan;33(1):1-6.
21. Helton ES, Chen X. p53 modulation of the DNA damage response. J Cell Biochem. 2007 Mar 1;100(4):883-96.
22. Meek DW. The p53 response to DNA damage. DNA Repair (Amst). 2004 Aug-Sep;3(8-9):1049-56.
23. Hajra KM, Liu JR. Apoptosome dysfunction in human cancer. Apoptosis. 2004 Nov;9(6):691-704.
24. Jin Z, El-Deiry WS. Overview of cell death signaling pathways. Cancer biology & therapy. 2005 Feb;4(2):139-63.
25. Owen-Schaub LB, Zhang W, Cusack JC, Angelo LS, Santee SM, Fujiwara T, et al. Wild-type human p53 and a temperature-sensitive mutant induce Fas/APO-1 expression. Mol Cell Biol. 1995 Jun;15(6):3032-40.
26. Pines J. Cyclins and cyclin-dependent kinases: a biochemical view. Biochem J. 1995 Jun 15;308 (Pt 3):697-711.
27. Kranenburg O, van der Eb AJ, Zantema A. Cyclin-dependent kinases and pRb: regulators of the proliferation-differentiation switch. FEBS Lett. 1995 Jun 26;367(2):103-6.
28. Nigg EA. Cyclin-dependent protein kinases: key regulators of the eukaryotic cell cycle. Bioessays. 1995 Jun;17(6):471-80.
29. MacLachlan TK, Sang N, Giordano A. Cyclins, cyclin-dependent kinases and cdk inhibitors: implications in cell cycle control and cancer. Crit Rev Eukaryot Gene Expr. 1995;5(2):127-56.
30. Gartel AL, Radhakrishnan SK. Lost in transcription: p21 repression, mechanisms, and consequences. Cancer Res. 2005 May 15;65(10):3980-5.
31. Rouault JP, Falette N, Guehenneux F, Guillot C, Rimokh R, Wang Q, et al. Identification of BTG2, an antiproliferative p53-dependent component of the DNA damage cellular response pathway. Nat Genet. 1996 Dec;14(4):482-6.
32. Smith ML, Chen IT, Zhan Q, Bae I, Chen CY, Gilmer TM, et al. Interaction of the p53-regulated protein Gadd45 with proliferating cell nuclear antigen. Science. 1994 Nov 25;266(5189):1376-80.
33. Smits VA, Klompmaker R, Vallenius T, Rijksen G, Makela TP, Medema RH. p21 inhibits Thr161 phosphorylation of Cdc2 to enforce the G2 DNA damage checkpoint. J Biol Chem. 2000 Sep 29;275(39):30638-43.

34. Hermeking H, Benzinger A. 14-3-3 proteins in cell cycle regulation. Semin Cancer Biol. 2006 Jun;16(3):183-92.
35. Kastan MB, Zhan Q, el-Deiry WS, Carrier F, Jacks T, Walsh WV, et al. A mammalian cell cycle checkpoint pathway utilizing p53 and GADD45 is defective in ataxia-telangiectasia. Cell. 1992 Nov 13;71(4):587-97.
36. Ohki R, Nemoto J, Murasawa H, Oda E, Inazawa J, Tanaka N, et al. Reprimo, a new candidate mediator of the p53-mediated cell cycle arrest at the G2 phase. J Biol Chem. 2000 Jul 28;275(30):22627-30.
37. Jin S, Tong T, Fan W, Fan F, Antinore MJ, Zhu X, et al. GADD45-induced cell cycle G2-M arrest associates with altered subcellular distribution of cyclin B1 and is independent of p38 kinase activity. Oncogene. 2002 Dec 12;21(57):8696-704.
38. di Masi A, Antoccia A, Dimauro I, Argentino-Storino A, Mosiello A, Mango R, et al. Gene expression and apoptosis induction in p53-heterozygous irradiated mice. Mutat Res. 2006 Feb 22;594(1-2):49-62.
39. Rozan LM, El-Deiry WS. p53 downstream target genes and tumor suppression: a classical view in evolution. Cell Death Differ. 2007 Jan;14(1):3-9.
40. Dimri GP. What has senescence got to do with cancer? Cancer cell. 2005 Jun;7(6):505-12.
41. Chang BD, Xuan Y, Broude EV, Zhu H, Schott B, Fang J, et al. Role of p53 and p21waf1/cip1 in senescence-like terminal proliferation arrest induced in human tumor cells by chemotherapeutic drugs. Oncogene. 1999 Aug 26;18(34):4808-18.
42. Achanta G, Huang P. Role of p53 in sensing oxidative DNA damage in response to reactive oxygen species-generating agents. Cancer Res. 2004 Sep 1;64(17):6233-9.
43. Mol CD, Arvai AS, Sanderson RJ, Slupphaug G, Kavli B, Krokan HE, et al. Crystal structure of human uracil-DNA glycosylase in complex with a protein inhibitor: protein mimicry of DNA. Cell. 1995 Sep 8;82(5):701-8.
44. Scherer SJ, Maier SM, Seifert M, Hanselmann RG, Zang KD, Muller-Hermelink HK, et al. p53 and c-Jun functionally synergize in the regulation of the DNA repair gene hMSH2 in response to UV. J Biol Chem. 2000 Dec 1;275(48):37469-73.
45. Yanamadala S, Ljungman M. Potential role of MLH1 in the induction of p53 and apoptosis by blocking transcription on damaged DNA templates. Mol Cancer Res. 2003 Aug;1(10):747-54.
46. Xu J, Morris GF. p53-mediated regulation of proliferating cell nuclear antigen expression in cells exposed to ionizing radiation. Mol Cell Biol. 1999 Jan;19(1):12-20.
47. Shimodaira H, Yoshioka-Yamashita A, Kolodner RD, Wang JY. Interaction of mismatch repair protein PMS2 and the p53-related transcription factor p73 in apoptosis response to cisplatin. Proc Natl Acad Sci U S A. 2003 Mar 4;100(5):2420-5.

48. Adimoolam S, Ford JM. p53 and DNA damage-inducible expression of the xeroderma pigmentosum group C gene. Proc Natl Acad Sci U S A. 2002 Oct 1;99(20):12985-90.
49. Hwang PM, Bunz F, Yu J, Rago C, Chan TA, Murphy MP, et al. Ferredoxin reductase affects p53-dependent, 5-fluorouracil-induced apoptosis in colorectal cancer cells. Nat Med. 2001 Oct;7(10):1111-7.
50. Hollander MC, Sheikh MS, Bulavin DV, Lundgren K, Augeri-Henmueller L, Shehee R, et al. Genomic instability in Gadd45a-deficient mice. Nat Genet. 1999 Oct;23(2):176-84.
51. Ford JM, Hanawalt PC. Li-Fraumeni syndrome fibroblasts homozygous for p53 mutations are deficient in global DNA repair but exhibit normal transcription-coupled repair and enhanced UV resistance. Proc Natl Acad Sci U S A. 1995 Sep 12;92(19):8876-80.
52. Shibue T, Taniguchi T. BH3-only proteins: integrated control point of apoptosis. Int J Cancer. 2006 Nov 1;119(9):2036-43.
53. Schinzel A, Kaufmann T, Borner C. Bcl-2 family members: integrators of survival and death signals in physiology and pathology [corrected]. Biochim Biophys Acta. 2004 Mar 1;1644(2-3):95-105.
54. Hacker G, Weber A. BH3-only proteins trigger cytochrome c release, but how? Arch Biochem Biophys. 2007 Jun 15;462(2):150-5.
55. Cory S, Adams JM. The Bcl2 family: regulators of the cellular life-or-death switch. Nature reviews. 2002 Sep;2(9):647-56.
56. Yee KS, Vousden KH. Complicating the complexity of p53. Carcinogenesis. 2005 Aug;26(8):1317-22.
57. Nemajerova A, Erster S, Moll UM. The post-translational phosphorylation and acetylation modification profile is not the determining factor in targeting endogenous stress-induced p53 to mitochondria. Cell Death Differ. 2005 Feb;12(2):197-200.
58. Erster S, Mihara M, Kim RH, Petrenko O, Moll UM. In vivo mitochondrial p53 translocation triggers a rapid first wave of cell death in response to DNA damage that can precede p53 target gene activation. Mol Cell Biol. 2004 Aug;24(15):6728-41.
59. Wesierska-Gadek J, Gueorguieva M, Herbacek I, Ranftler C. Effect of distinct anticancer drugs on the phosphorylation of p53 protein at serine 46 in human MCF-7 breast cancer cells. Ann N Y Acad Sci. 2007 Jan;1095:45-52.
60. Lu X. p53: a heavily dictated dictator of life and death. Curr Opin Genet Dev. 2005 Feb;15(1):27-33.
61. Wrighton KH, Prele CM, Sunters A, Yeudall WA. Aberrant p53 alters DNA damage checkpoints in response to cisplatin: downregulation of CDK expression and activity. Int J Cancer. 2004 Dec 10;112(5):760-70.
62. Thompson T, Tovar C, Yang H, Carvajal D, Vu BT, Xu Q, et al. Phosphorylation of p53 on key serines is dispensable for transcriptional activation and apoptosis. J Biol Chem. 2004 Dec 17;279(51):53015-22.

63. Lakin ND, Jackson SP. Regulation of p53 in response to DNA damage. Oncogene. 1999 Dec 13;18(53):7644-55.
64. Takagi M, Absalon MJ, McLure KG, Kastan MB. Regulation of p53 translation and induction after DNA damage by ribosomal protein L26 and nucleolin. Cell. 2005 Oct 7;123(1):49-63.
65. Chehab NH, Malikzay A, Stavridi ES, Halazonetis TD. Phosphorylation of Ser-20 mediates stabilization of human p53 in response to DNA damage. Proc Natl Acad Sci U S A. 1999 Nov 23;96(24):13777-82.
66. Zhang Y, Xiong Y. A p53 amino-terminal nuclear export signal inhibited by DNA damage-induced phosphorylation. Science. 2001 Jun 8;292(5523):1910-5.
67. Higashimoto Y, Saito S, Tong XH, Hong A, Sakaguchi K, Appella E, et al. Human p53 is phosphorylated on serines 6 and 9 in response to DNA damage-inducing agents. J Biol Chem. 2000 Jul 28;275(30):23199-203.
68. Dohoney KM, Guillerm C, Whiteford C, Elbi C, Lambert PF, Hager GL, et al. Phosphorylation of p53 at serine 37 is important for transcriptional activity and regulation in response to DNA damage. Oncogene. 2004 Jan 8;23(1):49-57.
69. Mayo LD, Seo YR, Jackson MW, Smith ML, Rivera Guzman J, Korgaonkar CK, et al. Phosphorylation of human p53 at serine 46 determines promoter selection and whether apoptosis is attenuated or amplified. J Biol Chem. 2005 Jul 15;280(28):25953-9.
70. Oda K, Arakawa H, Tanaka T, Matsuda K, Tanikawa C, Mori T, et al. p53AIP1, a potential mediator of p53-dependent apoptosis, and its regulation by Ser-46-phosphorylated p53. Cell. 2000 Sep 15;102(6):849-62.
71. Kurihara A, Nagoshi H, Yabuki M, Okuyama R, Obinata M, Ikawa S. Ser46 phosphorylation of p53 is not always sufficient to induce apoptosis: multiple mechanisms of regulation of p53-dependent apoptosis. Genes Cells. 2007 Jul;12(7):853-61.
72. Sakaguchi K, Sakamoto H, Lewis MS, Anderson CW, Erickson JW, Appella E, et al. Phosphorylation of serine 392 stabilizes the tetramer formation of tumor suppressor protein p53. Biochemistry. 1997 Aug 19;36(33):10117-24.
73. Kim YY, Park BJ, Kim DJ, Kim WH, Kim S, Oh KS, et al. Modification of serine 392 is a critical event in the regulation of p53 nuclear export and stability. FEBS Lett. 2004 Aug 13;572(1-3):92-8.
74. Saito S, Yamaguchi H, Higashimoto Y, Chao C, Xu Y, Fornace AJ, Jr., et al. Phosphorylation site interdependence of human p53 post-translational modifications in response to stress. J Biol Chem. 2003 Sep 26;278(39):37536-44.
75. Feng L, Hollstein M, Xu Y. Ser46 phosphorylation regulates p53-dependent apoptosis and replicative senescence. Cell Cycle. 2006 Dec;5(23):2812-9.
76. Fogal V, Hsieh JK, Royer C, Zhong S, Lu X. Cell cycle-dependent nuclear retention of p53 by E2F1 requires phosphorylation of p53 at Ser315. Embo J. 2005 Aug 3;24(15):2768-82.

77. Vousden KH. Outcomes of p53 activation--spoilt for choice. J Cell Sci. 2006 Dec 15;119(Pt 24):5015-20.
78. Yu Q. Restoring p53-mediated apoptosis in cancer cells: new opportunities for cancer therapy. Drug Resist Updat. 2006 Feb-Apr;9(1-2):19-25.
79. Chen X, Ko LJ, Jayaraman L, Prives C. p53 levels, functional domains, and DNA damage determine the extent of the apoptotic response of tumor cells. Genes Dev. 1996 Oct 1;10(19):2438-51.
80. Lai PB, Chi TY, Chen GG. Different levels of p53 induced either apoptosis or cell cycle arrest in a doxycycline-regulated hepatocellular carcinoma cell line in vitro. Apoptosis. 2007 Feb;12(2):387-93.
81. Lomazzi M, Moroni MC, Jensen MR, Frittoli E, Helin K. Suppression of the p53- or pRB-mediated G1 checkpoint is required for E2F-induced S-phase entry. Nat Genet. 2002 Jun;31(2):190-4.
82. Rieber M, Strasberg-Rieber M. Induction of p53 and melanoma cell death is reciprocal with down-regulation of E2F, cyclin D1 and pRB. Int J Cancer. 1998 May 29;76(5):757-60.
83. Braithwaite AW, Del Sal G, Lu X. Some p53-binding proteins that can function as arbiters of life and death. Cell Death Differ. 2006 Jun;13(6):984-93.
84. Samuels-Lev Y, O'Connor DJ, Bergamaschi D, Trigiante G, Hsieh JK, Zhong S, et al. ASPP proteins specifically stimulate the apoptotic function of p53. Mol Cell. 2001 Oct;8(4):781-94.
85. Bergamaschi D, Samuels Y, Jin B, Duraisingham S, Crook T, Lu X. ASPP1 and ASPP2: common activators of p53 family members. Mol Cell Biol. 2004 Feb;24(3):1341-50.
86. Bergamaschi D, Samuels Y, O'Neil NJ, Trigiante G, Crook T, Hsieh JK, et al. iASPP oncoprotein is a key inhibitor of p53 conserved from worm to human. Nat Genet. 2003 Feb;33(2):162-7.
87. Lasham A, Moloney S, Hale T, Homer C, Zhang YF, Murison JG, et al. The Y-box-binding protein, YB1, is a potential negative regulator of the p53 tumor suppressor. J Biol Chem. 2003 Sep 12;278(37):35516-23.
88. Kohno K, Izumi H, Uchiumi T, Ashizuka M, Kuwano M. The pleiotropic functions of the Y-box-binding protein, YB-1. Bioessays. 2003 Jul;25(7):691-8.
89. Zacchi P, Gostissa M, Uchida T, Salvagno C, Avolio F, Volinia S, et al. The prolyl isomerase Pin1 reveals a mechanism to control p53 functions after genotoxic insults. Nature. 2002 Oct 24;419(6909):853-7.
90. Wulf GM, Liou YC, Ryo A, Lee SW, Lu KP. Role of Pin1 in the regulation of p53 stability and p21 transactivation, and cell cycle checkpoints in response to DNA damage. J Biol Chem. 2002 Dec 13;277(50):47976-9.
91. Herold S, Wanzel M, Beuger V, Frohme C, Beul D, Hillukkala T, et al. Negative regulation of the mammalian UV response by Myc through association with Miz-1. Mol Cell. 2002 Sep;10(3):509-21.

92. Wu WS, Heinrichs S, Xu D, Garrison SP, Zambetti GP, Adams JM, et al. Slug antagonizes p53-mediated apoptosis of hematopoietic progenitors by repressing puma. Cell. 2005 Nov 18;123(4):641-53.
93. Kim E, Deppert W. The versatile interactions of p53 with DNA: when flexibility serves specificity. Cell Death Differ. 2006 Jun;13(6):885-9.
94. Chao C, Herr D, Chun J, Xu Y. Ser18 and 23 phosphorylation is required for p53-dependent apoptosis and tumor suppression. Embo J. 2006 Jun 7;25(11):2615-22.
95. Bunz F, Hwang PM, Torrance C, Waldman T, Zhang Y, Dillehay L, et al. Disruption of p53 in human cancer cells alters the responses to therapeutic agents. The Journal of clinical investigation. 1999 Aug;104(3):263-9.
96. Bouchet BP, de Fromentel CC, Puisieux A, Galmarini CM. p53 as a target for anti-cancer drug development. Critical reviews in oncology/hematology. 2006 Jun;58(3):190-207.
97. Hiraoka K, Kimura T, Logg CR, Tai CK, Haga K, Lawson GW, et al. Therapeutic efficacy of replication-competent retrovirus vector-mediated suicide gene therapy in a multifocal colorectal cancer metastasis model. Cancer Res. 2007 Jun 1;67(11):5345-53.
98. Rainov NG, Ren H. Clinical trials with retrovirus mediated gene therapy--what have we learned? J Neurooncol. 2003 Dec;65(3):227-36.
99. Eastham JA, Grafton W, Martin CM, Williams BJ. Suppression of primary tumor growth and the progression to metastasis with p53 adenovirus in human prostate cancer. J Urol. 2000 Sep;164(3 Pt 1):814-9.
100. Schuler M, Herrmann R, De Greve JL, Stewart AK, Gatzemeier U, Stewart DJ, et al. Adenovirus-mediated wild-type p53 gene transfer in patients receiving chemotherapy for advanced non-small-cell lung cancer: results of a multicenter phase II study. J Clin Oncol. 2001 Mar 15;19(6):1750-8.
101. Schuler M, Rochlitz C, Horowitz JA, Schlegel J, Perruchoud AP, Kommoss F, et al. A phase I study of adenovirus-mediated wild-type p53 gene transfer in patients with advanced non-small cell lung cancer. Hum Gene Ther. 1998 Sep 20;9(14):2075-82.
102. Vassilev LT, Vu BT, Graves B, Carvajal D, Podlaski F, Filipovic Z, et al. In vivo activation of the p53 pathway by small-molecule antagonists of MDM2. Science. 2004 Feb 6;303(5659):844-8.
103. Kramer DL, Vujcic S, Diegelman P, White C, Black JD, Porter CW. Polyamine analogue-mediated cell cycle responses in human melanoma cells involves the p53, p21, Rb regulatory pathway. Biochemical Society transactions. 1998 Nov;26(4):609-14.
104. Komarov PG, Komarova EA, Kondratov RV, Christov-Tselkov K, Coon JS, Chernov MV, et al. A chemical inhibitor of p53 that protects mice from the side effects of cancer therapy. Science (New York, NY. 1999 Sep 10;285(5434):1733-7.
105. Caron de Fromentel C, Gruel N, Venot C, Debussche L, Conseiller E, Dureuil C, et al. Restoration of transcriptional activity of p53 mutants in human

tumour cells by intracellular expression of anti-p53 single chain Fv fragments. Oncogene. 1999 Jan 14;18(2):551-7.
106. Tan J, Zhuang L, Leong HS, Iyer NG, Liu ET, Yu Q. Pharmacologic modulation of glycogen synthase kinase-3beta promotes p53-dependent apoptosis through a direct Bax-mediated mitochondrial pathway in colorectal cancer cells. Cancer research. 2005 Oct 1;65(19):9012-20.
107. Giard DJ, Aaronson SA, Todaro GJ, Arnstein P, Kersey JH, Dosik H, et al. In vitro cultivation of human tumors: establishment of cell lines derived from a series of solid tumors. Journal of the National Cancer Institute. 1973 Nov;51(5):1417-23.
108. Smith ML, Chen IT, Zhan Q, O'Connor PM, Fornace AJ, Jr. Involvement of the p53 tumor suppressor in repair of u.v.-type DNA damage. Oncogene. 1995 Mar 16;10(6):1053-9.
109. McGregor S. The role of p53 in Apoptotic Signalling Induced by Cytotoxic Chemotherapeutics [Honours]. Perth: Curtin University of Techonology; October 2005.
110. Labi V, Erlacher M, Kiessling S, Villunger A. BH3-only proteins in cell death initiation, malignant disease and anticancer therapy. Cell Death Differ. 2006 Aug;13(8):1325-38.
111. Liang SH, Clarke MF. Regulation of p53 localization. European journal of biochemistry / FEBS. 2001 May;268(10):2779-83.
112. Qi F, Zhang B, Xu Y. [Cisplatin-induced apoptosis in laryngeal squamous cell carcinoma strain and the influence on cell cycle]. Zhonghua yi xue za zhi. 1999 Apr;79(4):298-301.
113. Secchiero P, Corallini F, Gonelli A, Dell'Eva R, Vitale M, Capitani S, et al. Antiangiogenic activity of the MDM2 antagonist nutlin-3. Circulation research. 2007 Jan 5;100(1):61-9.
114. Marchenko ND, Zaika A, Moll UM. Death signal-induced localization of p53 protein to mitochondria. A potential role in apoptotic signaling. J Biol Chem. 2000 May 26;275(21):16202-12.
115. Bode AM, Dong Z. Post-translational modification of p53 in tumorigenesis. Nature reviews. 2004 Oct;4(10):793-805.